BERICHTE
aus dem Fachbereich Geowissenschaften
der Universität Bremen

No. 156

Moos, C.

RECONSTRUCTION OF UPWELLING INTENSITY AND PALEO-NUTRIENT GRADIENTS IN THE NORTHWEST ARABIAN SEA DERIVED FROM STABLE CARBON AND OXYGEN ISOTOPES OF PLANKTIC FORAMINIFERA

Berichte, Fachbereich Geowissenschaften, Universität Bremen, No. 156,
103 pages, Bremen 2000

ISSN 0931-0800

The "Berichte aus dem Fachbereich Geowissenschaften" are produced at irregular intervals by the Department of Geosciences, Bremen University.

They serve for the publication of experimental works, Ph.D.-theses and scientific contributions made by members of the department.

Reports can be ordered from:

Gisela Boelen

Sonderforschungsbereich 261

Universität Bremen

Postfach 330 440

D 28334 BREMEN

Phone: (49) 421 218-4124

Fax: (49) 421 218-3116

e-mail: boelen@uni-bremen.de

Citation:

Moos, C.

Reconstruction of upwelling intensity and paleo-nutrient gradients in the northwest Arabian Sea derived from stable carbon and oxygen isotopes of planktic foraminifera.

Berichte, Fachbereich Geowissenschaften, Universität Bremen, No. 156, 103 pages, Bremen, 2000.

ISSN 0931-0800

Reconstruction of upwelling intensity and paleo-nutrient gradients in the northwest Arabian Sea derived from stable carbon and oxygen isotopes of planktic foraminifera

Dissertation

zur Erlangung des Grades
Doktor der Naturwissenschaften
(Dr. rer. nat.)

am Fachbereich 5 - Geowissenschaften
der Universität Bremen

vorgelegt von

Christopher Moos

Bremen 2000

Tag des Kolloquiums:

09.06.2000

Gutachter:

Professor Dr. Gerold Wefer

Priv. Doz. Dr. Andreas Mackensen

Prüfer:

Professor Dr. Rüdiger Henrich

Professor Dr. Helmut Willems

Preface

The Asian Monsoon is one of the major atmospheric circulations in the earth's climate system and provides the rainfall that is needed to sustain about 60 % of the world's population. Natural and anthropogenic changes influence the monsoon system and cause climate anomalies affecting the agriculture of the Indian and Asian continents. To predict consequences of future climate variations we have to understand natural as well as anthropogenic mechanisms that control the climate system. Changes of the Asian Monsoon occur on different time scales. Instrumental climate observations are available mostly for the present situation covering the variability within the past ~50 years. The view into the past offers a rich source of information. The investigation of paleo time series covers the full range of variations in the mechanisms controlling the monsoon. Terrestrial and marine records are used to study variations and forcing mechanisms of the monsoon system as well as its interactions with the global climate during the past thousands to millions of years.

Important tools to reconstruct climate history are planktic foraminifera from marine sediments. Recent studies provide information about environmental conditions (e.g. temperature, light, food) preferred by different planktic foraminiferal species. The stable oxygen and carbon isotopes of their calcareous tests record hydrographic parameter of surface water masses favored by the analyzed species (e.g. Wefer, 1985; Hemleben et al., 1989). In this study stable isotope compositions of planktic foraminifera and seawater are used to trace modern and past water mass properties influenced by the monsoon circulation in the Arabian Sea.

This publication is submitted as PhD thesis at the University of Bremen and has been supervised by Professor Dr. G. Wefer. The study was conducted as part of the NEtherlands BRemen OCeanography cooperation (NEBROC) and funded by the Bundesministerium für Bildung, Wissenschaft, Forschung und Technologie (BMBF). All data presented in this thesis are archived in the Pangea database and are available via Internet (http://www.pangaea.de).

This study is subdivided into four parts. Part I refers to the main context of this study. Part II presents four manuscripts dealing with the main topic submitted or already published at reviewed scientific journals. To reduce repetitions the references were excluded from the manuscripts and combined in a separate chapter. Part III contains the conclusions of this thesis and gives implications for future research. Part IV refers to all references used for preparation of this study.

Table of Contents

Reconstruction of upwelling intensity and paleo-nutrient gradients in the northwest Arabian Sea derived from stable carbon and oxygen isotopes of planktic foraminifera

Abstract

The Asian Monsoon system dominates the climate over large areas of the Asian and Indian continents and the rainfall prevailing during SW-monsoon is decisive for the agriculture of the entire region. The atmospheric monsoon system dominates the oceanographic surface circulation of the northern Indian Ocean and causes strong upwelling off Somalia and Arabia during SW-monsoon and makes the northwestern Arabian Sea to one of the most productive areas in the world oceans. Thus, productivity and nutrient gradients in the northwestern Arabian Sea are important parameters for an understanding of the oceanic response to monsoonal forcing.

Stable oxygen and carbon isotopes ($\delta^{18}O$, $\delta^{13}C$) of seawater and planktic foraminifera reveal modern and past nutrient gradients in the monsoonal upwelling area of the northwestern Arabian Sea. The modern conditions were analyzed by hydrographic observations and seawater isotope measurements during the NE- and SW-monsoon season. The results were used to calibrate the oxygen and carbon isotopes of the modern planktic foraminifera *Globigerinoides ruber* (white) and *Neogloboquadrina dutertrei* derived from plankton tows and surface sediments. Foraminiferal $\delta^{13}C$ and $\delta^{18}O$ records from marine sediments off Oman were used to reconstruct past nutrient variations and their relation to monsoonal upwelling during the past 307 kyr.

Based on three research cruises the spatial distributions of $\delta^{13}C_{\Sigma CO2}$ and the concentrations of the nutrients PO_4 and NO_3 were investigated to infer seasonal and decadal changes. The analyzed water tracers reflect the strong stratification of the water column during NE-monsoon with a mixed layer depth around 80 m. In contrast, the distribution of all tracers is nearly homogenous in the upper 500 m during the upwelling period. The seasonal variability is relatively low near the sea surface due to summer heating and summer primary production. Therefore, the strongest seasonal differences of temperature, nutrient concentrations, and $\delta^{13}C_{\Sigma CO2}$ occur between 20 m and 80 m, where the seasonal range of $\delta^{13}C_{\Sigma CO2}$ is about 0.7 ‰ higher than at the sea surface. Below a depth of 150-200 m the seasonal gradient between upwelling and non-upwelling season decreases to zero.

The seasonal hydrographic observations and the stable oxygen and carbon isotopes of modern planktic foraminifera allow examining the environmental preferences of *G. ruber* (w) and *N. dutertrei*. *Globigerinoides ruber* (w) is adapted to the conditions of the upper water column and calcifies in oxygen isotope equilibrium with the ambient sea surface water. Due to the low seasonal $\delta^{13}C_{\Sigma CO2}$ gradient at the sea surface *G. ruber* (w) displays the high carbon isotope composition of nutrient depleted surface water, although nearly the half of the annual *G. ruber* (w) production occurs during upwelling season. *Neogloboquadrina dutertrei* seems to migrate vertically according to the strength of upwelling. The estimated depth habitat of *N. dutertrei* coincides with lowest $\delta^{13}C$ values of seawater (and the highest nutrient concentrations) observed in the upper water column during upwelling season. The carbon isotope compositions of both species show deviations relative to the $\delta^{13}C_{\Sigma CO2}$ of ambient seawater. Globigerinoides *ruber* (w) (in the 250-315 µm size fraction) is depleted in ^{13}C by 0.76 ‰ relative to $\delta^{13}C_{\Sigma CO2}$. In contrast, $\delta^{13}C$ in the shells of *N. dutertrei* is about 0.5 ‰ higher than in seawater. Within the observed range of upwelling variability the carbon isotope difference between *G. ruber* (w) and *N. dutertrei* ($\Delta\delta^{13}C$ *r-d*) is related to upwelling intensity and documents the maximum seasonal gradient of seawater $\delta^{13}C$.

The similarities between the carbon isotope record of *G. ruber* (w) and variations of the global marine carbon isotope signal of the past 307 kyr indicates again that $\delta^{13}C$ of *G. ruber* (w) traces nutrient depleted surface water masses and is mainly affected by global $\delta^{13}C_{\Sigma CO2}$ variations. The $\delta^{13}C$ in *N. dutertrei* is additionally influenced by the $\delta^{13}C$ of the nutrient enriched water during upwelling season. Hence, the $\Delta\delta^{13}C$ *r-d* variations of core GeoB 3005 is a measure of the nutrient availability of water masses affected by upwelling. Relative to the modern situation the foraminiferal $\Delta\delta^{13}C$ *r-d* difference suggests lower nutrient gradients during glacial periods. Highest nutrient availability is indicated at 6 kyr, 120 kyr 205 kyr, 240 kyr, and 265 kyr. Frequency analyses of the $\Delta\delta^{13}C$ *r-d* time series suggests cyclic changes in nutrient availability in accordance with Earth's orbital parameters of eccentricity and precession, as well as at periods of 12,5 kyr and 7,7 kyr. As indicated by a comparison between $\Delta\delta^{13}C$ *r-d*, tracers of productivity, and monsoon wind strength productivity depends mainly on nutrient availability, while upwelling intensity itself seems to be of lower importance during the past 307 kyr. Hence, the carbon isotopes of planktic foraminifera represent an important tool to distinguish between different control mechanisms of upwelling productivity during SW-monsoon and emphasize the importance of source water mass properties affected by upwelling.

Rekonstruktion von Auftriebsintensität und Paläonährstoffgradienten im nordwestlichen Arabischen Meer, abgeleitet von stabilen Kohlenstoff- und Sauerstoffisotopen in planktischen Foraminiferen

Zusammenfassung

In weiten Bereichen Asiens und Indiens wird das Klima durch den Einfluss des asiatischen Monsunsystems dominiert. Die Niederschläge des SW-Monsuns sind entscheidend für die landwirtschaftliche Entwicklung der gesamten Region. Zusätzlich beherrscht das atmosphärische Monsunsystem die Oberflächenzirkulation des nördlichen Indischen Ozeans und verursacht im Sommer starken Auftrieb vor den Küsten Somalias und Arabiens. Der Küstenauftrieb führt dazu, dass die Arabische See zu den produktivsten Gebieten der Weltozeane gehört. Daher sind Produktivität und Nährstoffgradienten unentbehrlich für das Verständnis der an das Monsunsystem gekoppelten Vorgänge im Ozean.

Stabile Sauerstoff- und Kohlenstoffisotope ($\delta^{18}O$, $\delta^{13}C$) des Meerwassers und planktischer Foraminiferen enthüllen heutige und vergangene Nährstoffgradienten im monsunbeeinflussten Auftriebsgebiet des nordwestlichen Arabischen Meers. Für eine Bewertung der heutige Situation wurden hydrographische Beobachtungen und Isotopenmessungen während des NE- und des SW-Monsuns durchgeführt. Isotopenmessungen an rezenten Exemplaren der planktischen Foraminiferen *Globigerinoides ruber* (weiß) und *Neogloboquadrina dutertrei* wurden an den heutigen hydrographischen Bedingungen kalibriert und mit saisonalen Kohlenstoffisotopenmessungen des gesamten gelösten anorganischen Kohlenstoffs ($\delta^{13}C_{\Sigma CO2}$) verglichen. Stabile Sauerstoff- und Kohlenstoffisotope planktischer Foraminiferenschalen aus marinen Sedimenten vor Oman ermöglichten die Rekonstruktion der Nährstoffvariationen der vergangenen 307.000 Jahre.

Drei Forschungsreisen bildeten die Grundlage für hydrographische Untersuchungen im nördlichen Arabischen Meer. Dabei wurden die räumliche Verteilungen sowie saisonale und dekadische Änderungen für $\delta^{13}C_{\Sigma CO2}$, PO_4 und NO_3 erfasst. Für die Zeit des NE-Monsuns geben die analysierten Wassertracer die Stratifizierung der Wassersäule wieder, mit Durchmischungstiefen von etwa 80 m. Während des Auftriebs ist die vertikale Verteilung aller Parameter innerhalb der oberen 500 m der Wassersäule annähernd homogen. Aufgrund der hohen Sonneneinstrahlung im Sommer, ebenso wie der verstärkten Primärproduktivität

während des Auftriebs, verringern sich die jahreszeitlichen Gegensätze von Temperatur, Nährstoffkonzentrationen und $\delta^{13}C_{\Sigma CO2}$ an der Wasseroberfläche. In Wassertiefen zwischen 20 m und 80 m wurden um 0.7 ‰ höhere Unterschiede zwischen NE- und SW-Monsun beobachtet, während unterhalb von 150 m bis 200 m nur noch sehr geringe Unterschiede erkennen sind.

Ein Vergleich von Isotopenmessungen an rezenten Foraminiferen der Arten *G. ruber* (w) und *N. dutertrei* mit saisonalen hydrographischen Beobachtungen ermöglichte es, die bevorzugten Milieubedingungen beider Arten zu erkunden. *Globigerinoides ruber* (w) bevorzugt die Bedingungen der Wasseroberfläche und kalzifiziert im Sauerstoffisotopengleichgewicht mit dem umgebenden Meerwasser der oberen Wassersäule. Das $\delta^{13}C$-Signal von *G. ruber* (w) spiegelt die hohen $\delta^{13}C_{\Sigma CO2}$-Werte von nährstoffarmen Oberflächenwässern wieder, obwohl die Häufigkeit von *G. ruber* (w) gleichmäßig auf beide Monsunperioden verteilt ist. Im Gegensatz zu *G. ruber* (w) scheint die Lebenstiefe von *N. dutertrei* in Abhängigkeit von der Auftriebsintensität zu variieren. Die ermittelten Lebenstiefen von *N. dutertrei* entsprechen den niedrigsten gemessenen $\delta^{13}C_{\Sigma CO2}$-Werten (den höchsten Nährstoffgehalten) des Meerwassers der oberen Wassersäule. Die Kohlenstoffisotopenverhältnisse beider Foraminiferenarten zeigen spezifische Abweichungen gegenüber der Isotopenzusammensetzung des Meerwassers. *Globigerinoides ruber* (w) (in einer Größenfraktion von 250-315 µm) zeigt um 0.76 ‰ niedrigere $\delta^{13}C$-Werte als das umgebende Meerwasser, während ^{13}C in den Gehäusen von *N. dutertrei* um etwa 0.5 ‰ angereichert ist. Die Kohlenstoffisotopendifferenz zwischen beiden Arten ($\Delta\delta^{13}C$ *r-d*) dokumentiert den maximalen jahreszeitlichen $\delta^{13}C_{\Sigma CO2}$-Gradienten und variiert mit der beobachteten Auftriebsintensität entlang der Arabischen Küste.

Während der vergangenen 307 ka entsprechen die $\delta^{13}C$-Variationen von *G. ruber* (w) den Abschätzungen globaler $\delta^{13}C_{\Sigma CO2}$ Änderungen und weisen darauf hin, dass *G. ruber* (w) während des gesamten Zeitraums nährstoffarmes Oberflächenwasser bevorzugte. Das $\delta^{13}C$ von *N. dutertrei* wird zusätzlich durch nährstoffreiches Auftriebswasser beeinflusst. Folglich kann die Differenz der Kohlenstoffisotope beider Arten als Messgröße für Nährstoffvariationen der auftriebsbeeinflussten Wassermassen verwendet werden. Gegenüber der heutigen Nährstoffsituation zeigt die $\Delta\delta^{13}C$ *r-d* Differenz geringere Nährstoffgradienten in glazialen Perioden an, während hohe Nährstoffverfügbarkeiten um 6, 120, 205, 240 und 265 ka angezeigt werden. Frequenzanalysen des $\Delta\delta^{13}C$ *r-d*-Signals weisen auf zyklische Nährstoffvariationen hin, die in Verbindung mit den orbitalen Erdbahnparametern der

Exzentrizität und der Präzession stehen. Zusätzlich wurden signifikante Variationen mit Perioden von 12.5 und 7.7 ka gefunden. Vergleiche zwischen Nährstoffvariationen ($\Delta\delta^{13}C$ *r-d*), Produktivitäts- und Windintensitätsanzeigern zeigen an, dass die Produktivität in den vergangenen 307 ka überwiegend von der Verfügbarkeit an Nährstoffen abhing. Änderungen der Auftriebsintensität selbst scheinen weniger bedeutsam gewesen zu sein. Folglich stellen Kohlenstoffisotope in planktischen Foraminiferen bedeutsame Werkzeuge dar, um verschiedene Kontrollmechanismen der Auftriebsproduktivität während des SW-Monsuns zu unterscheiden und betonen die Bedeutung der Wassereigenschaften der am Auftrieb beteiligten Ursprungswassermassen.

Part I - Introduction

1. Stable oxygen and carbon isotopes - paleoceanographic implications

1.1 Stable isotopes in planktic foraminifera

Stable oxygen and carbon isotope ratios of calcareous organisms are widely used to reconstruct paleoenvironmental parameters, for an overview see Wefer et al., 1999. Especially the planktic foraminifera represent an important group of organisms and the isotopic compositions of their calcite shells or tests are related to the hydrographic conditions of past ocean surface waters.

Planktic foraminifera are unicellular marine organisms living in the upper water column of the ocean (Figure 1). Each species favors certain environmental settings, with respect to temperature, salinity, food and light conditions (e.g. Hemleben et al., 1989). These ecological preferences result in characteristic seasonal and spatial distributions of each foraminiferal species over the world oceans. The fractionation of stable oxygen and carbon isotopes in tests of planktic foraminifera depends on the environmental conditions during calcification. Thus, faunal assemblages, and isotope compositions of foraminiferal shells allow reconstructing surface ocean hydrography. Due to these characteristics and because foraminiferal shells are often well preserved in ocean sediments they became important tools in paleoceanography.

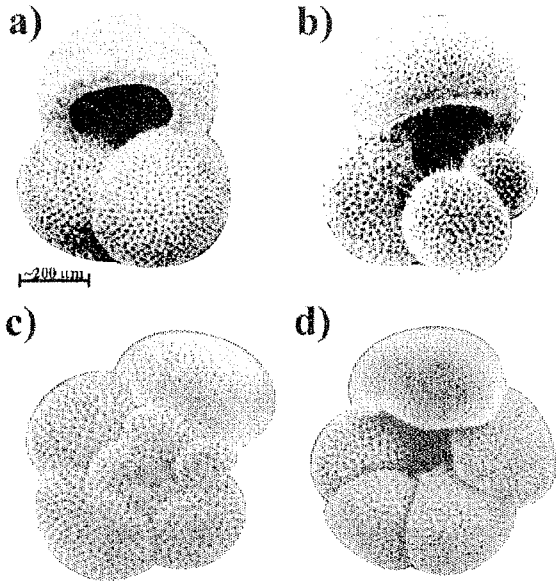

Figure 1. Examples of planktic foraminiferal species (Brummer and Kroon, 1988). **a)** *Globigerinoides ruber* (w), umbilical side (scale bar = 200 µm); **b)** *Globigerina bulloides*, umbilical side (x110); **c-d)** *Neogloboquadrina dutertrei*, trochospiral and umbilical side (x74, x62).

Potential problems when dealing with stable isotopes in planktic foraminifera are unknown factors like their preferred depth habitat and the season of maximum growth as well as deviations relative to isotope equilibrium expected for inorganic calcite precipitation, so- called "vital effects". Differences between the shells of living specimens and their dead counterparts in the sediment indicate that additional effects like secondary calcification and post depositional

calcite dissolution must be taken into account when interpreting oxygen and carbon isotopes (Berger and Gardner, 1975; Duplessy et al, 1981; Bouvier-Soumagnac and Duplessy, 1985). Additionally, each foraminiferal species accepts different ranges of environmental variations and react differently to changes in hydrography. Hence, regional paleoceanographic investigations require a calibration on the modern environment, if possible with respect to the variability expected for the past conditions.

A major mechanism controlling the stable isotopes of foraminiferal calcite is the isotope composition of seawater. Oxygen and carbon isotopes in seawater are influenced by global climate variations, which commonly exceed local effects. The use of isotope differences between foraminiferal species favoring different environmental conditions, according to seasonal and vertical preferences, allows to eliminate the global influence to the single isotope signals and to emphasize local differences.

1.2 Oxygen isotopes

Oxygen isotope composition of carbonate is mainly controlled by the temperature dependent fractionation and the oxygen isotope composition of seawater itself. The oxygen isotope composition of a sample is given by the ratio of ^{18}O versus ^{16}O and is expressed as the deviation relative to a standard and is reported as $\delta^{18}O$, in parts per thousand (per mil, ‰):

$$\delta^{18}O(‰) = \left[\frac{\left(^{18}O/^{16}O\right)_{sample} - \left(^{18}O/^{16}O\right)_{standard}}{\left(^{18}O/^{16}O\right)_{standard}} \right] * 1000 .$$

If the isotope composition of seawater is known, the temperature during calcification can be estimated from the $\delta^{18}O$ of the foraminiferal shell. Epstein et al. (1953) found an empirical relationship to calculate seawater temperatures from oxygen isotopes of calcareous shells from mollusks:

$$T(°C) = 16.5 - 4.3\left(\delta^{18}O_{cc} - \delta^{18}O_{w}\right) + 0.14\left(\delta^{18}O_{cc} - \delta^{18}O_{w}\right)^2 ,$$

where T is the temperature of seawater, and $\delta^{18}O_{cc}$ and $\delta^{18}O_{w}$ are the oxygen isotope compositions of carbonate and seawater, respectively. Later many modifications of this equation were developed for different marine organisms and several foraminiferal species (e.g. Bemis et al., 1998 and references therein). All of these paleotemperature equations show comparable slopes whereas the intercepts are significantly different demonstrating the general suitability of oxygen isotopes in calcareous organisms on the condition that specific fractionation effects are taken into account.

The $^{18}O/^{16}O$ ratio in seawater is mainly controlled by evaporation, precipitation, and river discharge. Evaporation removes preferentially $H_2{}^{16}O$ from the water while the remaining ocean becomes enriched in the heavier $H_2{}^{18}O$. Due to the isotope fractionation during evaporation oxygen isotopes in seawater correlate with salinity, as shown by Craig and Gordon (1965). Hence, calcite oxygen isotopes allow estimations of ocean salinity, provided that temperature is determined independently (e.g. Rosteck et al., 1993; Wolff et al., 1999). During glacial periods much of the $H_2{}^{16}O$ was fixed in the continental ice sheets, while the ocean water was enriched in $H_2{}^{18}O$. The growth and the decay of the global ice sheets caused oxygen isotopes variations of about 1.2 ‰ between the last glacial and postglacial periods (Dansgaard and Tauber, 1969; Shackleton and Opdyke, 1973). Hence, oxygen isotope variations display sea level changes as a function of the global ice volume. Due to the relation of oxygen isotopes to global climate variations foraminiferal $\delta^{18}O$ became important for stratigraphic framework, based on the studies of Shackleton and Opdyke (1973) and Imbrie et al. (1984).

1.3 Carbon isotopes

The ocean is the largest reservoir in the global carbon system (without considering carbonate sedimentary rocks) and the major long-term regulator for atmospheric CO_2. The ratio of the stable carbon isotopes $^{13}C/^{12}C$ is an important tracer of the carbonate system. As for $\delta^{18}O$ the carbon isotopes ratio $^{13}C/^{12}C$ of a given sample is expressed relative to a given standard in per mil:

$$\delta^{13}C(‰) = \left[\frac{\left(^{13}C/^{12}C\right)_{sample} - \left(^{13}C/^{12}C\right)_{standard}}{\left(^{13}C/^{12}C\right)_{standard}} \right] * 1000 .$$

Fractionation effects influencing the carbon isotope composition of dissolved CO_2 in seawater and in shells of planktic foraminifera are quite complex. The most important forcing factors are (1) the productivity-respiration cycle and (2) the gas exchange with the atmosphere. (1) Marine plants preferentially fix ^{12}C. During primary production the ocean surface water becomes enriched in the heavier isotope ^{13}C and depleted in ^{12}C and nutrients. Sinking organic matter is remineralized in deeper waters, lowering the $\delta^{13}C$ of dissolved inorganic carbon. Hence, $\delta^{13}C_{\Sigma CO2}$ in the ocean is inversely correlated with the nutrient content of ocean water (Broecker and Maier-Reimer, 1992; Broecker and Peng, 1982; Kroopnick, 1985). (2) Fractionation effects of carbon isotopes during the gas exchange between the atmosphere and ocean water depend on the sea surface temperature, the CO_2 exchange rate, and the water residence time at the sea surface (Siegenthaler and Münnich,

1981). Due to the thermodynamic effects and their strong regional variations the relationship of carbon isotopes and nutrients is not well defined at the sea surface. In ocean water carbon isotopes vary on different time scales. Seasonal changes depend on the relation of the carbon isotopes to the nutrient cycle. Due to the burning of fossil fuels and the release of isotopically light CO_2 into the atmosphere, the exchange between atmospheric and dissolved oceanic CO_2 has lead to a decrease in surface ocean $\delta^{13}C$ by about 0.4 ‰ during the past 2-3 decades (e.g. Quay et al., 1992). On geological time scales carbon isotope variations of planktic and benthic foraminifera indicate cyclic variations of about 1.0 ‰ related to the primary Earth's orbital periods (Shackleton et al., 1983).

Planktic foraminifera use the marine dissolved inorganic carbon to build their calcium carbonate tests. Hence, they have the potential to preserve the carbon isotope ratio of ancient water masses. This allows the reconstruction of past oceanic circulations and variations of the carbonate system and the underlying climatic changes. A general requirement for paleoceanographic reconstructions of $\delta^{13}C_{\Sigma CO2}$ is that the foraminifera calcify in equilibrium with ambient seawater or have predictable offsets (vital effects). In fact, $\delta^{13}C$ of the most foraminiferal species deviates from $\delta^{13}C$ of ambient seawater. Culture experiments and field studies have identified ontogenetic and metabolic effects, kinetic fractionation and the carbonate chemistry of seawater as additional mechanisms affecting foraminiferal $\delta^{13}C$ (e.g. Spero and Lea, 1996; Wefer and Berger, 1991; Ravelo and Fairbanks, 1995, Spero et al., 1997). Because the foraminiferal carbon isotope offsets (vital effects) are different for each species individual calibrations are required for paleoceanographic implications. If vital effects and the preferred vertical as well as the seasonal habitat of the analyzed species are known, differences in $\delta^{13}C$ between planktic foraminifera allow reconstructions of seasonal and vertical nutrient changes, independent of global ΣCO_2 variations. In the northwestern Arabian Sea, where modern productivity shows strong seasonal gradients due to atmospheric forcing, foraminiferal carbon isotope records of marine sediments are important tracers of paleo-climate reconstructions.

2. Monsoon climate

2.1 The Indian Monsoon system

The Indian Monsoon system is part of the large-scale circulation of the Asian Monsoon and dominates the atmospheric and oceanographic circulation of the Indian subcontinent and the Arabian Sea. The monsoon is caused by the seasonal reversal of strong pressure gradients between the Tibetan plateau and the southern Indian Ocean (Figure 2) (Findlater, 1974; Flohn, 1950).

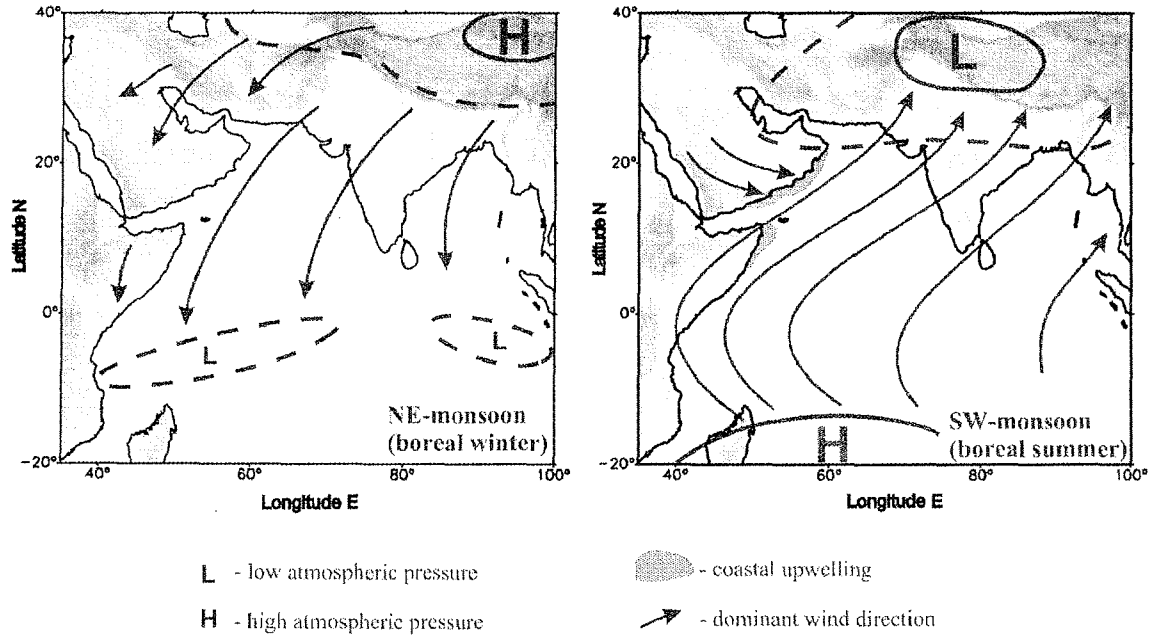

Figure 2. Map of the northern Indian Ocean and the Himalayan region showing the atmospheric monsoon circulation (after Weischet, 1988); during NE-monsoon (December-March) (left) and SW-monsoon (May-September) (right).

During northern hemisphere winter season low solar insolation and a high albedo, due to the snow cover of the Himalaya, cause an atmospheric high-pressure cell over Central Asia. At the same time an atmospheric heat low is established over the relatively warm southern Indian Ocean. The resulting pressure gradient causes the cold, dry northeast monsoon winds to blow from the Tibetan plateau over the Arabian Sea. Increasing solar insolation in spring causes atmospheric warming and rising. This results in a low-pressure center over Asia and a reversal of the atmospheric circulation during boreal summer. From May to September the summer monsoon establishes and strong winds blow from the southwest over the Indian Ocean along the coasts of Africa and Arabia. The SW-monsoon circulation transports moist air from the Indian Ocean to the Asian continent and releases large amounts of latent heat

over the Himalayan, causing a reinforcement of SW-monsoon winds. Because the monsoon dynamic mainly depends on the annual insolation cycle, the end of the SW-monsoon is marked by the decrease of northern hemisphere insolation in autumn.

2.2 Ocean circulation setting in the Arabian Sea

Because of the landmasses forming the northern boundary of the Arabian Sea the oceanographic circulation and the water exchange in the Arabian Sea are strongly different from those in other ocean basins. The major water exchange takes place with the southern Indian Ocean and to lower extents with the Red Sea and the Persian Gulf.

The surface circulation is strongly affected by the variability of the atmospheric monsoon circulation, which is responsible for a seasonal reversal of the oceanographic current system in the Arabian Sea (Figure 3a, b). A subtropical gyre, comparable to the Atlantic Ocean is not well defined during NE-monsoon season and there is only a little net transport of surface water to the north (Tomczak and Godfrey, 1994). Low-saline water is transported from the Bay of Bengal northwestward along the Indian shelf from early November to January against the prevailing NE-monsoon wind direction. The Somali current responds quickly to the onset of the SW-monsoon winds in April and the East Arabian current, its northward continuation, is fully established by the mid of May. Initiated by SW-monsoon winds, the Somali and East Arabian currents, the SW-monsoon current, and the South-Equatorial current form a strong anticyclonic gyre in the Indian Ocean north of 10°S (Wyrtki, 1973). During the transitions between the two monsoon seasons (March-April and October-November) the circulation is less well defined.

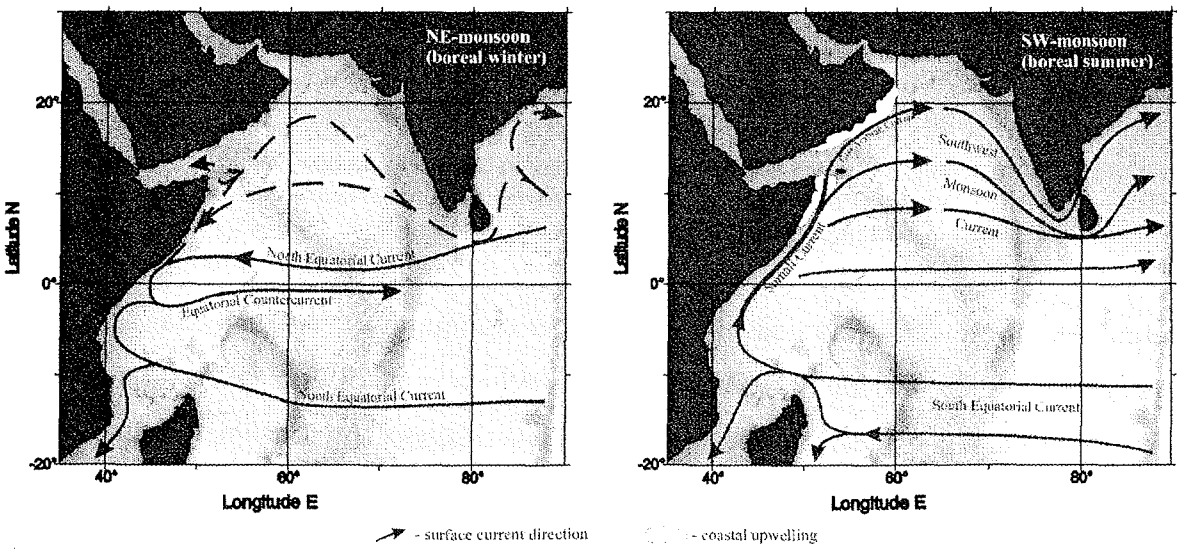

Figure 3. Map of the Arabian Sea showing the main ocean circulation patterns (after Tomczak and Godfrey, 1994); during NE-monsoon period (December-March) (left) and SW-monsoon period (May-September) (right).

2.3 Productivity and upwelling in the northwestern Arabian Sea

The main hydrographic feature of the monsoon circulation is the strong upwelling along the coasts of Somalia and Arabia from May to September. Upwelling owes its existence to the wind field, the oceanographic current system and the Coriolis force producing an offshore transport within the Ekman layer (Figure 4). While upwelling occurs cold, nutrient rich subsurface water rises into the photic zone. Productivity reaches its annual maximum, and about 70 % of biogenic sediments are deposited during summer upwelling (Smith et al., 1998). Another remarkable feature of the Arabian Sea upwelling is that the annual sea surface temperature maximum does not occurs in summer, but during the spring transition from the NE- to the SW-monsoon. The seawater temperatures are lowered by about 5°C during upwelling (Wyrtki, 1973).

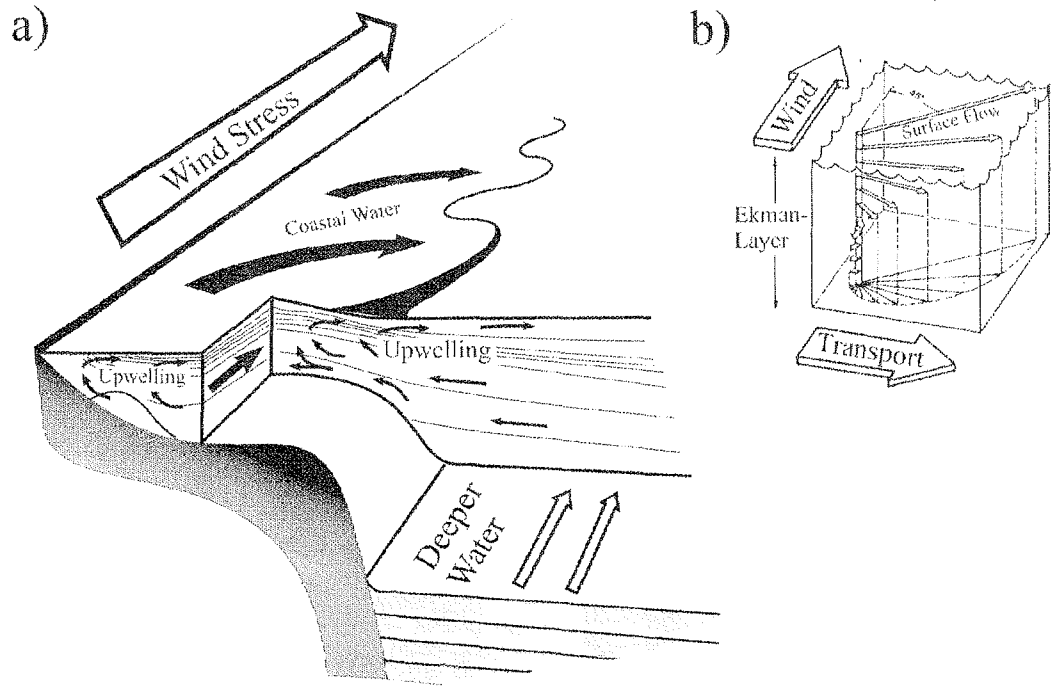

Figure 4. Schematic diagrams of the upwelling system off Oman; **a)** upwelling circulation during SW-monsoon (after Hart and Currie, 1960); **b)** Ekman pumping in the northern hemispher (Arntz and Fahrbach, 1991). The direction of the integrated mass transport within the Ekman layer is 90° to the right (northern hemisphere) versus the prevailing wind direction.

During the inter-monsoon periods the upper water column of the Arabian Sea is generally stratified and can be considered as oligothrophic (Jochem et al., 1993; Owens et al., 1993). The winter season is generally associated with low primary production, except for the northern area of the Arabian Sea where cold NE-monsoon winds produce a convective overturn, and winter blooms can occur in the coastal areas of Yemen and Oman (Banse and McClain, 1986; Shetye et al., 1991).

2.4 Modern variations of monsoon climate

Although the general Indian Monsoon circulation pattern shows a remarkable regularity from year to year, there are important interannual variations in the amount and the spatial distribution of monsoon rainfall as well as in the strength, the duration and the onset of the monsoon periods. A widely used term of modern monsoon intensity is the All-India rainfall Index (AIRI), a measure of the total summer rainfall over India (Mooley and Parthasarathy, 1984). The AIRI identifies decades with higher and lower interannual variability superimposed on multidecadal changes of wet and dry periods between 1871 and 1993, with a higher variability of the Indian rainfall during dry periods. Insolation is the outstanding mechanism driving the modern circulation of the Indian Monsoon. Under present conditions insolation is almost constant from year to year and does not explain the large interannual variability of the monsoon (Clemens et al., 1996). The identification and the quantification of additional controlling mechanisms is a major purpose for a better understanding of monsoon dynamics. Direct observations of the modern atmospheric and hydrographic situations cover the present variations of the past 3-4 decades. Furthermore, the recent investigations help to calibrate climate proxy indicators that allow carrying out examinations on longer time scales.

Several mechanisms were identified affecting monsoon dynamics. The sea surface temperature anomalies of the subtropical Indian Ocean have an important impact on the distribution and the effect of the monsoon convection (Clemens et al., 1991). Correlations between rainfall anomalies reveal the monsoon as internal part of the Southern Oscillation and confirm that El Niño significantly influences the Indian Summer Monsoon (e.g. Webster et al., 1998). In essence, drought years over India are often associated with anomalous warm sea surface temperatures in the equatorial eastern and central Pacific Ocean (El Niño), while exceedingly wet years are related to "cold" events (La Niña). Another important processes associated with the monsoon circulation might be the snow cover over Eurasia affecting the land surface albedo. The potential link between monsoon strength and the snow cover over Eurasia is still discussed. Some model results suggest a negative correlation between Himalayan snow cover and monsoon rainfall. Most of these connections have been found also in geological records (Clemens et al., 1991; Sirocko, 1996).

2.5 Past variations of monsoon climate

The view into the past by studying geological records of climate history is one important way to identify physical key processes affecting monsoon climate. Paleoclimatic examinations of monsoon climate are focused on time series of marine sediments providing a broad space of parameter related to ocean and monsoon history (e.g. dust and pollen particles transported by monsoonal winds; ocean sea surface temperatures, marine productivity).

With respect to marine geological tracers in sediments, SW-monsoon winds in the Arabian Sea carry lithogenic dust into the ocean, and they induce upwelling of cold nutrient rich subsurface waters, which is accompanied by enhanced productivity. Hence, tracers related to upwelling productivity or to monsoonal wind strength, like the relative abundance of the planktic foraminifera *G. bulloides*, the lithogenic grain size component of marine sediments, and pollen records allow identifying strong and weak monsoon periods (Anderson and Prell, 1991; Clemens et al., 1991; Prell and Van Campo, 1986). Recent studies suggest that SW-monsoon winds and coastal upwelling were generally weaker during glacial periods. Spectral analyses of monsoon tracers indicate a dominant sensitivity to orbital forcing at the obliquity and the precession periods (41,000 yr and 23,000 yr) as well as in the sub Milankovitch domain near the half precession cycle (Clemens et al., 1996). Temporal lags between monsoon tracers and orbital parameters indicate that there is a delayed response of the monsoon strength to its forcing mechanisms. Within the precession cycle the maximum of the SW-monsoon intensity lags the maximum of the northern hemisphere insolation by about 9 kyr. Hence, besides solar radiation additional forcing mechanisms of the monsoon must be taken into consideration. Stronger Arabian Sea SW-monsoon winds in the past were generally associated with increased summer radiation over central Asia, reduced global ice masses, and enhanced latent heat transport from the southern Indian Ocean (e.g. Anderson and Prell, 1991, 1993; Clemens et al., 1991; Sirocko et al, 1996).

3. Focus of this study

Strong seasonal changes related to atmospheric forcing mechanisms, and discrete water exchange with other ocean basins make the north-western Arabian Sea to an ideal area to study the coupling of atmospheric and oceanic regimes in the climate system. Yet, the present and the past dynamics and control mechanisms of the Indian Monsoon are not completely understood. For investigations of monsoon history forcing mechanisms must be identified and reconstructed by proxies. As discussed above several climate proxies may be used for studying past monsoons and for inferring monsoon dynamics. Most proxies are influenced by secondary mechanisms. The first step before applying proxies is their calibration and the assessment of their application on geological time scales.

The focus of this thesis is the use of carbon isotope compositions of planktic foraminifera as tracer to reconstruct water mass properties and productivity in the Arabian Sea and to provide a better understanding of monsoon climate. The results are used to infer changes in the monsoon system over the past 307 kyr. As a prerequisite the modern relationships between the carbon isotope composition of seawater, nutrient concentrations, and productivity were evaluated and used for the calibration of foraminiferal $\delta^{13}C$. This main section of this thesis is incorporated in Part II.

Part II contains four manuscripts submitted to or already published in reviewed scientific journals and books.

1. The South Atlantic Carbon Isotope Record of Planktic Foraminifera

Published as:
Mulitza, S., H. Arz, S. Kemle-von Mücke, C. Moos, H.-S. Niebler, J. Pätzold, and M. Segl, 1999, The South Atlantic Carbon Isotope Record of Planktic Foraminifera, in G. Fischer, and G. Wefer, eds., Use Of Proxies In Paleoceanography, Berlin, New York, Springer, p. 427-445.

This manuscript reviews the general use of carbon isotopes in paleoceanography and underlines the role of the oceans in the global carbon cycle. The effects controlling the isotope fractionation between the carbon reservoirs and the recent distribution of $\delta^{13}C_{\Sigma CO2}$ in the world oceans are discussed. For paleoceanographic reconstructions additional mechanisms referring to $\delta^{13}C$ in planktic foraminiferal tests are taken into consideration and for several modern foraminiferal species deviations to the $\delta^{13}C$ of inorganic calcite precipitated in isotope equilibrium are derived. Additionally examples for the late quaternary period are given for global $\delta^{13}C$ variations as well as for different hydrographic environments of the South Atlantic Ocean.

2. Seasonal and decadal changes in carbon isotope composition of the north-western Arabian Sea

Submitted as:
Moos, C. A., G.-J. A. Brummer, G. Ganssen, W. Helder, A. Hupe, R. Kloosterhuis, R. Lendt, R. R. Schneider, and G. Wefer, Seasonal and decadal changes in carbon isotope composition of the north western Arabian Sea, Deep-Sea Research I, submitted 1999.

The article discusses modern changes of carbon isotopes of dissolved inorganic carbon ($\delta^{13}C_{\Sigma CO2}$), based on spatial, seasonal and decadal hydrographic observations and isotope measurements in the northwestern Arabian Sea. The manuscript outlines hydrographic and seawater isotopes of both monsoon seasons. All measured water mass properties display the stratification of the water column during NE-monsoon and the dynamic and the effects that occur during upwelling. To determine the $\delta^{13}C_{\Sigma CO2}$/nutrient relationships additionally the stoichiometry of Arabian Sea waters and the effects of denitrification within the oxygen minimum zone are treated. The results allow a comparison of modern $\delta^{13}C_{\Sigma CO2}$ data with former values of GEOSECS and provide an opportunity to investigate the influence of anthropogenic CO_2 to Arabian Sea waters.

3. Stable isotopes in planktic foraminifera recording monsoonal upwelling in the northwest Arabian Sea

Submitted as:
Moos, C. A., R. Schiebel, R. R. Schneider, and G. Wefer, Stable isotopes in planktic foraminifera recording monsoonal upwelling in the northwest Arabian Sea, Marine Micropaleontology, submitted 2000.

This manuscript is focused on a calibration of carbon isotopes in recent planktic foraminifera and an assignment of different species to their preferred depth habitat and season of growth. For a better understanding of foraminiferal $\delta^{13}C$ signals, plankton tow and surface sediment samples off Arabia were analyzed and compared with the seasonal hydrographic conditions and the carbon isotope variations of seawater. The results allow assigning the two foraminiferal species *G. ruber* (w) and *N. dutertrei* to seasonal hydrographic end member of the two monsoon seasons. Furthermore, the isotope results of *Globigerinoides ruber* (w) and *Neogloboquadrina dutertrei* were used to evaluate variations of upwelling intensity and seasonal changes of nutrient gradients along the Arabian coast.

4. Carbon isotopes of planktic foraminifera recording nutrient and productivity variations in the northwest Arabian Sea during the past 300,000 yr

To be submitted as:
Moos, C. A., D. Budziak, R. R. Schneider, and G. Wefer, Carbon isotopes of planktic foraminifera recording nutrient and productivity variations in the northwestern Arabian Sea during the past 300,000 yr, Geology, submitted 2000.

The main objective of this thesis is to investigate upwelling history and paleo-nutrient gradients in the monsoonal upwelling area off Oman. Carbon isotopes of the planktic foraminifera *G. ruber* (w) and *N. dutertrei* allow a reconstruction of the nutrient availability in Arabian Sea surface water masses during the past 307 kyr. Cross-spectral analyzes between planktic foraminiferal $\delta^{13}C$ time series and monsoon and productivity tracers reveal general examinations about cyclical changes of environmental settings in the Arabian Sea. The comparison of the geological records indicates that upwelling was always strong enough to transport the nutrients, available in the upper water column, to the sea surface. Thus, productivity variations off Oman are mainly affected by the nutrient availability of the water masses affected by upwelling, but upwelling intensity itself seems to be of lower importance.

Part II - Publications

1. The South Atlantic Carbon Isotope Record of Planktic Foraminifera

(published in " G. Fischer and G. Wefer, 1999, Use Of Proxies In Paleoceanography")

S. Mulitza[1*], H. Arz[1], S. Kemle-von Mücke[1], C. Moos[1], H.-S. Niebler[1,2], J. Pätzold[1] and M. Segl[1]

[1] *Universität Bremen, Fachbereich Geowissenschaften, Postfach 33 04 40, D-28334 Bremen, Germany*
[2] *Alfred-Wegener-Institut für Polar- und Meeresforschung, Postfach 12 01 61, D-27515 Bremerhaven, Germany*
**corresponding author (e-mail): smul@palmod.uni-bremen.de*

Abstract: We reviewed the paleoceanographic application of the carbon isotope composition of planktic foraminifera. Major controls on the distribution of $\delta^{13}C$ of dissolved CO_2 ($\delta^{13}C_{\Sigma CO2}$) in the modern ocean are photosynthesis-respiration cycle, isotopic fractionation during air-sea exchange, and circulation. The carbon isotope composition of surface waters is not recorded without perturbations by planktic foraminifera. Besides $\delta^{13}C_{\Sigma CO2}$ of the surrounding seawater, the $\delta^{13}C$ composition of planktic foraminifera is affected by vital effects, the water depth of calcification and postdepositional dissolution. We compared several high-resolution (>10cm/ka) carbon isotope records from the Southern Ocean, the Benguela upwelling system, and the tropical Atlantic. In the Southern Ocean, carbon isotope values are about 1.2 ‰ lower during the LGM and up to 1.7 ‰ lower during the last deglaciation, when compared to the Holocene. These depletions might be explained with a combination of a subsurface nutrient enrichment and reduced air-sea exchange due to an increased stratification of surface waters. In the Benguela Upwelling system, waters originating in the south are upwelled. While the deglacial minimum is transferred and recorded in its full extent in the $\delta^{13}C$ record of *Globigerina bulloides*, glacial values show only little changes. This might suggest, that the lower glacial $\delta^{13}C$ values of high-latitude surface waters are not upwelled off Namibia, or that *G. bulloides* records post-upwelling conditions, when increased seasonal production has already increased surface-water $\delta^{13}C$. Synchronous to the $\delta^{13}C$ depletions in high latitudes, low $\delta^{13}C$ values were recorded in *Globigerinoides sacculifer* during the LGM and during the last deglaciation in the nutrient-depleted western equatorial Atlantic. Hence, part of the glacial-interglacial variability presumably transferred from high to low latitudes seems to be related to changes in thermodynamic fractionation. The variability in $\delta^{13}C$ is lowest in the northernmost core M35003-4 from the eastern Caribbean, implying that the Antarctic Intermediate Water might have acted as a conduit to transfer the deglacial minimum to tropical surface waters.

Introduction

During the Quaternary the climate of our planet underwent a succession of cold periods in which large parts of the northern hemisphere were covered by ice. Most scientists believe that variations in the distribution of insolation are the major driving force for the ice ages (Hays et al. 1976; Imbrie et al. 1984). However, insolation alone cannot explain the amplitude and hemispheric synchronism of the temperature changes (Short et al. 1991). Hence, additional feedback mechanisms must play an important role. Ice-core studies have shown that part of the glacial cooling was presumably due to lower atmospheric CO_2 contents. The origin of the glacial CO_2 decrease must lie in the ocean, because it is the largest active carbon reservoir and a key component as a sink and a transfer agent for the motion of carbon through the world system. Consequently, in order to understand global climate

From FISCHER G, WEFER G (eds), 1999, *Use of Proxies in Paleoceanography: Examples from the South Atlantic.* Springer-Verlag Berlin Heidelberg, pp 427-445

changes, it is necessary to understand the oceanic carbon system. An important tracer of the carbon system is the ratio of the stable carbon isotopes $^{13}C/^{12}C$. Through the fractionation effects involved in the transfer of carbon between reservoirs, this ratio yields important information regarding the environment from which a sample comes. Like many marine organisms, single-celled planktic foraminifera use the dissolved carbon to build their calcium carbonate skeletons. For this reason, and because they are widely distributed on the sea floor, planktic foraminifera have the potential to preserve the carbon isotope ratios of ancient water masses in their shells and to provide information about the past oceanic carbon system and its role in climate change. This paper reviews the present-day distribution of $\delta^{13}C$ in the ocean, the recording of $\delta^{13}C$ by planktic foraminifera and the late Quaternary carbon isotope record of planktic foraminifera in the tropical and South Atlantic.

Carbon Isotopes

Isotopes are variations of an element containing different numbers of neutrons. There are three different carbon isotopes: ^{12}C, ^{13}C and ^{14}C. ^{12}C is the most abundant, while ^{13}C and ^{14}C only comprise 1% and 10^{-10} % of the total carbon, respectively. Our study concentrates on the two stable isotopes ^{12}C and ^{13}C. Due to the different atomic weight, fractionation during the geochemical transfer of carbon produces variations in the distribution of the isotopes of carbon. Craig (1953) first identified that certain biochemical processes alter the equilibrium between the carbon isotopes. Some processes, such as photosynthesis, favor one isotope over another, so after photosynthesis, the isotope ^{13}C is depleted by 1.8% in comparison to its natural ratios in the atmosphere (Harkness 1979). Conversely, the inorganic carbon dissolved in the oceans is generally enriched by 0.7% in ^{13}C relative to atmospheric carbon dioxide. The isotopic composition of the sample being measured is expressed as delta $\delta^{13}C$:

$$\delta^{13}C(‰) = \left[\frac{(^{13}C/^{12}C)_{\text{sample}} - (^{13}C/^{12}C)_{\text{standard}}}{(^{13}C/^{12}C)_{\text{standard}}} \right] \cdot 1000$$

which represents the parts per thousand difference (per mil) between the sample $^{13}C/^{12}C$ ratio and that of the international PDB standard carbonate. PDB refers to the Cretaceous belemnite formation at Peedee in South Carolina, USA. This nomenclature has recently been changed to VPDB (Coplen 1996). The basic principles of mass spectrometry and the preparation of carbonate samples are described by Hoefs (1987). A good description for the preparation of CO_2 from water samples is given by Bard et al. (1987).

Distribution and Controls of Carbon Isotopes in the Ocean

$\delta^{13}C_{\Sigma CO2}$ is related to nutrient cycles and biological productivity. Plants preferentially fix ^{12}C in organic matter, leaving the surface ocean enriched in ^{13}C and depleted in nutrients. In deeper waters organic matter is remineralized, lowering the $\delta^{13}C$ of the total dissolved CO_2. Along with this decrease in ^{13}C, nutrient concentrations increase and oxygen concentrations decrease. For this reason, the $^{13}C/^{12}C$ ratio in the ocean is inversely correlated to the nutrient concentration. According to Broecker and Peng (1982), the proportionality constant of this relationship can be approximated by:

$$\Delta\delta^{13}C = \Delta\delta^{13}C_{\text{plant - }\Sigma CO2} \frac{C/N_{\text{organic matter}}}{\Sigma CO_2{}_{\text{mean ocean}}} \cdot \Delta NO_3^-$$

$\Delta\delta^{13}C_{\text{plant-}\Sigma CO2}$ is about -20 ‰, the C/N ratio is about 7 and the mean ΣCO_2 content is 2200 µmol/kg. Hence the slope of the relationship between $\Delta\delta^{13}C$ and ΔNO_3^- is about 0.064 ‰/µmol/kg. This value agrees well with the observed slope (Kroopnick 1985), suggesting that nutrient-cycling is an important control for the $\delta^{13}C_{\Sigma CO2}$ distribution in the ocean. Besides the photosynthesis-respiration cycle, the distribution of ^{13}C is also influenced by advective and diffusive transport processes within the ocean. Fig. 1b shows the distribution of $\delta^{13}C_{\Sigma CO2}$ on a transect through the Atlantic (GEOSECS, Kroopnick 1985). The major water masses can be distinguished in this plot. A tongue of isotopically heavy and nutrient-poor NADW extends from the regions of deep water formation in the North

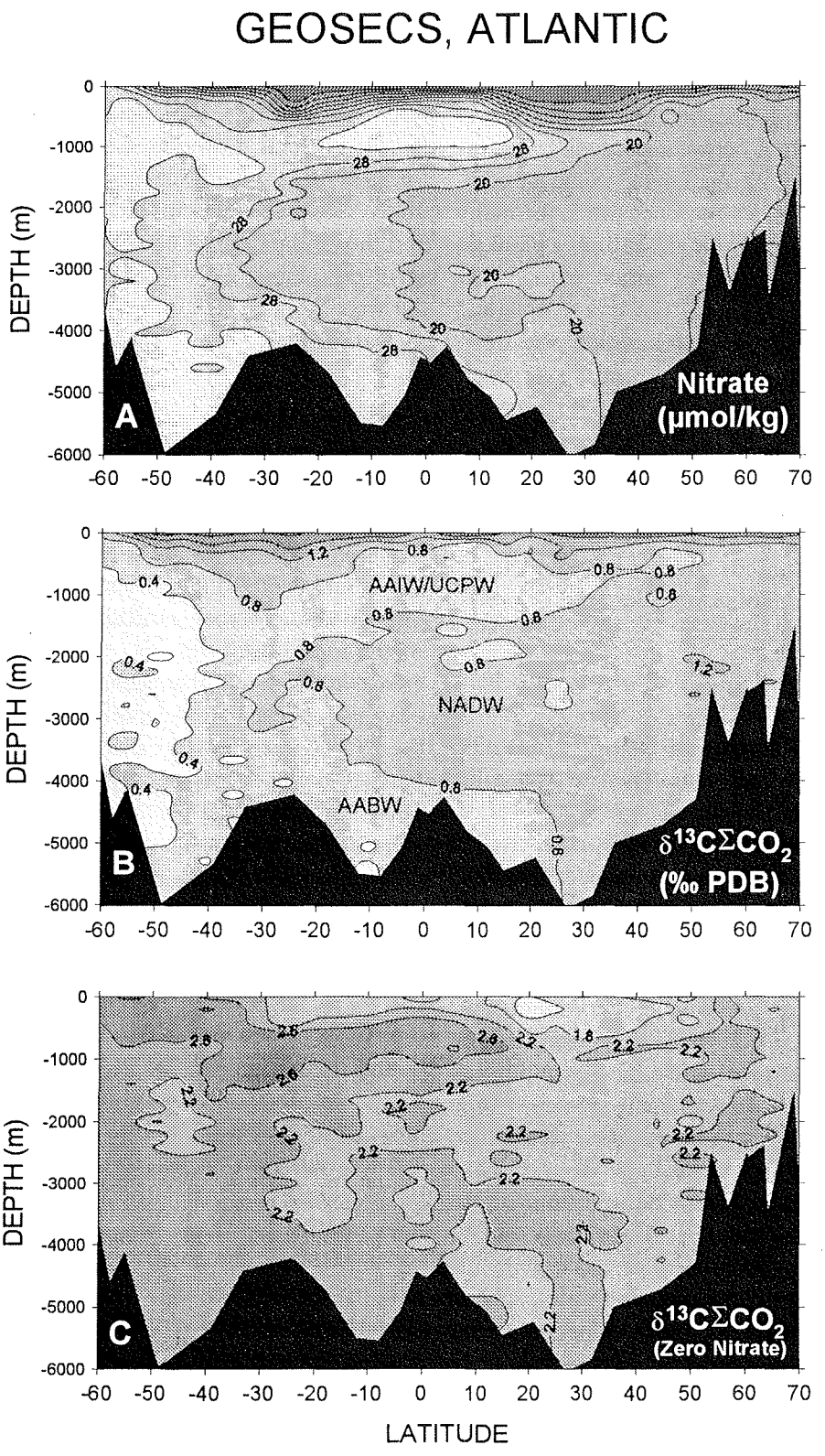

Fig. 1. **(a)** GEOSECS nitrate concentrations; **(b)** GEOSECS carbon isotope composition of dissolved CO_2; **(c)** $\delta^{13}C$ corrected for nutrient components.

Atlantic into the South Atlantic. This water mass is truncated by isotopically light and nutrient-rich bottom and intermediate water masses of Antarctic origin (Fig. 1a,b).

A second reason for $\delta^{13}C_{\Sigma CO2}$ variations in the ocean comes from the fact that carbon circulates in the atmosphere as well. Isotopic fractionation occurs during the exchange of CO_2 between atmosphere and ocean, because ^{13}C is more soluble than ^{12}C. The extent of this fractionation depends on sea-surface temperature, but also on the CO_2 exchange rate and surface-water residence times. Seawater completely equilibrated with the atmosphere at 0°C should have a $\delta^{13}C$ value which is about 3‰ higher than the same seawater at 25°C (Mook et al. 1974; Siegenthaler and Münnich 1981).

To illustrate the effects of air-sea exchange, we normalized the GEOSECS $\delta^{13}C_{\Sigma CO2}$ values to zero nitrate (Fig. 1c). This was done by subtracting 0.064 ‰ from $\delta^{13}C_{\Sigma CO2}$ for every µmol/kg nitrate. This procedure should remove the effect of nutrient-cycling from the $\delta^{13}C_{\Sigma CO2}$ values. A tongue of thermodynamically enriched water descends from the Antarctic Polar Front to the North, coinciding with the Antarctic Intermediate Water (AAIW) and the Upper Circumpolar Water (UCPW) (Fig. 1c). This enrichment is due to higher gas-exchange rates at colder temperatures close to the Polar Front, where intermediate waters are formed (Charles and Fairbanks 1990). In contrast, the NADW is labeled by a relative depletion, presumably because equilibration occurs at warmer temperatures before cooling and sinking processes (Lynch-Stieglitz et al. 1995). This demonstrates that the thermodynamic influence differs among water masses and is a significant source of variability. It must be noted, however, that the correction to zero nitrate, employed here, does not account for regional variations in the Redfield Ratio and in the isotopic composition of organic matter. But, as pointed out by Charles et al. (1993), this would not change the most important features in Fig. 1c dramatically.

Due to the addition of isotopically light fossil fuel and forest soil CO_2, the $\delta^{13}C$ value of the atmosphere has decreased from -6.4 ‰ to -7.8 ‰ and is further decreasing (Friedli et al. 1986). As the CO_2 of the surface water exchanges with the atmosphere the $\delta^{13}C_{\Sigma CO2}$ value of the surface water also decreased since pre-industrial time. This process is known as the "^{13}C Suess-effect".

Another source of variations for marine $\delta^{13}C_{\Sigma CO2}$ is freshwater runoff. Since most of the CO_2 dissolved in groundwater derives from organic matter degradation, river water has very low $\delta^{13}C$. In the surface waters of the Guinea Basin, admixture of Niger freshwater results in a linear relationship between salinity and $\delta^{13}C_{\Sigma CO2}$ (Fig. 2, Duplessy 1972). This relationship to salinity has been used to reconstruct the Niger freshwater supply (Pastouret et al. 1978).

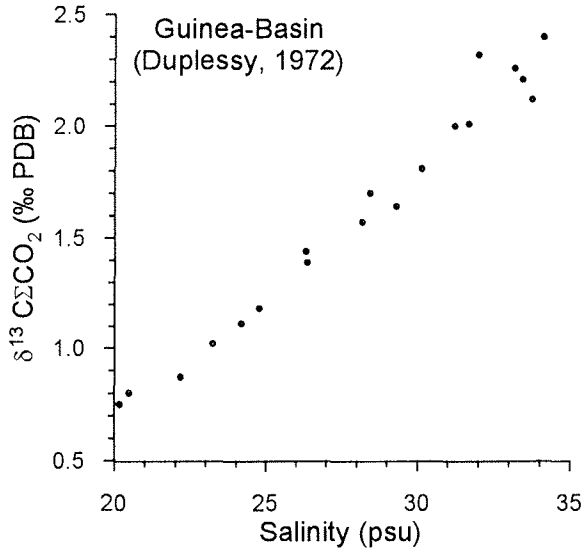

Fig. 2. Relationship between surface water $\delta^{13}C_{\Sigma CO2}$ and salinity in the Guinea Basin due to admixture of Niger freshwater. Data are from Duplessy (1972).

Recording of $\delta^{13}C$ by Planktic Foraminifera

Disequilibrium Effects

Planktic foraminifera are the primary tool for the reconstruction of the paleo-carbon isotopic composition of surface waters. In order to use foraminiferal $\delta^{13}C$ as a proxy for $\delta^{13}C_{\Sigma CO2}$, a first requirement is that foraminifera secrete their calcite in equilibrium or have predictable offsets. A number of experimental studies used inorganic car-

bonate precipitates to examine the carbon isotopic fractionation as a function of carbonate mineralogy, temperature and precipitation rate (Emrich et al. 1970, Turner 1982, Romanek et al. 1992). Emrich et al. (1970) suggested that the fractionation between precipitating calcite and surrounding bicarbonate increases by 0.035‰ per degree temperature increase. In contrast, a recent study of Romanek et al. (1992) indicates that the $\delta^{13}C$ enrichment factor of calcite is 1‰ (within the experimental error of ± 0.2‰) between 10 and 40°C and that the temperature dependence observed by Emrich et al. (1970) might reflect an increase in the proportion of aragonite in their samples. Following Romanek et al. (1992) the best estimate for equilibrum calcification in waters warmer than 10°C might be:

$$\delta^{13}C_{equilibrium} = \delta^{13}C_{seawater} + 1.0‰$$

Hence, a foraminiferal shell calcified in equilibrium should be 1‰ heavier than the dissolved CO_2 of the surrounding seawater. To evaluate the ability of foraminifera to record the seawater carbon isotopic composition, researchers normally compare the carbon isotopic composition of foraminiferal shells to the predicted carbon isotopic composition of inorganic calcite in equilibrium. Combined plankton tow holes and CTD casts provide the opportunity to compare the $\delta^{13}C$ of naturally grown foraminifera directly to that of the dissolved inorganic carbon in equilibrium. Here, we show data from plankton tow GeoB 1402-2 obtained from the eastern equatorial Atlantic (Fig. 3). First, we determined the position of calcification by assuming that $\delta^{18}O$ is close to equilibrium (Ortiz et al. 1996). Then, $\delta^{13}C_{\Sigma CO2}$ of the ambient seawater was calculated on the basis of its relationship to apparent oxygen utilization (AOU) (Kroopnick 1985). Fig. 4 shows plots of $\delta^{13}C_{equilibrium}$ vs. the $\delta^{13}C$ of the planktic species *Neogloboquadrina dutertrei*, *Puleniatina obliquiloculata* and *Globigerinoides sacculifer* (left panel) and plots of the deviation from the equilibrium vs. ambient temperature measured with a CTD-probe at the tow site (right panel). All three foraminiferal species are too light with respect to equilibrium calcite. However, *N. dutertrei* shows a constant offset of about 0.5 ‰ to the $\delta^{13}C_{\Sigma CO2}$ of the ambient seawater and therefore seems to be a reliable recorder of the $\delta^{13}C_{\Sigma CO2}$. In contrast, *P. obliquiloculata* and *G. sacculifer* exhibit vital effects up to 2.4 ‰ and no correlation to $\delta^{13}C_{\Sigma CO2}$. The carbon isotope disequilibrium of *P. obliquiloculata* increases with increasing temperature (Fig. 4). The $\delta^{13}C$ of *G. sacculifer* does not show any correlation either to $\delta^{13}C_{\Sigma CO2}$ or temperature. Apparently, all *G. sacculifer* were grown at the same $\delta^{13}C_{\Sigma CO2}$, but differ up to 1.8 ‰ from each other. The observed offsets must be due to fractionation processes during the uptake of carbon into calcite, the so-called vital effects. Generally three major types of vital effects can be distinguished (Ravelo and Fairbanks 1995): (1) incorporation of light metabolic carbon, (2) photosynthetic utilization of light carbon by symbionts which increases the available ^{13}C for calcification, (3) kinetic fractionation effects related to biological processes.

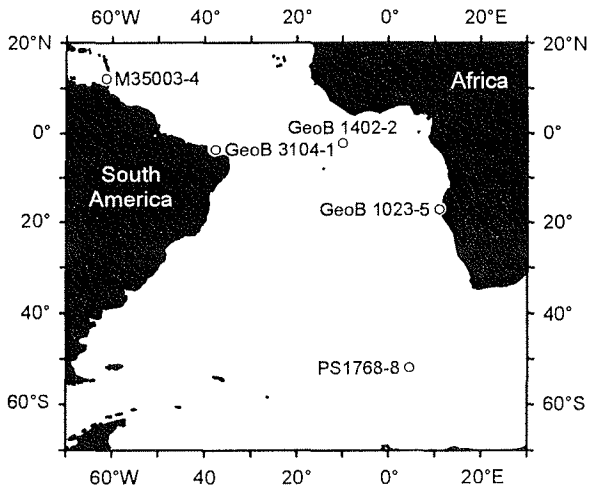

Fig. 3. Geographical positions of the examined sites.

Foraminifera have been extensively investigated with regard to metabolic effects on skeletal $\delta^{13}C$. Many studies documented the effect of low metabolic CO_2 on the $\delta^{13}C$ of foraminiferal carbonate (Ravelo and Fairbanks 1995 and references therein). These studies show that the carbon pool used for carbonate crystallization may contain a

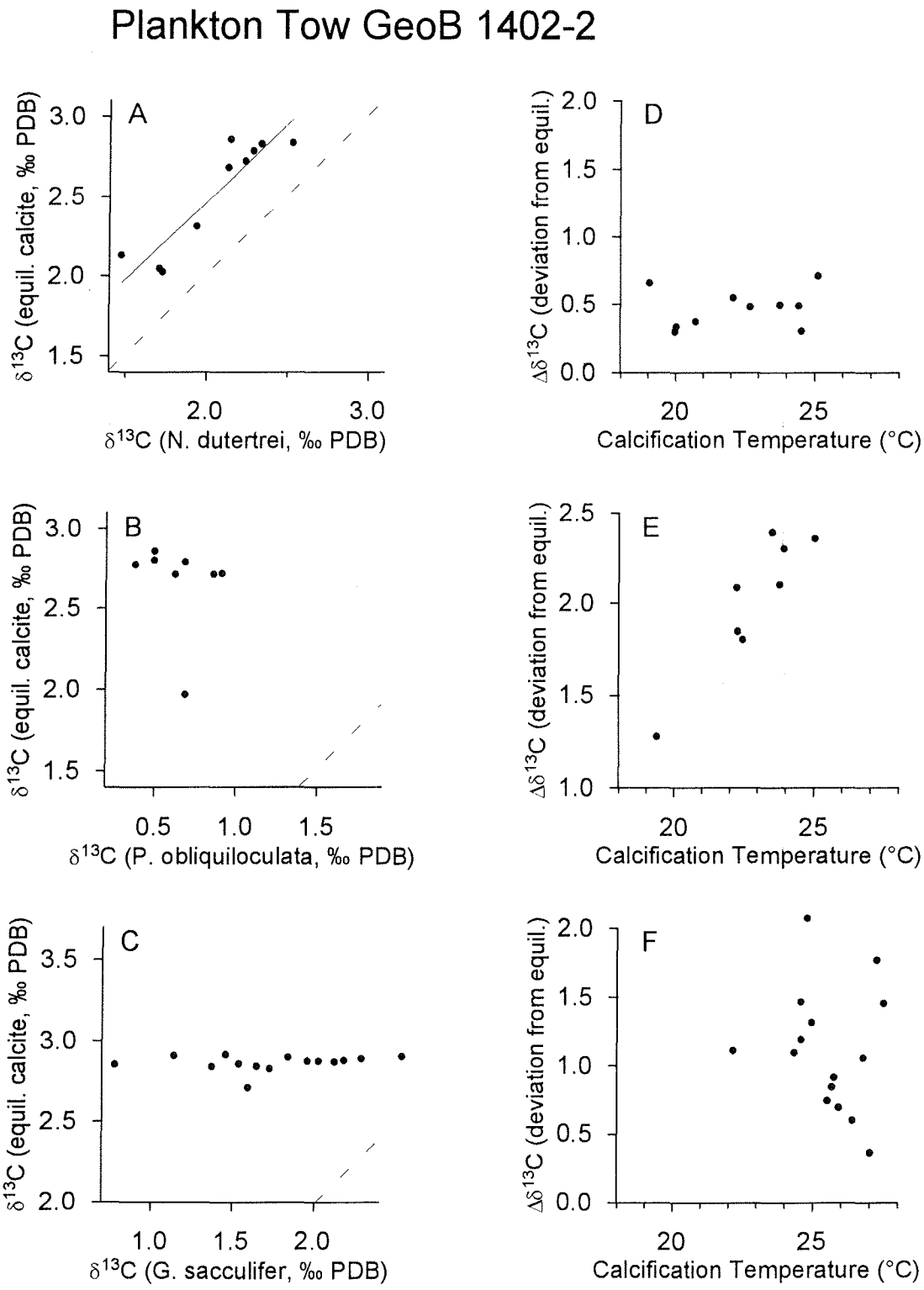

Fig. 4. (a-c) $\delta^{13}C$ of *N. dutertrei*, *P. obliquiloculata* and *G. sacculifer* versus $\delta^{13}C_{\Sigma CO2}$ in the depth of calcification. Depth of calcification was calculated from $\delta^{18}O$. $\delta^{13}C_{\Sigma CO2}$ was calculated from apparent oxygen utilization (AOU). **(d-f)** Deviation of foraminiferal $\delta^{13}C$ from equilibrium versus calcification temperature. Temperature, salinity and oxygen concentration were measured at the trap site with a CTD-Probe.

considerable amount of respired light carbon. Spero and Lea (1996) concluded from a feeding experiment that the planktic foraminifera *Globigerina bulloides* contains about 8% respired CO_2. If we assume an organic carbon composition of -20‰ and a $\delta^{13}C_{\Sigma CO2}$ of 1.5, we can easily shift the foraminiferal $\delta^{13}C$ by more than -1.8 ‰ relative to equilibrium calcite. Therefore, the incorporation of metabolic carbon into the shells could be one explanation for the observed vital effects.

Apparently, the deviations from equilibrium values are temperature-dependent in *P. obliquiloculata*. The isotopic disequilibrium in *P. obliquiloculata* increases with increasing temperature. This strongly suggests that, in this species, the respiration rate and hence the amount of incorporated metabolic CO_2 increases with increasing temperature as previously hypothesized for other species (Ravelo and Fairbanks 1995; Ortiz et al. 1996; Spero and Lea 1996). Interestingly, the slope of $\Delta\delta^{13}C$:T in *P. obliquiloculata* is very close to that observed by Ortiz et al. (1996) using different species. However, the shells of *N. dutertrei* were also calcified over a comparable large temperature range and exhibit no temperature-dependent offset. This shows that the concept of temperature-dependent "metabolic" vital effects does not hold for all species.

Besides metabolic effects, fractionation can also be due to photosynthesis. Some spinose foraminifera (e.g. *G. sacculifer*) harbor symbiontic algae. Photosynthesis of symbiontic algae preferentially utilizes ^{12}C and should leave the ambient environment enriched in $\delta^{13}C$. Therefore, symbiont activity increases the shell $\delta^{13}C$. The photosynthetic effect on the $\delta^{13}C$ of *G. sacculifer* has been demonstrated in culture experiments (Spero and Lea 1993). Chambers secreted under higher light levels were enriched by 1.1 to 1.7 ‰ relative to chambers grown in the dark. As small tests usually grow under lower light levels than large tests (Spero and Lea 1993) and because symbiont density increases with increasing chamber irradiance, *G. sacculifer* shows a pronounced increase in $\delta^{13}C$ related to size (Fig. 5). However, as small *G. sacculifer* are lighter than equilibrium calcite, another process must be invoked. In the culture experiments of Spero and Lea (1993) smallest *G. sacculifer*, grown under low light levels, deviate by about -0.4 ‰ from $\delta^{13}C_{\Sigma CO2}$ of ambient seawater and hence by about -1.4 ‰ from equilibrium calcite. This is comparable to the deviation found in small *G. sacculifer* from plankton tow GeoB 1402-2. It seems likely, that respired light carbon was incorporated into small shells. As *G. sacculifer* grows, the increasing symbiont activity shifts the carbon isotope values closer to equilibrium (Fig. 5). For paleoceanographic purposes, large individuals (>800 µm!) of symbiont bearing species with small variations in size downcore (preferably ±25 µm) gave most consistent results among different cores (Oppo and Fairbanks 1989).

Another type of vital effect is due to kinetic fractionation. Kinetic discrimination against ^{13}C and ^{18}O originates from the slow isotopic equilibration during hydration and hydroxylation reactions between CO_2 and HCO_3^- during the calcification process (McConnaughey et al. 1997). This kind of

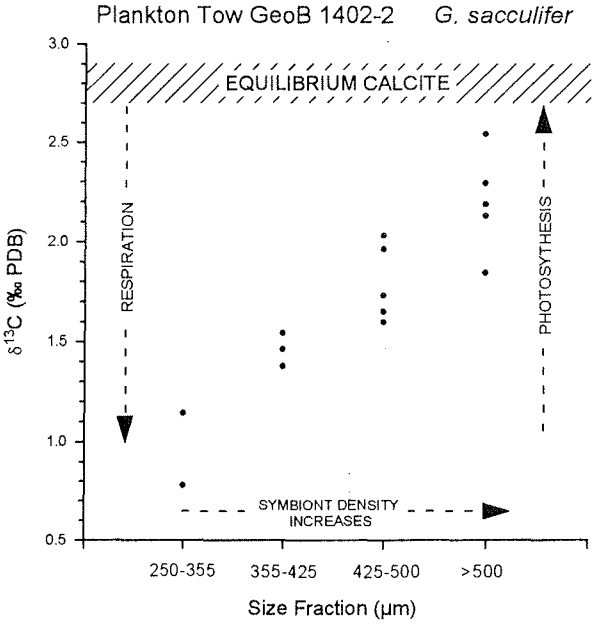

Fig. 5. $\delta^{13}C$ of *G sacculifer* versus size from multinet GeoB 1402-2. Small *G sacculifer* deviate from the equilibrium due to the uptake of light metabolic CO_2. Increase of photosynthesis and symbiont activity in larger shells increases the $\delta^{13}C$ toward equilibrium values.

fractionation tends to produce linear correlations between $\delta^{13}C$ and $\delta^{18}O$. The time for oxygen and carbon isotopic equilibration is in the order of minutes, close to the time for calcite precipitation in foraminifera (Ortiz et al. 1996). Thus, the extent of disequilibrium may be a function of the organisms' calcification rate. Another parameter possibly affecting the kinetic disequilibrium was recently discovered by Spero et al. (1997) (see also Bijma et al. this volume). They found that the $\delta^{13}C$ and $\delta^{18}O$ of foraminiferal calcite decreases with increasing seawater $[CO_3^{2-}]$. The proportional decrease in $\delta^{18}O$ and $\delta^{13}C$ also suggests a kinetic origin. The exact mechanism is still unknown.

Habitat Effects

It is clear from the last paragraph that vital effects play an important part in controlling the carbon isotope value of planktic foraminifera. In order to use the carbon isotopic composition of planktic foraminifera as a paleoceanographic tool, we must also know where and when the species under study calcified (i.e. the water depth or the season of calcification). In Fig. 6 the $\delta^{13}C$ values of *N. dutertrei* are plotted against the water depth of calcification inferred from oxygen isotopes. Depending on where calcification took place in the water column, the $\delta^{13}C$ among individual *N. dutertrei* differs up to 1 ‰. It is clear from this example, that $\delta^{13}C$ variations of *N. dutertrei* in the past could either be interpreted as a changing $\delta^{13}C_{\Sigma CO2}$ signal or as changing calcification depth. This problem is complicated by the fact that most planktic foraminifera add a considerable amount of gametogenetic calcite (also called "calcite crust") in deeper water masses. Hence, the $\delta^{13}C$ value might be a mixture of several depth levels. However, if a species is confined to a certain deep depth interval, its $\delta^{13}C$ composition might provide useful information about the carbon isotopic composition of subsurface depth levels. A good example is given by the species *Globorotalia truncatulinoides* which is a typical "thermocline-dweller" (Hemleben et al. 1985; Mulitza et al. 1997).

While plankton tows provide a regional snapshot of the isotopic composition of living planktic foraminifera, core-top measurements allow to compare the isotopic composition of a species over a range of hydrographic regimes. In Fig. 7, we contoured the $\delta^{13}C$ of thermocline-dwelling *G. truncatulinoides* from Holocene core-top samples (32°S to 10°N, Fig. 7b) and the phosphate concentration in 100 m water depth (Fig. 7a). *G. truncatulinoides* exhibits highest values in the subtropical gyre center near 30° S, whereas relatively low values occur in the tropical Atlantic and at the eastern boundary. The southwesterly directed decrease of phosphate shows distinct similarity to the carbon isotope ratios of *G. truncatulinoides*. Thus, this species might be a good recorder of thermocline nutrient levels (Mulitza et al. 1998).

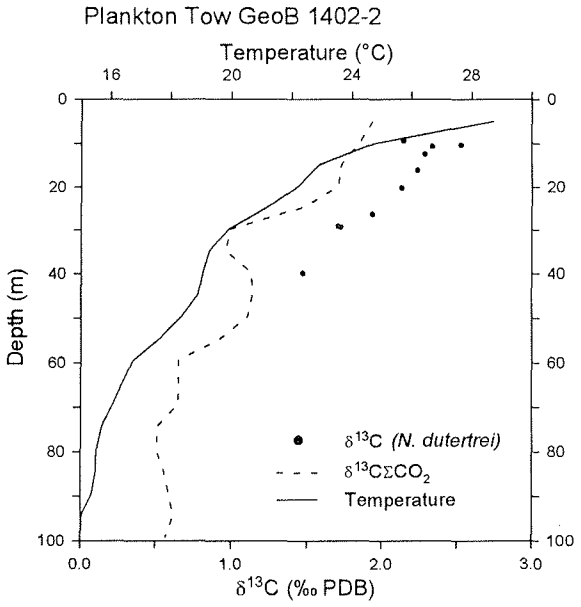

Fig. 6. Comparison of the $\delta^{13}C$ of *N. dutertrei* with the vertical distribution of $\delta^{13}C_{\Sigma CO2}$ (calculated from AOU). Depth of calcification was calculated from $\delta^{18}O$.

Dissolution Effects

In the modern ocean, carbonate dissolution increases with depth and in regions with high sedimentation rates of organic matter. Carbonate dissolution could also contribute to variations in stable carbon isotope records (Berger 1971; Savin and Douglas 1973; Shackleton and Opdyke 1976;

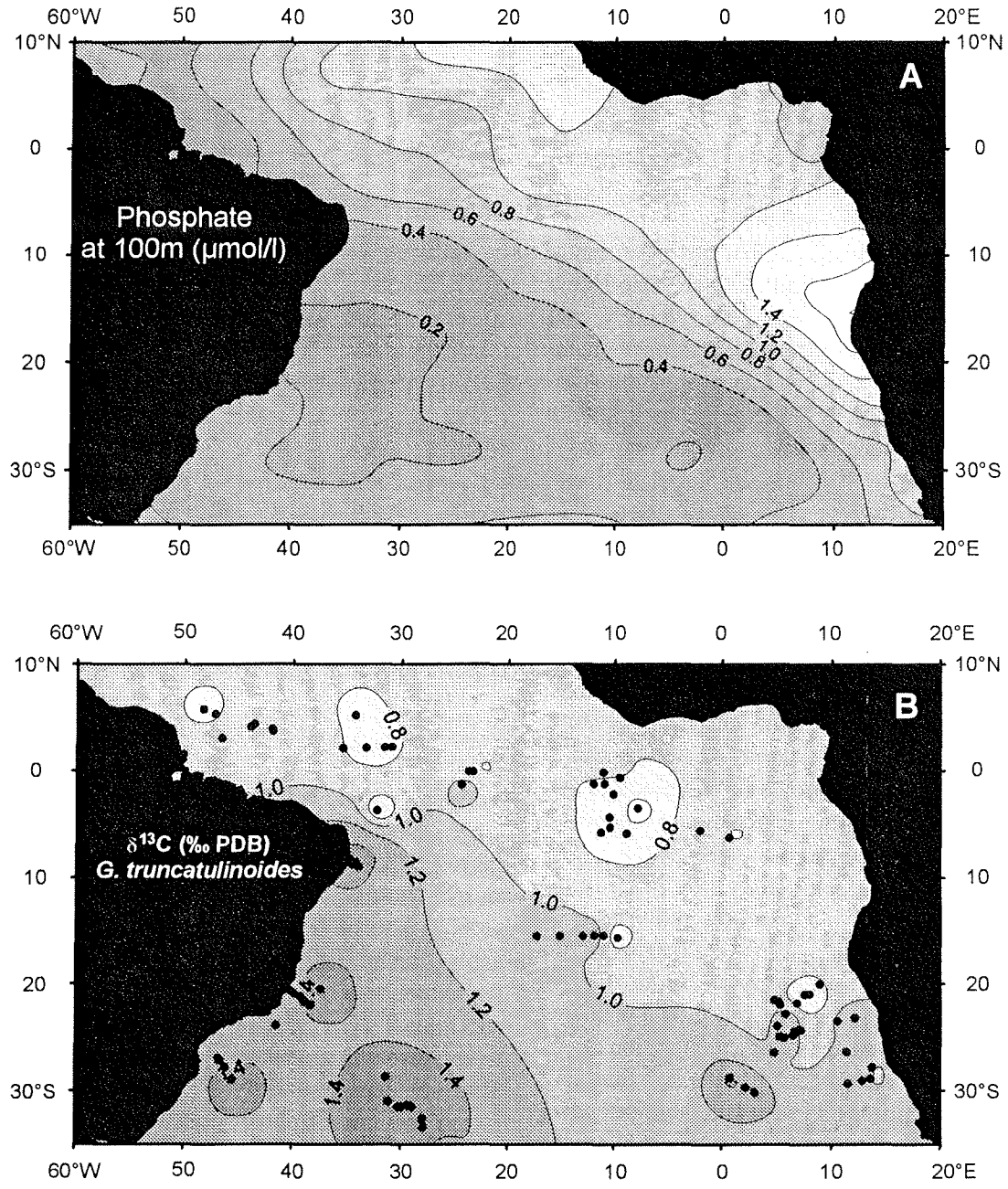

Fig. 7. (a) Phosphate concentration at 100 m water depth (Conkright et al. 1994). **(b)** $\delta^{13}C$ of *G. truncatulinoides* (550-600 µm) from core tops (redrawn after Mulitza et al. 1998).

Berger and Killingley 1977; Bonneau et al. 1980). We have shown in Fig. 5 that the distribution of $\delta^{13}C$ in foraminiferal shells is far from being homogenous. If certain parts of the shell are removed by dissolution the $\delta^{13}C$ value of the remnants should change. For example, Wu and Berger (1989) measured the carbon isotope composition of *P. obliquiloculata* and *G. sacculifer* from surface sediments of the Ontong Java Plateau which were recovered from a depth range between 1598 and

4441m (Fig. 8). The results suggest strong dissolution effects in deep waters. The carbon isotopic composition of the different species, however, is affected in different ways. While the shells of *P. obliquiloculata* deviate to heavier values in deep waters, *G. sacculifer* shows lighter values than shells picked from shallow sediment samples (Fig. 8). This opposite response to dissolution must reflect differences in the distribution of carbon isotopes in the shells of *G. sacculifer* and *P. obliquiloculata* due to different life cycles. *G. sacculifer* starts to calcify in the mixed layer and adds up to 30% calcite crust in deeper thermocline waters (Duplessy et al. 1981; Lohmann 1995). Therefore, the initial shell of large *G. sacculifer* specimens is relatively heavy while the calcite crust is isotopically light. As the crust is typically more resistant to dissolution than the initial shell, the whole-shell $\delta^{13}C$ will be shifted towards lighter values, if dissolution takes place. Additionally, isotopically heavy specimens that have no crust might be dissolved from the sea-floor population. *P. obliquiloculata* dwells in the upper portion of the thermocline and therefore calcifies over a smaller range of $\delta^{13}C_{\Sigma CO2}$ than *G. sacculifer*. Since the chambers formed during early growth stages in warmer waters are isotopically very light, presumably due to uptake of metabolic CO_2 (see above), dissolution of the initial chambers increases $\delta^{13}C$ of the remnants towards higher $\delta^{13}C$ values. Generally, dissolution effects tend to fluctuate in concert with glacial-interglacial variations (Berger and Vincent 1986) and are therefore hard to separate from climate related signals. It is obvious that strong dissolution must be avoided to obtain reliable carbon isotope records.

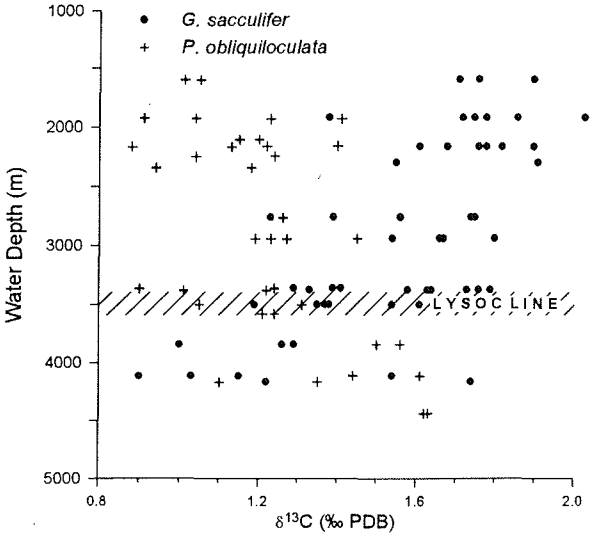

Fig. 8. Effect of dissolution on the carbon isotope composition of *G. sacculifer* and *P. obliquiloculata* from Holocene samples of the Ontong Java Plateau. Data are from Wu and Berger (1989).

Late Quaternary $\delta^{13}C$ Records

Global Variations

One of the first attempts to use the $\delta^{13}C$ composition of foraminiferal calcite for paleoceanography was published by Shackleton (1977). He analyzed tests of the benthic foraminifer *Uvigerina*. Shackleton's $\delta^{13}C$ records exhibit lower $\delta^{13}C$ ratios at the last glacial maximum than during the Holocene. This depletion must have been of global character, because lower glacial carbon isotope values were observed in all three ocean basins and also in shallow-dwelling planktic foraminifera. Since the only important reservoir of light carbon is the continental biosphere (ca. -25 ‰), Shackleton interpreted the lower values as an injection of light terrestrial carbon into the ocean. Later, it became evident that *Uvigerina* is not an optimal recorder of deep water $\delta^{13}C$ because of its infaunal habitat (Zahn and Sarnthein 1987). Recent estimates of the global shift in $\delta^{13}C$ are 0.3 to 0.4 ‰ (Curry et al. 1988; Duplessy et al. 1988). It should be noted, however, that changes in the $\delta^{13}C$ value of the dissolved organic carbon (Rau et al. 1991) or a change in the foraminiferal disequilibrium offset in response to the changing carbonate chemistry of the ocean (Spero et al. 1997; Bijma et al. this volume; Lea et al. this volume) might also contribute to a global glacial reduction of the foraminiferal $\delta^{13}C$.

Regional Variations in the Tropical Atlantic and the Southern Ocean

Although the recording of $\delta^{13}C$ in planktic foraminifera is yet not fully understood, deviations from the global signal may provide hints about regional changes in the carbon isotope chemistry of surface waters. This approach requires that disequilibrium effects are invariant through time, which might be unrealistic in the light of the studies which use the extent of the vital effect as a proxy itself (see Bjima et al. and Lea et al. this volume). However, two main strategies to deal with carbon isotope records of planktic foraminifera can be found in the literature. The first is to use carbon isotope differences of different foraminiferal species (in most cases benthic and planktic) in the same core (e.g. Shackleton and Pisias 1985; Steens et al. 1992; Schneider et al. 1994; Wefer et al. 1996). Because global effects should be cancelled out, this method can provide information about the vertical or seasonal differences in the carbon isotope composition of water masses. The other strategy, applied to both benthic and planktic records, is to compare carbon isotope records from different sites, e.g. from high and low latitudes within the same time frame (e.g. Labeyrie and Duplessy 1985; Oppo and Fairbanks 1987; Ninnemann and Charles 1997; Duplessy et al. 1988). This method should allow to differentiate relative changes between water masses of different regions. Following the latter strategy, we will now present four high-resolution (>10 cm/ka), ^{14}C-dated planktic $\delta^{13}C$ records from key regions within the South and Equatorial Atlantic (Fig. 3, see Table 1 for positions and references). All shown ^{14}C-data were only corrected by the modern reservoir age of surface waters (Bard 1988).

Southern Ocean. The Southern Ocean is the ventilation area for a great part of the world ocean where the initial isotopic composition of water masses leaving the surface can be monitored. Core PS1768-8 is located just south of the present-day Antarctic Polar Front (APF), a primary source region for the Antarctic Intermediate Water (Molinelli 1981; Tsuchia et al. 1994). The salient feature of core PS1768-8 is a strong deglacial $\delta^{13}C$-minimum dated to about 12.1 ka (Fig. 9a, Frank et al. 1996). The carbon isotope values at the deglacial minimum are more than 1.7 ‰ lower than during the latest Holocene (core-top). The glacial-Holocene difference is about 1.2 ‰, which is much more than observed in carbon isotope records from a comparable latitude in the Indo-Pacific sector of the Southern Ocean (Ninnemann and Charles 1997).

It seems that the Atlantic sector of the Southern Ocean is the region of the world where the greatest glacial-interglacial changes in $\delta^{13}C$ of planktic foraminifera occur (Ninnemann and Charles 1997). Most authors interpret the low glacial $\delta^{13}C$ values of *N. pachyderma* in the Southern Ocean as a nutrient enrichment in surface waters (Charles and Fairbanks 1990; Charles et al. 1996; Ninnemann and Charles 1997). Such an

Core	Latitude	Longitude	Depth (m)	Species	Reference
PS1768-8	52°35.6'S	4°28.5'E	3270	*N. pachy.*(sin.)	Frank et al. (1996)
GeoB 1023-5	17°09.5'S	11°00.5'E	1980	*G. bulloides*	Schneider et al. (1992)
GeoB 3104-1	3°40,0'S	37°43,0'W	767	*G. sacculifer*	Arz et al. (1998)
M35003-4	12°05,4'N	61°14,6'W	1299	*G. ruber* (pink)	Rühlemann et al. (in prep)

Table 1. Core locations, references and species used for stable isotope analyses.

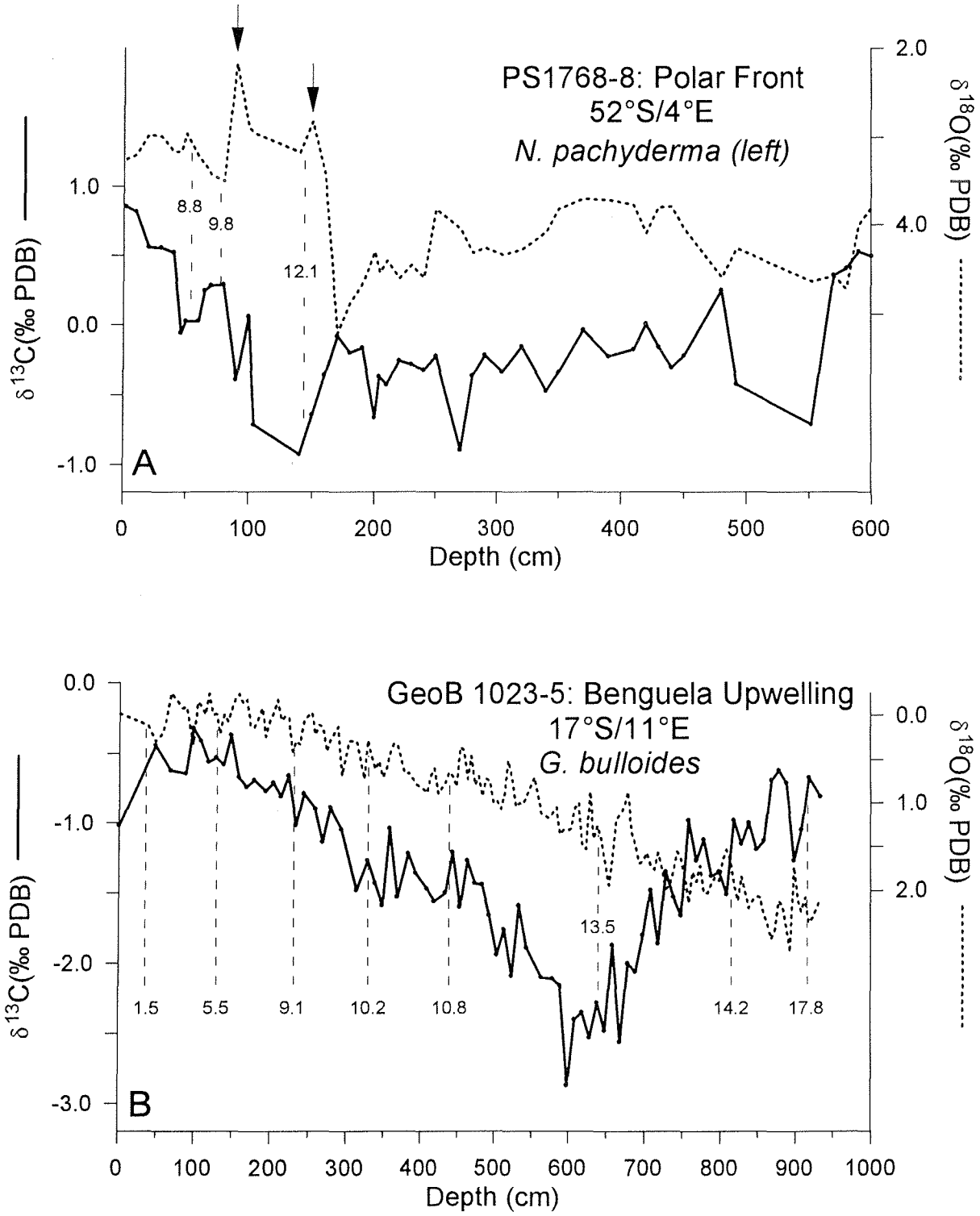

Fig. 9. (a) $\delta^{13}C$ and $\delta^{18}O$ of *N. pachyderma* from core PS1768-8 (Niebler 1995). ^{14}C-Datings are from Frank et al. (1996). **(b)** $\delta^{13}C$ and $\delta^{18}O$ of *G. bulloides* from the Benguela Upwelling System (Schneider et al. 1992).

increase in nutrient levels might result from any combination of (1) decreased biological activity, (2) increased upwelling rates or (3) increased nutrient concentrations of source waters. Charles and Fairbanks (1990) proposed that the increased nutrient concentrations in the Southern Ocean during the LGM were due to a reduced contribution by nutrient poor NADW. This hypothesis is supported by by the isotopic composition of benthic foraminifera, which record a comparable high glacial-interglacial $\delta^{13}C$ shift of about 1.3‰ in the Southern Ocean (see compilation and references in Michel et al. 1995). Cd/Ca and Ba/Ca ratios of benthic foraminifera, however, suggest that the nutrient concentrations within CPDW remained close to the modern level (Lea 1995; Boyle and Rosenthal 1996). Additionally, the nutrient utilization was increased south of the APF and remained unchanged north of the APF (Francois et al. 1997). This should result, at least south of the APF, in higher $\delta^{13}C$-values of surface waters.

The discrepancy between the data might be resolved by considering the habitat of *N. pachyderma* and the hydrologic changes in the Southern Ocean during the LGM. Results from plankton tows indicate that *N. pachyderma* secretes ¾ of its shell in water depth between 50 and 200 m (Kohfeld et al. 1997; Carstens et al. 1997). Duplessy et al. (1996) have shown that the salinity of surface waters in the Antarctic Zone were considerably reduced during the LGM which probably resulted in an increased vertical stratification. Since the modern upper water column is relatively well mixed in the Southern Ocean, *N. pachyderma* records surface water conditions despite its deeper habitat. Under more stratified conditions, however, their habitat would be enriched in nutrients and hence their shells would record a lower $\delta^{13}C$. Support for this hypothesis comes from shallow dwelling *G. bulloides* which records a much lower glacial/interglacial amplitude in the subantarctic zone (Ninnemann and Charles 1997).

Due to the higher stratification or sea ice cover, the gas exchange between atmosphere and ocean might have been considerably reduced during the glacial. This would cause an additional decrease of the $\delta^{13}C$ of surface waters and probably also in the water masses sinking down from Southern Ocean surface waters. Fig. 1c indicates that nowadays the exchange with the atmosphere increases the $\delta^{13}C$ of surface waters in the vicinity of the Polar Front by about 0.4 ‰. Hence, a reduction in air-sea exchange could only explain part of the deglacial and glacial minimum and does not resolve the cadmium/$\delta^{13}C$ discrepancy (Michel et al. 1995).

The deglacial minimum can also be explained with changes in surface water hydrology. Zielinski et al. (1998) have shown that deglacial temperatures recorded in core PS1768-8 were up to 3°C warmer than during the late Holocene. This warming and an additional surface freshening (Niebler 1995) may have produced the huge negative $\delta^{18}O$ anomaly in *N. pachyderma* during the last deglaciation as measured in core PS1768-8 (arrows in Fig. 9a). The warmer temperatures may indicate that surface waters originated further north, where equilibration with atmospheric CO_2 took place at warmer temperatures.

An alternative explanation for the $\delta^{13}C$ variability in planktic foraminifera was provided by Lea et al. (this volume). They attributed the low glacial $\delta^{13}C$ values of *G. bulloides* and *N. pachyderma* to higher carbon ion contents of Southern Ocean surface waters. Although this effect might cause the glacial reduction in foraminiferal $\delta^{13}C$, it cannot explain the huge deglacial $\delta^{13}C$ - minimum, because increasing atmospheric CO_2 during deglaciation constrains decreased carbon ion content of deglacial subantarctic surface waters (Lea et al. this volume).

Benguela Upwelling. To what extent is the glacial-interglacial variability of high latitudes transferred to the World Ocean? The answer to this question provides hints about changes in the general circulation pattern. In this regard, upwelling regions are important, because nutrients are normally not fully utilized and changes in the chemistry of upwelled waters should directly be transferred to surface waters. Most carbon isotope studies, intended to monitor the upwelling regions in the past, used *G. bulloides* because this species is well adapted to upwelling conditions. Isotope studies of plankton tows and core tops have shown that the $\delta^{13}C$ value of *G. bulloides* increases in upwelling regions relative to open ocean conditions (Ganssen 1983; Kroon and Ganssen 1988;

Schneider et al. 1994). This has been attributed to the late seasonal occurrence of *G. bulloides* when primary production has already decreased the nutrient concentrations and increased the $\delta^{13}C$ of surface waters. Another factor increasing the $\delta^{13}C$ of *G. bulloides* in upwelling regions is temperature. Culturing experiments indicated that the $\delta^{13}C$ of *G. bulloides* increases by about 0.1‰ per degree of temperature decrease (Bemis and Spero 1997). Hence, increased upwelling might also increase the $\delta^{13}C$ of *G. bulloides* by cooling SSTs.

Core GeoB 1023-5 is located in the Benguela Upwelling Region off Namibia and has been extensively studied by Schneider et al. (1992). In sharp contrast to the high-latitude core PS1768-8, the glacial-interglacial $\delta^{13}C$ difference of *G. bulloides* is close to zero (Fig. 9b). Taking into account a negative global $\delta^{13}C$ shift of 0.3-0.4 ‰ from the Holocene to the last glacial, there must have been a local increase in glacial surface water $\delta^{13}C$ relative to the global ocean, or a surface water cooling of about 3-4 °C. A cooling of about 4°C has been observed for the nearby core GeoB 1710-3 (Kirst et al. 1998). Hence, the negative global $\delta^{13}C$ shift during the LGM is nearly compensated by a positive $\delta^{13}C$ shift due to a cooling of ambient surface waters, and no additional effects are necessary to explain the glacial carbon isotope values of *G. bulloides*.

The deglaciation in Core GeoB 1023-5 is marked by a strong $\delta^{13}C$-minimum at about 13 ka. According to Oppo and Fairbanks (1989) and Schneider et al. (1992), the deglacial minimum might either reflect an increased upwelling of subsurface waters, or a change in the preformed isotopic composition of source waters. Since there were no indications of higher upwelling during deglaciation, Schneider et al. (1992) suggested that the minimum is due to a change in the isotopic composition of the upwelled source waters. Today, waters upwelled off Namibia originate from the South Atlantic Central Water level at 200-400 m depth. The modern source area of this water type is near the Subtropical Front (e.g. Gordon 1981). We have already shown that Southern Ocean surface waters exhibit a strong deglacial minimum with comparable timing (Fig. 9a). Therefore, it seems to be reasonable that the deglacial minimum is due to a change in the preformed isotopic composition of the upwelled waters. Problems with this scenario are that cores closer to the potential source area (e.g. Ninneman and Charles 1997) show a much smaller deglacial minimum than observed in core GeoB 1023-5. However, future work might show that upwelled central waters originated further south, or that the deglacial $\delta^{13}C$ depletion was actually larger at the Subtropical Front.

Oligotrophic Tropical Atlantic. In contrast to the high latitudes and the upwelling regions, cores recovered from the tropical Atlantic provide the opportunity to study carbon isotope records from nutrient-depleted surface waters. Changes in the carbon isotope composition of tropical surface waters should be mainly due to processes unrelated to nutrient cycling. Core GeoB 3104-1 comes from the western equatorial Atlantic off Brazil, from a water depth of about 767 m. The isotope records and ^{14}C-datings were measured on the shallow-dwelling species *G. sacculifer* (Fig. 10a, Arz et al. 1998). As already shown in Fig. 5, *G. sacculifer* exhibits a strong size-trend in $\delta^{13}C$. By using a narrow size range (350-400 µm in this case) the effects of ontogeny should be minimized. Generally, the variability of tropical $\delta^{13}C$-records is lower than in high- and mid-latitudes. Glacial values in core GeoB 3104-1 are about 0.8 ‰ lower than Holocene values. Like all other cores presented in this study, GeoB 3104-1 contains a strong deglacial minimum dated to about 13 ka. Although, the magnitude of the observed changes in core 3104-1 is much lower than in the high and mid-latitude cores, the changes are too great to be solely explained with global changes in carbon inventories. Since tropical surface waters are always depleted in nutrients, changes in the thermodynamic imprint must be responsible for the glacial and deglacial depletion in $\delta^{13}C$. As benthic foraminifera from cores located in the Antarctic Intermediate Water contain a synchronous deglacial $\delta^{13}C$-minimum, Oppo and Fairbanks (1989), and later Lynch-Stieglitz et al. (1994), suggested that the deglacial minimum might be due to changes in the preformed $\delta^{13}C$ signal of intermediate waters and transferred to surface waters by upwelling. We have presented indications for both mechanisms, changes in preformed $\delta^{13}C$ of AAIW source waters (PS1768-8)

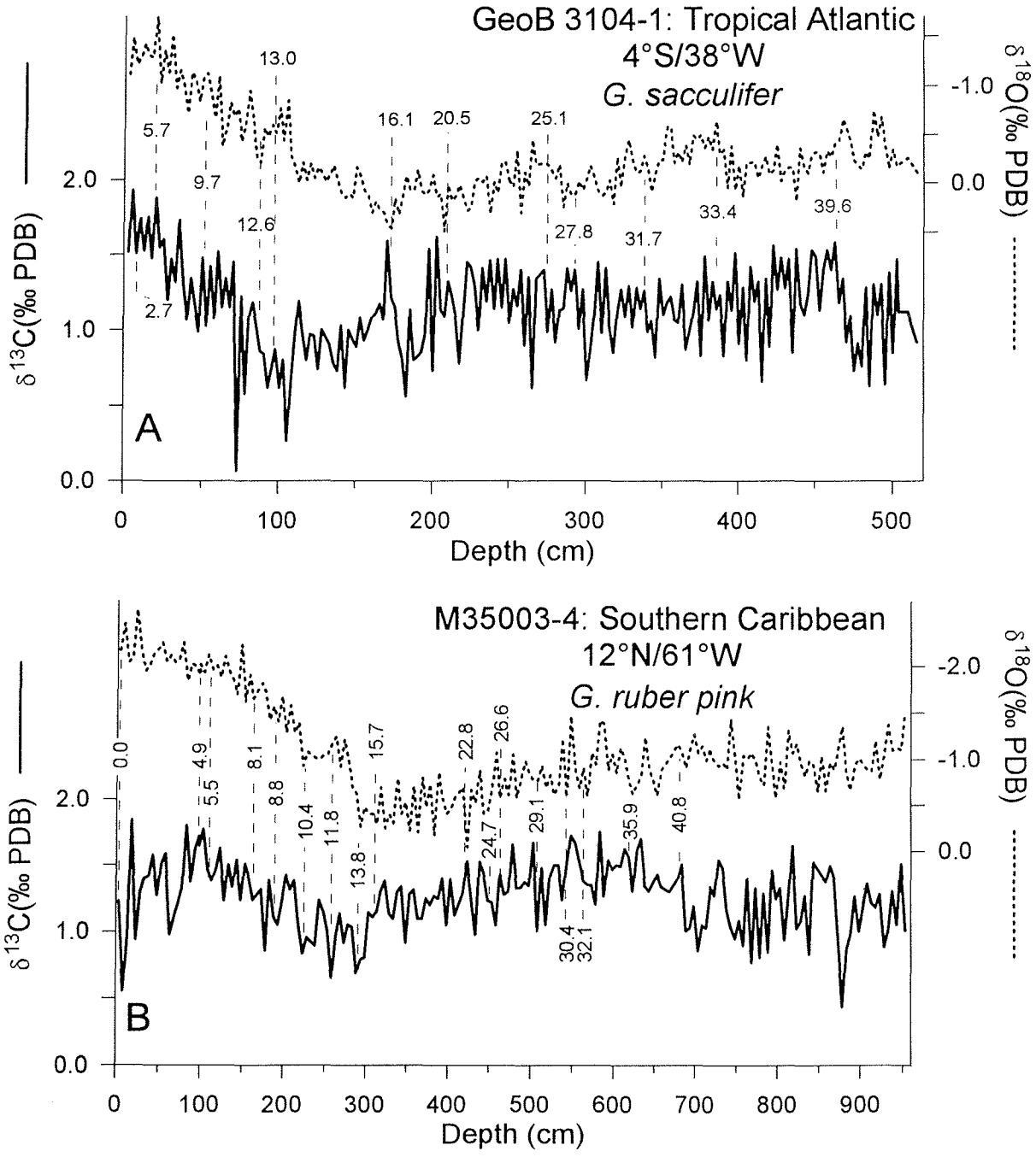

Fig. 10. (a) $\delta^{13}C$ and $\delta^{18}O$ from the tropical Atlantic core GeoB 3104-1 (Arz et al. 1998). **(b)** $\delta^{13}C$ and $\delta^{18}O$ of *G. ruber* (pink) from the Caribbean core M35003-4.

as well as the signal transfer to surface waters in the coastal upwelling regions (GeoB 1023-5). However, if the hypothesis is correct that the thermodynamic imprint is transferred by AAIW, regions with little or no AAIW should record a different signal. The Southern Caribbean is a region where the AAIW is already considerably diluted by Upper North Atlantic Deep Water. Core M35003-4

was taken at 12°N/61°W close to Barbados. In fact, the difference between the Holocene (0-5 ka) and the deglacial minimum (12.5-13.5 ka) amounts to only 0.2 ‰ in core M35003-4, and is much less pronounced than in the *G. sacculifer* record from GeoB 3104-1. This observation strongly supports the hypothesis of a high southern origin of the deglacial minimum.

The large glacial-interglacial variability of high latitudes (e.g. core PS1768-8, Fig. 9a) is obviously not transferred to lower latitudes to the same extent as the deglacial minimum. One explanation for this observation could be the glacial circulation pattern. Benthic $\delta^{13}C$ values indicate that the glacial intermediate depth equatorial Atlantic was cut off from the southern intermediate water source (Oppo and Fairbanks 1987; Boyle and Keigwin 1987; Duplessy et al. 1988). Hence, there might have been no effective conduit to transfer the high-latitude signal to the low latitudes.

Conclusions

The carbon isotope distribution in the ocean provides important information about the ocean's circulation state. The $\delta^{13}C$ of shallow-dwelling planktic foraminifera is an indispensable tool to define the preformed $\delta^{13}C$ composition of past water masses. Besides the carbon isotope composition of the surrounding seawater, important controls of the shell's $\delta^{13}C$ are (1) disequilibrium vital effects, (2) the habitat of the used species, and (3) postdepositional dissolution. Vital effects vary from species to species and cannot be reduced to a single mechanism. The carbonate system, photosynthesis, and the incorporation of light metabolic CO_2 seem to be major candidates to explain disequilibrium effects. However, once resolved, vital effects might provide additional proxies for temperature and the carbonate system. Knowledge of the habitat is also critical for the interpretation of the $\delta^{13}C$ composition of planktic foraminifera. On the other hand, if the depth of calcification is well known, carbon isotope differences between foraminiferal species can yield information about the nutrient stratification of surface waters.

Low glacial $\delta^{13}C$ values in the Atlantic sector of the Southern Ocean are presumably due to a combination of decreased air-sea exchange, subsurface nutrient enrichment, and environmentally controlled vital effects. At present, it seems to be difficult to quantify the contribution of the different effects to the total record. The variability in the oligotropic tropical Atlantic is much lower and might by explained with a combination of global variations and changes in the thermodynamic imprint of source waters. Despite their different amplitudes, the $\delta^{13}C$ records from various parts in the tropical and South Atlantic exhibit some striking similarities. An event common to both high and low latitudes is the deglacial $\delta^{13}C$ minimum near 13 ka. Our study shows that the deglacial minimum is associated with huge hydrographic changes in the Atlantic sector of the Southern Ocean just south of the Polar Front. We have presented strong support for the hypothesis that the AAIW provides a conduit to transfer the deglacial minimum from the Antarctic surface to tropical Atlantic surface waters. However, to further strengthen this hypothesis, a more precise geographic pattern of $\delta^{13}C$ variability is required.

Acknowledgments

The preparation of this paper was supported by EC Grant CHRX-CT 92-0066 (received by S. Mulitza during a postdoctoral stay at the Centre des Faibles Radioactivités, Gif-sur-Yvette) and the Deutsche Forschungsgemeinschaft (Sonderforschungsbereich 261 at University of Bremen; Contribution Nr. 222). We thank E. Michel and an anonymous referee for careful reviews and J. Bijma and R.R. Schneider for discussion and comments. Thanks to P. Grootes and staff of the Leibnitz-Labor in Kiel for providing AMS- ^{14}C datings of core M35003-4. Data available under www.pangaea.de/Projects/SFB261.

2. Seasonal and decadal changes in carbon isotope composition of the north-western Arabian Sea

(submitted to "Deep Sea Research Part I")

Christopher A. Moos[1,*], Geert-Jan A. Brummer[2], Gerald Ganssen[3], Willem Helder[2], Axel Hupe[4], Rikus Kloosterhuis[2], Ralf Lendt[4], Ralph R. Schneider[1] and Gerold Wefer[1].

[1] Fachbereich Geowissenschaften, University of Bremen, Klagenfurter Strasse, D-28359 Bremen, Germany

[2] Netherlands Institute for Sea Research, P.O. box 59, 1790 AB Den Burg, Texel, The Netherlands

[3] Institute of Earth Sience, de Boelelaan 1085, 1081 HV Amsterdam, The Netherlands

[4] Institute of Biogeochemistry and Marine Chemistry, University of Hamburg, Bundesstrasse 55, D-2146 Hamburg 13, Germany

Abstract

Based on three research cruises in the northern Arabian Sea during the SW-monsoon season of 1992 and late NE-monsoon of 1993 and 1995, we investigated the spatial and vertical distributions of $\delta^{13}C$ of dissolved inorganic carbon ($\delta^{13}C_{\Sigma CO2}$) and the concentration of PO_4, NO_3, ΣCO_2, and O_2 related to decadal and seasonal changes. The seasonal variability of these tracers reflects the summer upwelling and advection of subsurface water (SW-Monsoon) and the stratification of the water column during the winter season. The strongest gradients between SW- and NE-monsoon season occur at water depths between 20 and 80 m. In this depth range the seasonal variation of $\delta^{13}C_{\Sigma CO2}$, temperature, salinity, and phosphate amounts 1.3 ‰, 7 °C, 0.45 psu, and 1.8 µMol kg^{-1}, respectively.

* Corresponding author. Fax: 0049 421 218 3116; e-mail: moos@allgeo.uni-bremen.de

The ΣCO_2 and $\delta^{13}C_{\Sigma CO2}$ data were combined with nutrient data for comparison with data of the GEOSECS Indian Ocean expedition 1977. While the stoichiometry of the NO_3/PO_4 ratio shows no obvious changes, the nutrient normalised carbon isotope values reflect a decrease of 0.3 ‰ at the sea surface between 1977 and 1993 indicating an anthropogenic CO_2 increase.

Keywords: carbon isotopes, dissolved inorganic carbon, nutrient concentration, upwelling, seasonality, anthropogenic effect

Regional index terms: Indian Ocean, Arabian Sea, Gulf of Aden

1. Introduction

1.1 Carbon isotopes of dissolved inorganic carbon as tracers for carbon cycle and ocean circulation

The carbon isotope composition of ocean surface water is mainly affected by primary production. Thus annual changes in $\delta^{13}C$ of dissolved inorganic carbon are mainly related to seasonal variability of primary production and nutrient utilisation. Long-term trends reflect changes like the anthropogenic increase of the atmospheric CO_2 concentration.

The ocean is the largest reservoir of the global carbon system and the major long-term regulator for atmospheric CO_2. Thus, to understand the ocean carbon cycle is the key to predict climate changes owing to anthropogenic CO_2 emissions. An important tracer of the carbon system is the ratio of the stable carbon isotopes ^{13}C and ^{12}C. The carbon isotope composition of dissolved inorganic carbon (ΣCO_2) in the ocean is related to the nutrient cycle, biological productivity and its regeneration. Marine organic matter produced by photosynthesis preferentially fixes ^{12}C and shows $\delta^{13}C$ values around −19 ‰. Hence, the surface ocean becomes enriched in ^{13}C and depleted in nutrients. In contrast, oxidation of sinking organic matter releases ^{12}C rich CO_2 into the reservoir and lowers $\delta^{13}C$ of deeper water. Simultaneously the nutrient concentration increases while the oxygen concentration decreases. Therefore $\delta^{13}C_{\Sigma CO2}$ in the ocean is inversely correlated with the nutrient content of ocean water (Broecker and Maier-Reimer, 1992; Broecker and Peng, 1982; Kroopnick, 1985). Broecker and Peng (1982) derived a theoretical relationship formulated in equation (1).

$$\delta^{13}C(\text{zero } PO_4) = \delta^{13}C_{\Sigma CO_2} - \left[\frac{\delta^{13}C\text{plant}}{\Sigma CO_2 \text{mean ocean}}\left(\frac{C}{P}\right)_{org}\right] * PO_4 \quad (1)$$

for the $\delta^{13}C$*plant* and ΣCO_2*mean ocean* values used by Broecker and Maier-Reimer (1992) and a C/P ratio observed for the Arabian Sea by Millero et al., (1998) the equation becomes

$$\delta^{13}C(\text{zero } PO_4)(‰) = \delta^{13}C_{\Sigma CO_2}(‰) - \left[\frac{-19}{2200}\left(\frac{‰\ kg}{\mu Mol}\right)125\right] * PO_4\left(\frac{\mu Mol}{kg}\right)$$

$$= \delta^{13}C_{\Sigma CO_2} + 1.1 * PO_4 \quad (2)$$

For areas where nitrogen fixation is a negligible and NO_3 reflects the hole nitrogen concentration the equation can also be formulated for nitrate ((C/N)*org* = 7 (Redfield et al., 1963)):

$$\delta^{13}C(\text{zero } NO_3) = \delta^{13}C_{\Sigma CO_2} + 0.06 * NO_3 \quad (3)$$

The biological coefficients of 1.1 and 0.06, in equation (2) and (3) reflect the fixation of $\delta^{13}C_{\Sigma CO2}$ by fractionation during photosynthesis and describe the slope of the $\delta^{13}C$/nutrient relationship as illustrated in Figure 6.

A second major control of the $^{13}C/^{12}C$ ratio of seawater is the isotope fractionation, which occurs during the exchange of CO_2 between the atmosphere and the surface ocean. The air-sea fractionation depends on several thermodynamic control mechanisms. The fractionation factors vary as a function of sea surface temperature, CO_2 exchange rate, and water residence time at the sea surface (Siegenthaler and Münnich, 1981). As reported from ice core data and atmospheric observations CO_2 and $\delta^{13}C$ show a general covariation during the past 150 years. Due to the addition of CO_2 derived from fossil fuel with $\delta^{13}C$ values around –27 ‰ the isotope composition of the atmosphere has changed from –6.4 ‰ in pre-industrial times to modern values near -7.8 ‰ (Friedli et al., 1986). The CO_2 concentration in the atmosphere increased continuously from its pre-industrial value near 280 parts per million to 363 in 1997 (Keeling and Whorf, 1998; Neftel et al., 1994). Hence the changes in the amount of ^{13}C of the surface ocean reflect a combination of changes in the isotope composition and the increase of dissolved inorganic carbon. Therefore the $\delta^{13}C_{\Sigma CO2}$ tracks the penetration of anthropogenic CO_2 in the ocean and offers an independent way to assess the oceanic CO_2 uptake (Siegenthaler and Sarmiento, 1993; Heimann and Maier-Reimer, 1996).

Several authors used $\delta^{13}C_{\Sigma CO2}$ to calculate the ocean uptake of CO_2 over decades or since pre-industrial times using direct observations or model calculations (Bacastow et al., 1996; Heimann and Maier-Reimer, 1996; Joos and Bruno, 1998; Keir et al., 1998; Quay et al., 1992;

Tans et al., 1993). Heimann and Maier-Reimer (1996) showed by a simulation with the Hamburg model that discrepancies between ocean uptake rates based on different analysis methods probably reflect uncertainties of the observational database. Most of the available $\delta^{13}C_{\Sigma CO2}$ data originate from areas, which act preferentially as sinks for atmospheric CO_2. However, little is known about the long-term trends of the carbon isotope composition of high productivity areas with strong seasonal changes.

One of the objectives of the Netherlands Indian Ocean Program (NIOP) and the investigations of the University of Bremen was to obtain a data set, which includes monsoonal variations and long-term trends of the carbon isotope composition in relation to nutrient and dissolved inorganic carbon concentrations in the Gulf of Aden and the upwelling area off Yemen and Oman.

We present a detailed description of spatial and seasonal distribution in $\delta^{13}C_{\Sigma CO2}$, ΣCO2, PO_4, NO_3, and O_2 during SW-monsoon 1992 and NE-monsoon 1993 and 1995 from the Gulf of Aden. A comparison of our data with previous data from the GEOSECS program in the late-70's are interpreted in terms of the influence of anthropogenic $^{13}CO_2$ in the north-western Arabian Sea.

1.2 Circulation patterns of the northwestern Arabian Sea

Strong seasonal changes related to atmospheric forcing mechanisms and discrete water exchange with other ocean basins make the northern Arabian Sea to an ideal area to study the coupling of climatic and oceanographic regimes. The hydrological conditions of the northern Arabian Sea are different from most other ocean basins. Because of the landmasses forming the northern boundary of the Arabian Sea the major water exchange takes place with the southern Indian Ocean and to some extent with the Red Sea and the Persian Gulf. Especially the Indian Monsoon system has a dominant influence on the extreme seasonal variation of the sea surface circulation and the distribution of water tracers in the upper water column. From May to September the surface water circulation is affected by SW-monsoon winds and causes upwelling along the coastal areas of Somalia, Yemen, and Oman while the strong Somali current is established. During this period, cold, nutrient rich subsurface water rises to the sea surface and the primary production reaches its annual maximum. In contrast, during the inter-monsoon periods (March-May and October-December) the water column of the Arabian Sea is stratified and can be considered as oligothrophic (Jochem et al., 1993; Owens et al., 1993). The surface circulation reverses to an anticyclonic circulation from December to March

(Schott et al., 1990; Wyrtki, 1973). The winter season is generally associated with low primary production, except for the northern area of the Arabian Sea where winter blooms can occur in the coastal areas of Oman (Banse and McClain, 1986).

The dissolved oxygen concentration is extremely low (less than 20 μMol kg^{-1}) in the northern Arabian Sea between 150 and 1400 m. This is due to the locally high primary production and the oxidation of organic matter. In addition the ventilation of the water masses in intermediate depth is rather slow (Morrison et al., 1998; Swallow, 1984; Wyrtki, 1973). The inflow of Red Sea Water (RSW) into the Gulf of Aden occurs at 500-800 m depth within the oxygen minimum zone. RSW is characterised by a salinity maximum of 36.7 psu and a density of 27.2 kg m^{-3} in the northern Arabian Sea (Wyrtki, 1971). Outflow water from the Persian Gulf has slightly lower densities (26.7 kg m^{-3} and above) and is found at about 250-300 m in the northern Arabian Sea (Tomczak and Godfrey, 1994).

2. Methods and Materials

Materials

Three oceanographic research cruises between 1992 and 1995 were carried out in the north-western Arabian Sea and cover both monsoon seasons. During these cruises oceanographic stations were sampled for measurements of the carbon isotope composition, phosphate and nitrate content and dissolved inorganic carbon of the water column.

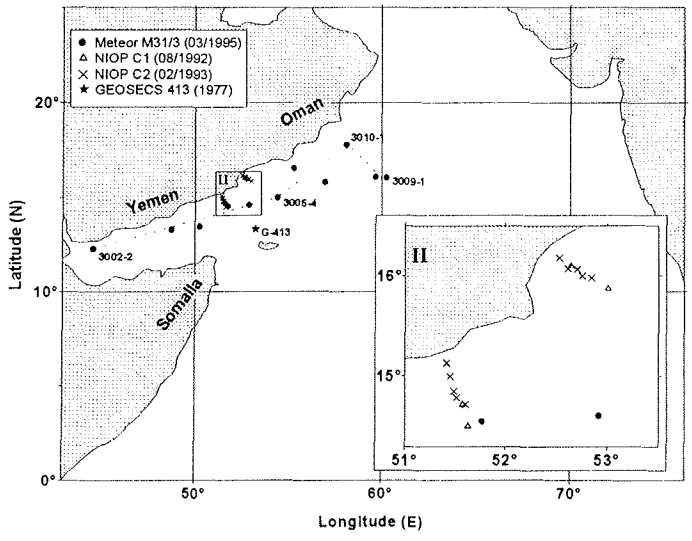

Figure 1. Sampling locations of Meteor cruise M31/3 and NIOP cruises C1 and C2.

During Meteor cruise M31/3 eleven hydrographic stations were sampled in the north-western Arabian Sea, between 40-60° E longitudes and 12-18° N latitudes (Figure 1) at the end of NE-monsoon (March 1995). Continuous information on the hydrographic conditions

was obtained using a *GO 7* rosette equipped pressure-, temperature-, conductivity-, and oxygen sensors. Water samples were collected with an automatic rosette of 12*10 l Niskin bottles for determination of stable carbon isotope ratios and ΣCO_2 measurements. Duplicate samples of 50 ml were taken. A total of 164 water samples were recovered and stored in brown borosilicate glass bottles. The samples were poisoned with 1 ml saturated $HgCl_2$ solution and bottles were sealed with melted paraffin.

All samples for ΣCO_2 were poisoned with saturated $HgCl_2$ and stored in 250 ml borosilicate glass bottles. Dissolved inorganic carbon was measured onshore using a coulometric detector (model 5001 of UIC Inc., USA) combined with a CO_2 extraction unit (Robinson and Williams, 1991) to purge the CO_2 from an acidified seawater sample into the coulometric cell. The principle of the ΣCO_2 analysis is described in the DOE handbook of methods for CO_2 measurements (Department of Energy (DOE), 1994). The reliability of the coulometric titration was regularly checked with sodium carbonate standards. The analytical precision was about ± 5 μMol kg^{-1}.

During both NIOP cruises C1 (SW-monsoon) and C2 (NE-monsoon) two transects were sampled off eastern Yemen (Figure 1). Sampling for $\delta^{13}C_{\Sigma CO2}$ was carried out in much the same way as during the Meteor cruise except that single samples were taken down to a depth of 800 m that and poisoned with about 0.5 ml of a I_2-KI solution in dematerialized water (15 and 30 gram $liter^{-1}$, respectively). From the same CTD-rosette bottles, nutrient samples were taken and analysed colorimetrically shipboard by the TRAACS 800 autoanalyzer with a precision better than 0.04 μM for phosphate, 0.15 μM for nitrate and 0.15 μM for silicate. CTD oxygen sensors were calibrated by Winkler titration using conventional procedures. No samples for ΣCO_2 were taken.

More details are given in the cruise reports *Meteor-Berichte 96-4* (Hemleben et al., 1996) and (Baars, 1994; Van Hinte et al., 1995). The hydrographic stations sampled during NIOP cruises (1992-1993) and GeoB cruise M31/3 (1995) as well as the analysed parameters are summarised in Tab. 1.

Determination of $\delta^{13}C_{\Sigma CO2}$

For $\delta^{13}C$ analysis dissolved inorganic carbon was extracted as CO_2 gas from the water samples. Under vacuum conditions 50 ml of sea water were filled in a glass tube and acidified with 5 ml 99 % phosphoric acid. The extracted CO_2 was condensed into a sample tube by cooling with liquid N_2 and dried by passing through traps cooled with a dry ice-ethanol

mixture. In general the acid extraction of the ΣCO_2 followed the method of Kroopnick (1974). Isotope measurements were carried out at the University of Bremen and the Netherlands Institute for Sea Research. The carbon isotopes of the CO_2 gas were measured using triple collector mass spectrometers (*Finnigan Delta, VG optima*). Measurements were related to the VPDB standard through an internal standard gas. Measurements of duplicate samples (Meteor M31/3) and duplicate analyses of the same samples (NIOP C1, C2) show a statistical reproducibility of ± 0.16 ‰.

Spikes in $\delta^{13}C$ data

The carbon isotope profiles show a large number of spikes with exceedingly low $\delta^{13}C$ values down to -5 ‰. These spikes were found in profiles of all cruises and independent of the used toxin ($HgCl_2$ or KI). These values are reproducible by remeasurements of the same sample (KI samples), but not in general for the analyses of duplicate samples ($HgCl_2$ samples).

Possibly these values are the result of organic matter oxidation produced by late or insufficient poisoning or by oxidation of the used toxin itself. Similar problems are described by Kroopnick (1985) for GEOSECS samples from the Pacific and Atlantic Ocean.

Since the spikes are negative, we removed all samples, which exceeded the 95 % prediction level by iterative polynomial regression against associated state variables, until the standard deviation became symmetrical. In our procedure $\delta^{13}C_{\Sigma CO2}$ was

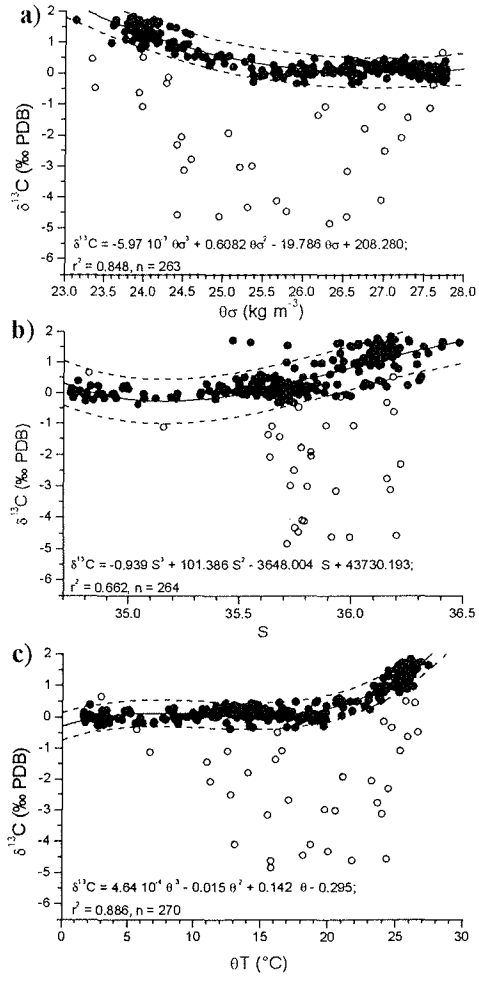

Figure 2. Identification of spikes within the $\delta^{13}C_{\Sigma CO2}$ data by correlation with hydro-graphic state variables; filled dots – resulted $\delta^{13}C_{\Sigma CO2}$ values; open dots – spikes, identified by all state variables; dashed lines - standard deviation of the polynomial fitting function; correlation with (a) sigma theta; (b) salinity and (c) potential temperature.

correlated separately with temperature, salinity, and density (including GEOSECS data of stations 413 (Kroopnick, 1985)). Only samples wit exceedingly low $\delta^{13}C_{\Sigma CO2}$ in all three state variables were identified as spikes (Figure 2a-c). To confirm the identification of the spikes, the NIOP samples were also correlated with NO^{3-}, PO_4^{3-} and O_2, which are associated with the cycling of organic matter. Independently, this method removed the same samples from the data-set as did the other three state variables.

Calibration of $\delta^{13}C$ data

In order to compare our data with the GEOSECS data we corrected for offsets due to different preparation techniques and laboratory standards by the following procedure. Assuming no significant changes occurred in the $\delta^{13}C_{\Sigma CO2}$ of the deep Arabian Sea water masses (below 700 m) within the past 15 years. We calculated a mean carbon isotope profile for GeoB and for the GEOSECS data (Figure 3), with a resolution of 25 m between 0 and 250 m water depth and 250 m between 250 and 2500 m. For calibration we only used data below an estimated penetration depth of 600 m (± 20 %) for a fossil fuel induced $\delta^{13}C$ anomaly as assumed by Broecker and Peng (1993) for the period from 1970-1990. To establish a calibration for samples of the same water masses we compared the corresponding temperature, salinity, and density measurements of our profiles with the GEOSECS data. As calibration reference we used GEOSECS position 413 in a depth range between 750 and 2500 m. The average profile calculated from our data is offset by 0.28 ‰ (± 0.05 ‰) relative to the GEOSECS profile.

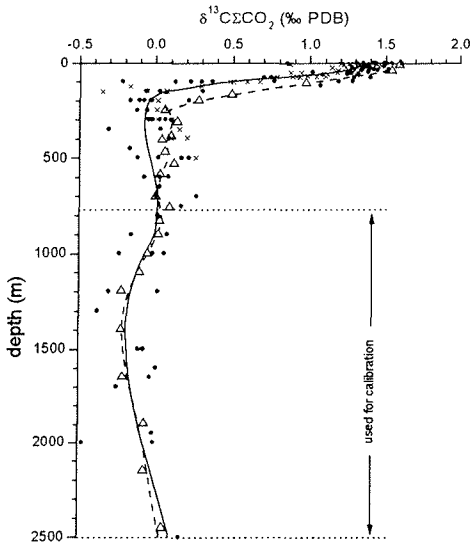

Figure 3. Calibrated $\delta^{13}C_{\Sigma CO2}$ data compared to GEOSECS station 413; dots – Meteor M31/3, crosses – NIOP C2, open triangles – GEOSECS station 413, solid line – spline smoothed average profile of Meteor M31/3 and NIOP C2 data, dashed line - spline smoothed profile of GEOSECS data; horizontal dotted lines mark the interval used for calibration.

We consider no significant deviation caused by fossil fuel CO_2 between the NIOP cruises and Meteor cruise M31/3 as the time in between was very short. Because NIOP did not

sample deep water extensively we compared the average profiles within a depth range between 100 and 500 m. We found no obvious differences between the NIOP and the calibrated GeoB profiles. Hence no additional calibration needed to be applied to the NIOP data.

Table 1. Sampling locations and measured parameters of NIOP and Meteor cruises

Station	cruise	date	LongE	LatN	CTD	$\delta^{13}C$	NO_3	PO_4	O_2	ΣCO_2
3002-2	Meteor M31/3	05.03.95	44,64	12,29	x	x	-	-	-	x
3003-1	Meteor M31/3	06.03.95	50,28	13,49	x	x	-	-	-	x
3004-3	Meteor M31/3	07.03.95	52,92	14,60	x	x	-	-	-	x
3005-4	Meteor M31/3	09.03.95	54,45	15,01	x	x	-	-	-	x
3006-1	Meteor M31/3	10.03.95	57,00	15,83	x	x	-	-	-	x
3008-4	Meteor M31/3	13.03.95	59,69	16,09	x	x	-	-	-	x
3009-1	Meteor M31/3	14.03.95	60,27	16,05	x	x	-	-	-	x
3010-1	Meteor M31/3	16.03.95	58,15	17,76	x	x	-	-	-	x
3011-4	Meteor M31/3	18.03.95	55,33	16,53	x	x	-	-	-	x
3012-3	Meteor M31/3	19.03.95	51,77	14,55	x	x	-	-	-	x
3013-3	Meteor M31/3	20.03.95	48,78	13,31	x	x	-	-	-	x
305-2	NIOP C1	17.08.92	51,57	14,73	x	x	x	x	x	-
306-2	NIOP C1	17.08.92	51,63	14,51	x	x	x	x	-	-
309-2	NIOP C1	19.08.92	52,64	16,11	x	x	x	x	x	-
313-5	NIOP C1	22.08.92	53,01	15,88	x	x	x	x	x	-
918-1	NIOP C2	25.02.93	52,84	15,98	x	x	x	x	x	-
919-1	NIOP C2	25.02.93	52,84	15,98	x	x	x	x	x	-
920-1	NIOP C2	27.02.93	52,70	16,07	x	x	x	x	x	-
921-1	NIOP C2	27.02.93	52,61	16,07	x	x	x	x	x	-
922-1	NIOP C2	28.02.93	52,53	16,18	x	x	x	x	x	-
924-1	NIOP C2	02.03.93	51,60	14,72	x	x	x	x	x	-
925-1	NIOP C2	02.03.93	51,52	14,79	x	x	x	x	x	-
926-1	NIOP C2	03.03.93	51,49	14,85	x	x	x	x	x	-
927-1	NIOP C2	03.03.93	51,45	15,00	x	x	x	x	x	-
928-2	NIOP C2	03.03.93	51,42	15,13	x	x	x	x	x	-

3. Results

North-west Arabian Sea transect

The distribution of water masses and the stratification of the water column in the northwestern Arabian Sea during March 1995 are well reflected in the physical properties. Figure 4a-d illustrates the lateral and vertical distribution of salinity, potential temperature (θ), $\delta^{13}C_{\Sigma CO2}$, and ΣCO_2 concentration along the WSW-ENE transect of Meteor cruise M31/3. Salinity shows a lateral variability of 0.2 to 0.3 psu in the upper 400 m. RSW with a core of 37.2 psu, θ = 17.7 °C and a potential density of σ(θ) =27.2 causes laterally higher salinity gradients of 1.5 psu in a depth range of 350-1200 m in the western Gulf of Aden (Figure 4a).

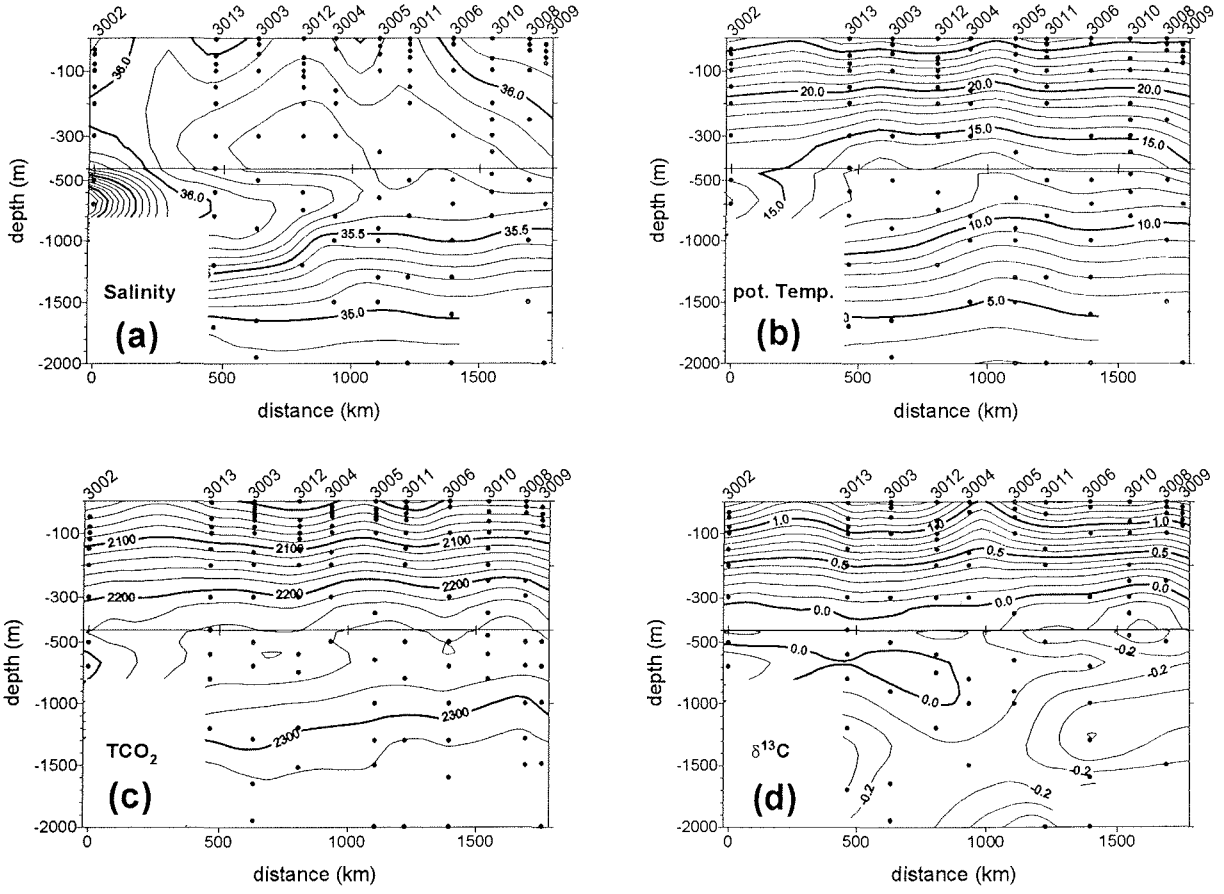

Figure 4. Spatial and vertical distribution of water tracers in the Gulf of Aden during Meteor cruise M31/3; (a) salinity (psu); (b) potential temperature T (°C); (c) phosphate concentration PO_4 (μMol kg^{-1}); and (d) $\delta^{13}C_{\Sigma CO2}$ (‰ PDB)

This corresponds to the signature of RSW in the Gulf of Aden given by Wyrtki (1971) for RSW. Potential temperature shows only in the depth interval of RSW significant lateral changes of 6 °C. Temperature decreases from 26 °C at the surface to 18 °C at 300 m. Below the thermocline potential temperature drops to 3 °C at 2000 m (Figure 4b). ΣCO_2 increases with depth from surface values of 1980-2030 μMol kg^{-1} to 2330 μMol kg^{-1} at 2000 m and

shows only for RSW a remarkable variation (Figure 4c). $\delta^{13}C_{\Sigma CO2}$ varies between 1.2 and 1.6 ‰ PDB in the upper 50 m of the water column. From 50 to 130 m the $\delta^{13}C_{\Sigma CO2}$ decreases to about –0.1 ‰. Below the thermocline the values vary only in a small range between –0.3 and 0.2 ‰, with a slight secondary maximum of 0.0-0.1 ‰ at 700-800 m. The lowest values around –0.3 ‰ are observed between 1200 and 1600 m (Figure 3). Apparently, significant lateral variation occurs at depths below 300 m that are related to the RSW and the oxygen minimum zone. RSW shows a relative $\delta^{13}C$ maximum of 0.2 ‰ in its core in the western Gulf of Aden decreasing to nearly 0.0 ‰ north of Socotra (Figure 4d).

Seasonal variability

To describe the seasonal changes of the coastal upwelling system we used the carbon isotope composition of the water column, in combination with the nutrient and CTD measurements. Figure 5 shows the vertical $\delta^{13}C_{\Sigma CO2}$, phosphate, salinity, and temperature distribution in the upper 500 m of the water column during SW- and NE-monsoon season for the NIOP cruises C1 and C2, respectively. The strong seasonal difference between NE- and SW-monsoon season is shown by all parameters.

NE-monsoon samples show nearly constant values in the upper 50 to 80 m of the water column and strong gradients within the thermocline between water depths of 50-150 m. At greater depth, down to 500 m, all parameters are nearly constant. During the NE-monsoon season the $\delta^{13}C_{\Sigma CO2}$ varies between 0.9 and 1.5 ‰ in the upper 50 m of the water column and drops to values around 0 ‰ below a water depth of 150 m. Phosphate concentrations vary inversely with the carbon isotope composition with a minimum in the upper 30 m of 0.26 µMol kg^{-1} and a subsequent increase to 2.6 µMol kg^{-1} at 500 m. Changes in salinity show a distribution similar to the other parameters. Surface values between 36.1 and 36.2 psu drop to a minimum around 35.6 psu at a water depth of 150-250 m, increases to 35.94 psu at 500 m. Temperature shows similar variation to $\delta^{13}C_{\Sigma CO2}$ with a maximum of 26.7 °C at the surface and minimum values between 12.5 and 18 °C below the thermocline. In contrast to other parameters potential temperature decreases continuously below the thermocline to 12.0 °C at 500 m.

The vertical variability of all analysed parameters is much lower during SW-monsoon season. In contrast to the NE-monsoon the most pronounced vertical gradients occur in the uppermost 30 m of the water column. Average surface temperatures are around 21.0 °C with maximum values of 25.7 °C (station 313-5). Between 30 and 500 m temperature decreases

from 18 to 13 °C. Salinity shows the least variation ranging between 35.62 and 35.75 psu in the upper 500 m, except at station 313-5 with a value of 35.97 psu near the surface. The average phosphate concentration is 1.6 μMol kg^{-1} in the upper 30 m. $\delta^{13}C$ varies in the range of -0.1 ‰ below 30 m to 1.0 ‰ at the sea surface. PO_4 and $\delta^{13}C$ are nearly homogenous between 30 and 500 m, with values of 2.5 μMol kg^{-1} and 0.0 ‰, respectively.

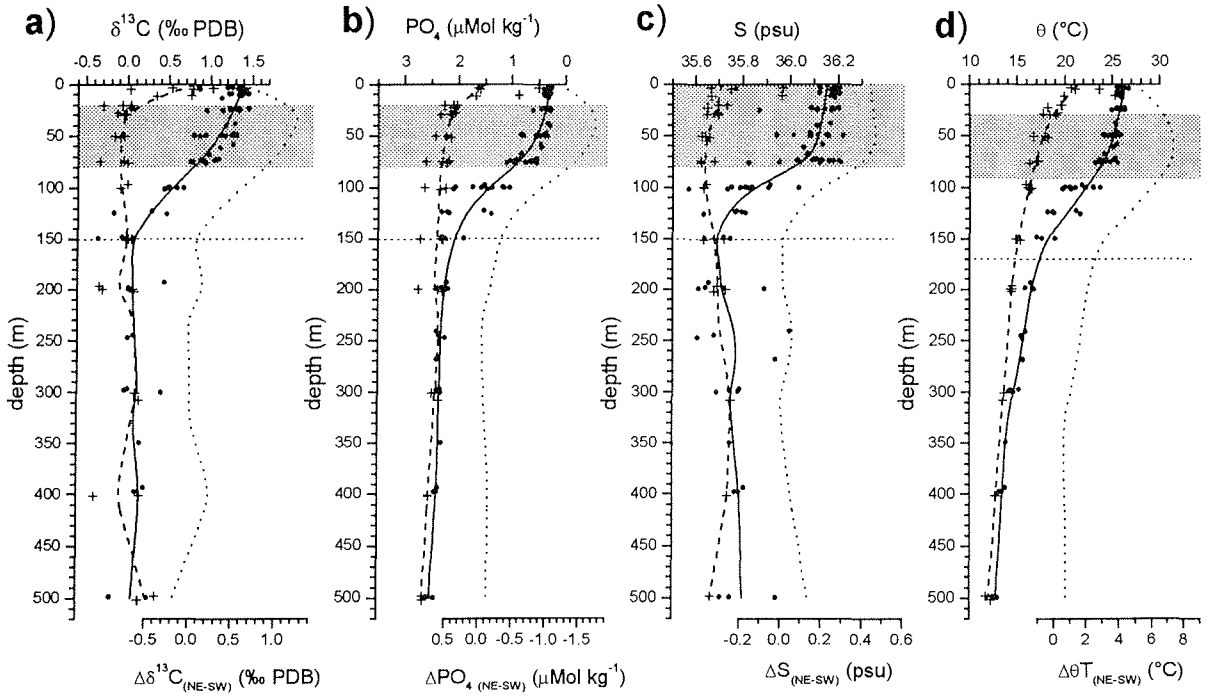

Figure 5. Hydrographic parameters versus depth of NIOP cruises C1 and C2. Crosses - SW-monsoon data; filled dots - NE-monsoon data, dashed lines - average profile of SW-monsoon data, solid lines - average profiles of NE-monsoon data, dotted lines - difference of averaged profiles (NIOP C2-C1), the shaded areas mark the depth range of the highest seasonal difference; above the dotted, horizontal line a clear seasonal gradient is observed; (a) $\delta^{13}C_{\Sigma CO2}$; (b) phosphate; (c) salinity; (d) potential temperature.

The largest seasonal variation for all parameters occurs in the depth interval between 20-80 m. The seasonal difference in the carbon isotope composition $\Delta\delta^{13}C$(NE-SW) is 0.6 ‰ at the sea surface and reaches a maximum of 1.3 ‰ at 30 m, decreasing to nearly 0 ‰ below 150 m. ΔPO_4(NE-SW) shows a similar variation with a maximum of 1.8 μMol kg^{-1} at 30 m and a surface difference of only 1.2 μMol kg^{-1}. The seasonal temperature difference is only 4.5 °C at the surface, but increases to more than 7 °C at 60 m. Salinity is the only parameter with a nearly constant seasonal difference of 0.45 psu in the uppermost 80 m. Below the difference decreases to 0-0.1 psu.

Redfield ratio and Long-term variability

To asses long-term changes in the carbon budget we compared our data with those from GEOSECS position 413. Figure 6 illustrates the differences of total carbon dioxide normalised to constant salinity ($N\Sigma CO_2=\Sigma CO_2 * 35/S$) and the ratios of NO_3/PO_4, $\delta^{13}C/PO_4$, and $\delta^{13}C/NO_3$ between GEOSECS and the Meteor M31/3 - NIOP data, respectively. The normalisation of ΣCO_2 to a constant salinity (35 psu) removes the variations due to mixing, evaporation or dilution. To compare $N\Sigma CO_2$ of GEOSECS and Meteor cruise M31/3 the data were interpolated to common depth intervals. The two $N\Sigma CO_2$ data-sets of GEOSECS and M31/3 do not show a continuous 1:1 relation. A shift around 20 µMol kg^{-1} can be observed for the upper 200 m.

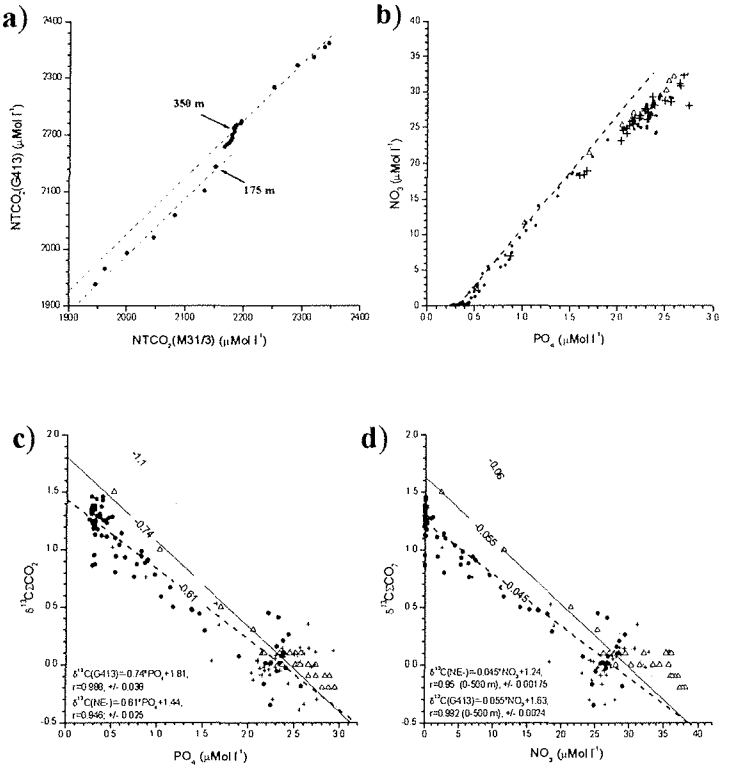

Figure 6. Relationships between nutrient tracers and carbon isotope composition of ΣCO_2. (a) correlation of $N\Sigma CO_2$ between GEOSECS and M31/3. Data are linear interpolated to depth of GEOSECS samples. (b)-(d) filled dots - NIOP C2 data of NE-monsoon season, crosses - NIOP C1 data of SW-monsoon season, triangles - GEOSECS station 413. (b) NO_3/PO_4 ratios, the dashed line reflects the Redfield ratio.

The ratio of nitrogen to phosphorus was NO_3/PO_4=13.32 ±0.15 for NE-monsoon samples of NIOP cruise C2 and 0.12 higher than those of NIOP cruise C1 (13.44 ±0.27). The estimated slope for all NIOP samples is 13.19 ± 0.13. This is lower than the global Redfield ratio ($\Delta N/\Delta P$ = 16) (Redfield et al., 1963), but is in general agreement with the values given by Millero et al. (1998) ($\Delta N/\Delta P$ = 13.53 ± 0.06) and Hupe et al. (1998) ($\Delta N/\Delta P$ = 13) for Arabian Sea waters. Considering the effect of denitrification Hupe and Karstensen (2000) found a $\Delta N/\Delta P$ ratio of 14.4 within the oxygen minimum zone of the northern Arabian Sea. Because of NO_3 oxidisation in the oxygen minimum layer, we compared an expected NO_3

concentration with the in situ measured nitrate concentrations. The calculation based on an idea of Broecker and Peng (1982) who multiplied the global $\Delta N/\Delta P$ ratio of Redfield (1963) with the phosphate concentration to estimate an expected NO_3 concentration. Gruber and Sarmiento (1997) defined a quasi-conservative nitrogen tracer N* which is mainly affected by denitrification and nitrogen fixation. This tracer contains the difference between the observed and the expected nitrate concentration. Figure 7 shows the calculated tracer N* and the oxygen concentration plotted versus depth. NE-monsoon samples show NO_3 depletion between -2 and -3 μMol kg^{-1} in the upper 100 m of the water column. The highest deviation of -8 to -10 from the expected Nitrate concentration was found between 150 and 250 m. Below 250 m the values range within -5 to -10 μMol kg^{-1}. These values coincide generally with oxygen concentration lower than 20 μMol kg^{-1} below 150 m. SW-monsoon samples show a more homogenous distribution. Below 30 m N* shows concentrations in a range of -4 to -8 μMol kg^{-1} and coincides again with oxygen concentration below 20 μMol kg^{-1}. At the sea surface oxygen covers a range between 130-230 μMol l^{-1} and N* varies within (–2)-(-5) μMol l^{-1}.

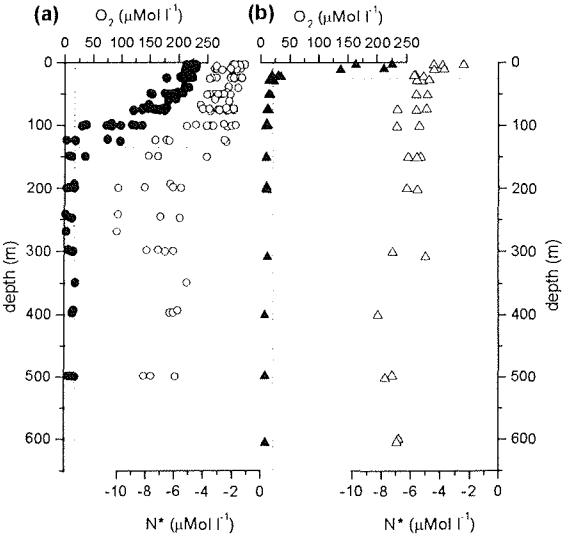

Figure 7. Oxygen concentration in the water column compared with a calculation of the seasonal nitrate deficit relative to phosphate using a quasi-conservative tracer N* defined by Gruber & Sarmiento (1997). (a) NE-monsoon season; (b) SW-monsoon season

Because of the biological fixation of dissolved inorganic carbon and nutrients, the carbon isotope composition of sea water changes by about -1.1 ‰ per μMol kg^{-1} increase in PO_4 concentration, if there was no air-sea fractionation (Broecker and Maier-Reimer, 1992). The changes of $\delta^{13}C$ due to NO_3 are 0.062 ‰ per μMol kg^{-1} if there was no additional influence of the nitrogen cycle. Changes in the photosynthesis-respiration cycle as well as changes in the $^{13}C/^{12}C$ ratio lead to different slopes of $\delta^{13}C_{\Sigma CO2}$ versus PO_4 or NO_3. The observed slopes for GEOSECS data ($\delta^{13}C/PO_4 = -0.74$; $\delta^{13}C/NO_3 = -0.055$) are less steep than expected from biological fractionation alone ($\delta^{13}C/PO_4 = -1.0$; $\delta^{13}C/NO_3 = -0.06$), but steeper

than measured in February and March 1993 ($\delta^{13}C/PO_4 = -0.61$; $\delta^{13}C/NO_3 = -0.045$) 15 years later. The $\delta^{13}C_{\Sigma CO2}$ values of GEOSECS station 413 are around 0.3 ‰ heavier than the NIOP data at the sea surface. Below a water depth of 250 m all data vary within the same range (Figure 4c, d). Most samples of August 1992 (NIOP C1) show $\delta^{13}C_{\Sigma CO2}$ values between –0.2 and 0.2 ‰ or NO_3 of 22-30 µMol kg^{-1}. These SW-monsoon values correspond to NE-monsoon data below 200 m.

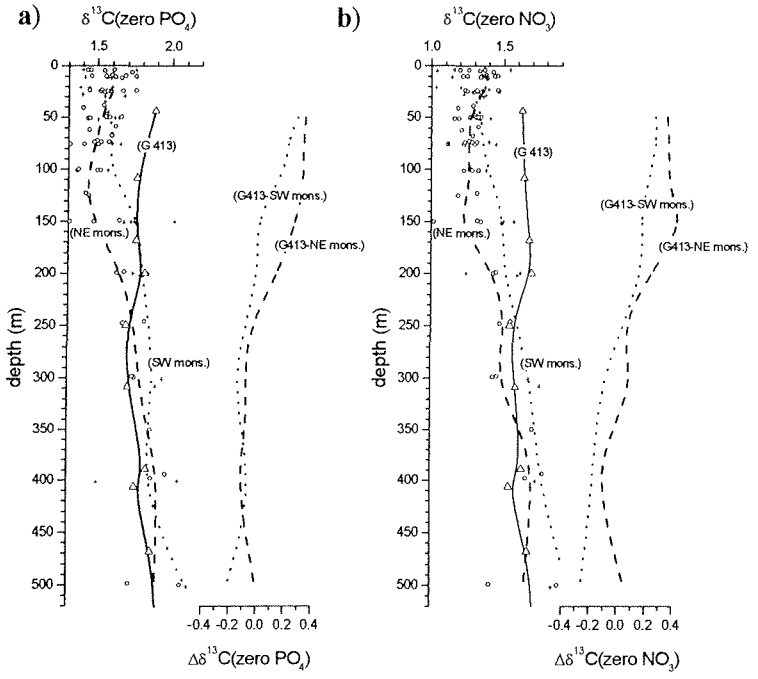

Figure 8. Nutrient normalised profiles of 1992/93 in comparison to GEOSECS data of 1977. (a) $\delta^{13}C_{\Sigma CO2}$ normalised to zero phosphate; (b) $\delta^{13}C_{\Sigma CO2}$ normalised to zero nitrate. Dots – NE-monsoon values; crosses – SW-monsoon values; triangles – GEOSECS data; dashed line – average profile of NE-monsoon samples; dotted line – average profile of SW-monsoon samples; straight line – average profile of NE-monsoon samples. The two profiles on the right in the figures a) and b) show the difference of the averaged profiles to GEOSECS; dotted line – dashed line - GEOSECS-(NE-monsoon); GEOSECS-(SW-monsoon).

To analyse the difference between GEOSECS and our data we normalised the NIOP data to zero phosphate or nitrate, based on the $\delta^{13}C/PO_4$, $\delta^{13}C/NO3$ relationship determined by the GEOSECS data of 1977 (Figure 8). Between phosphate and nitrate normalised $\delta^{13}C_{\Sigma CO2}$ data a general difference of 0.23 ‰ can be observed. This due to a PO_4 content of 0.31 µMol kg^{-1} while the corresponding NO_3 concentration is zero (see Figure 6b). However, phosphate and nitrate normalised $\delta^{13}C_{\Sigma CO2}$ data of both NIOP cruises show a deviation to GEOSECS in the same order and direction, althoughthe amount varies with depth. Because we used the GEOSECS relation for the normalisation the corresponding GEOSECS profileshows no obvious variations with depth, only a slight decrease of 0.1 ‰ in $\delta^{13}C_{\Sigma CO2}$ is observed between 200 and 250 m. In contrast normalised $\delta^{13}C_{\Sigma CO2}$ of NIOP cruise C2 (C1) increases below 150 m (100 m) from 1.6 ‰ at the surface to values about 1.9 ‰ at 500 m.

4. Discussion

Seasonal variability of hydrographic conditions

All analysed parameters mirror the structure of the water column prevailing during the sampling periods. Samples collected during NIOP cruise C2 and Meteor cruise M31/3 reflect the strong stratification of the water column during the winter season. Samples of NIOP cruise C1 show the vertical homogenisation of the water column while upwelling occurs during summer season. Except for salinity, all parameters show strong vertical gradients near the sea surface during SW-monsoon. Salinity shows a nearly complete homogenisation of the water column in the upper 500 m. Thus salinity is the only parameter, which clearly indicates the presence of freshly upwelled water at the sea surface. Temperature increases because of summer heating, while the decrease of nutrient concentration and the corresponding increases of $\delta^{13}C_{\Sigma CO2}$ reflect the influence of primary production. Generally the seasonal differences cover four depth ranges: (1) The upper 20-30 m. Due to primary production, seasonal heating, and mixing processes the signature of upwelled water in the uppermost 20 m reflects not the maximum upwelling signal. Thus the seasonal gradient close to the sea surface is lower than the maximal difference. (2) The maximal seasonal gradient between 30-80 m. The surface signal of all parameters extends to 80 m depth during the NE-monsoon. During upwelling season the water signature in the range from 20-80 m corresponds to subthermocline water of NE-monsoon. Hence the seasonal variation is largest in this depth interval. (3) Depth interval of the winter thermocline (80-150 m). While upwelling occurs the water column is nearly homogenised below 20-30 m. In contrast in the depth range of the winter thermocline the strongest vertical gradients exist. (4) None of the parameters shows significant inter annual variability below 150-200 m.

Variations of the NO_3/PO_4 ratio, denitrification

As shown in Figure 6b and summarized in Table 2 the NO_3/PO_4 ratio in the northwestern Arabian Sea is lower than the relation of Redfield et al. (1963). The dashed line shows the global Redfield ratio (NO_3/PO_4=16). Values below this line indicate a loss of nitrate relative to phosphate concentration. All samples show significant nitrate depletion in the upper 600 m of the water column. A reason for this loss of nitrate might be the denitrification process in the oxygen minimum zone where nitrate is used as oxidising agent. For the Arabian Sea denitrification is described by Mantoura et al. (1993); Naqvi (1987); Naqvi and Noronha (1991); Naqvi and Sen Gupta (1985). We found high nitrate depletion coinciding with oxygen concentrations below 20 $\mu Mol\ l^{-1}$. Therefore we checked the NO_3/PO_4 relation for oxygen

concentrations above and below 20 μMol kg^{-1}. NE-monsoon samples show O_2 concentrations >20 μMol kg^{-1} in the upper 150 m of the water column. The NO_3/PO_4 ratio of these samples is 14.12 (± 0.19) and is in good agreement with observation of Millero et al. (1998) for Arabian Sea surface water. For samples with oxygen concentrations below 20 μMol kg^{-1} we found a much lower slope of 11.49 (± 1.03) for the NO_3/PO_4 ratio. Comparable results are found by Hupe et al. (1998) in the Arabian Sea for a water depth below 500 m. The different ratios between nitrate and phosphate are summarised in Table 2. The large uncertainty in the relation of low oxygen water is due to generally high nutrient concentrations and the small range covered in our data. Additionally it must be taken into account, that a variable intensity of denitrification causes no constant nutrient ratios in the water column.

However, we find different NO_3/PO_4 ratios in the upper water column and for both monsoon seasons. If these variations are due to significant NO_3 depletion within the oxygen minimum layer nutrient normalised $\delta^{13}C_{\Sigma CO2}$ values must show clear differences between phosphate and nitrate normalised profiles. Because we found a good agreement between NO_3/PO_4 ratios of GEOSECS and our data we assume no changes in the nutrient budget. The GEOSECS data show a NO_3/PO_4 of 13.98 (± 0.31) which is close to our value of NE-monsoon samples with oxygen concentrations > 20 μMol kg^{-1} (14.12, ± 0.19). For our nutrient normalisation of $\delta^{13}C_{\Sigma CO2}$ we used the GEOSECS correlation between $\delta^{13}C_{\Sigma CO2}/PO_4$ and $\delta^{13}C_{\Sigma CO2}/NO_3$. In comparison to GEOSECS the difference of nitrate and phosphate normalised profiles is within the error of the $\delta^{13}C$ values. Thus we assume that denitrification in the Arabian Sea is an important factor compared to the global ocean, but the seasonal loss of nitrate plays only a secondary role.

Long-term trend of $\delta^{13}C_{\Sigma CO2}$

The nutrient normalised $\delta^{13}C_{\Sigma CO2}$ values show a decrease of 0.3 ‰ at the sea surface from 1977 to 1993. This is near the value of 0.4 ‰ given by Quay et al. (1992) estimated from data of the Pacific Ocean for a period of twenty years (1970-1990). Generally the release of fossil fuel CO_2 and the uptake by the oceans is associated with the lowering of $\delta^{13}C_{\Sigma CO2}$ of seawater. This is not self evident for upwelling areas which act frequently as sources of CO_2 into the atmosphere. Goyet et al. (1999) for example observed a net ΔpCO_2(atm-sea) in the order of 50 μatm in the upwelling area of Yemen and Oman during SW-monsoon.

Therefore, additional possibilities have to be taken into account to explain the variability of carbon isotope composition in the northwestern Arabian Sea. For this purpose we use the

correlation between $\delta^{13}C_{\Sigma CO2}$ and our other hydrographic measurements. Because $^{13}C/^{12}C$ variations in seawater are mainly controlled by the photosynthesis-respiration cycle, we use equation (1) formulated by Broecker and Peng (1982) to asses the effect of the single parameters to the $\delta^{13}C$/nutrient relationship. The difference between the real biological fractionation and the measured $\delta^{13}C_{\Sigma CO2}$ reflect the common influence of a thermodynamic and a fossil fuel induced effect. Although we can neither quantify the real slope of the biological fractionation nor determine the thermodynamic effect or a pre-industrial $\delta^{13}C_{\Sigma CO2}$ value, we can use the differentce in the gradients of the $\delta^{13}C$/nutrient relationships between two data-sets to discuss the variability of the hydrographic system. Different slopes of the data-sets correspond to changes of the $\delta^{13}C_{\Sigma CO2}$ and/or to variations in the photosynthesis-respiration cycle. To discuss alternative effects to a fossil fuel induced alteration of the $^{13}C/^{12}C$ ratio we assume that variations in $\delta^{13}C_{\Sigma CO2}$ are exclusively controlled by the parameters considered in equation (1).

The biological coefficients of equations (2) and (3) are theoretical approximations and the parameter of the equations vary within the ocean. Francois et al. (1993) observed pCO_2-independent variations of $\delta^{13}C$*plant* near 5 ‰ in the equatorial Indian Ocean, which entails a change of the coefficient of 0.29 for a phosphate and 0.016 for a nitrate-based normalisation. For surface waters of the Arabian Sea and the equatorial Pacific Ocean the $\Delta C/\Delta P$ ratio varies in a range of 90-125 Millero et al. (1998); Steinberg et al. (1998), corresponding to changes in the $\delta^{13}C/PO_4$ slope of 0.26. To estimate the influence of changes in the $N\Sigma CO_2$ concentration we compare the GEOSECS data with M31/3 measurements (Figure 6a). The gradient of the GEOSECS 413 data as a function of $N\Sigma CO_2$(M31/3) is close to one and the intercept is near zero. The observed variations are lower than 30 µMol kg^{-1}. Even if an additional calibration offset around 30 µMol kg^{-1} is taken into account, the slope of the $\delta^{13}C$/phosphate relation (equation 1) changes less than 0.05 ‰ kg μMol^{-1}. To cause changes in the observed range the concentration of ΣCO_2 must increase over 400 µMol kg^{-1}. There are no distinguishable differences in the nutrient and carbon measurements between GEOSECS and NIOP or M31/3, respectively. Hence there is no possibility to explain the different of the $\delta^{13}C$/nutrient relationships only by changes in concentrations of the parameters discussed above. For changes in $\delta^{13}C$*plant* we have no measurements that support a variability of the phytoplankton community and its isotope composition. Nevertheless an influence on the $^{13}C/^{12}C$ ratio induced by variations of the phytoplankton community cannot be excluded. Thus we believe that the $\delta^{13}C_{\Sigma CO2}$ changes are due to a variation of the carbon isotope composition itself.

Our data are consistent with a long-term decrease of $\delta^{13}C_{\Sigma CO2}$ in the order of 0.3 ‰ induced by the ocean uptake of fossil fuel CO_2. At the sea surface the effect is evident for samples from both NIOP cruises (Figure 8). The vertical, nutrient normalised $\delta^{13}C_{\Sigma CO2}$ profiles of summer upwelling season seem to be shifted upward for 100-150 m relative to the NE-monsoon data. Thus the difference between the normalised $\delta^{13}C$ profiles of SW- and NE-monsoon season indicate different water types participate in the upwelling process.

Additionally a downward transport of anthropogenic CO_2 by the marine biosphere might be a reason for the difference between the normalised $\delta^{13}C$ profiles of NE- and SW-monsoon season. If the marine biosphere prefers ^{12}C the seasonally high primary production could buffer an anthropogenic induced lowering of the $^{13}C/^{12}C$ ratio of the ΣCO_2 by calcification and photosynthesis. After the death of marine organisms and sinking to deeper water levels the remineralisation of calcite tests and organic matter to ΣCO_2 causes a large penetration depth of fossil fuel CO_2 when seasonal upwelling finished. Such a redistribution of carbon isotopes is also noted by Heimann and Maier-Reimer (1996). For the seasonal upwelling system of the northern Arabian Sea this hypothetical idea can be described by a simplified annual cycle. Marine organisms cause a fixation of ^{12}C during upwelling season and a downward transport after their death, when upwelling finished, followed by remineralisation to dissolved inorganic carbon. This is in general agreement with the observation of the low seasonal gradient of nutrient concentration and $\delta^{13}C_{\Sigma CO2}$ near the sea surface, which implies that primary production is fast enough to strip surface water nearly free of nutrients while upwelling occurs.

Table 2: Comparison of stoichiometric NO_3/PO_4 ratios for different water types of the Arabian Sea.

	Remarks	$\Delta N/\Delta P$	Error (±)
Redfield et al. (1963)		16	
Millero et al. (1998)	Surface water	14.19	0.05
Millero et al. (1998)	Surface + deep water	13.53	0.06
GEOSECS	Northwest Arabian Sea	13.98	0.31
This study	NE-monsoon (0-600 m)	13.19	0.13
This study	SW-monsoon (0-600 m)	13.44	0.27
This study	NE- + SW-monsoon (0-600 m)	13.32	0.15
This study	NE-monsoon (0-150 m) $O_2 \geq 20$ µMol kg^{-1}	14.12	0.19
This study	SW- & NE-monsoon $O_2 < 20$ µMol kg^{-1}	11.49	1.03

5. Conclusions

All analysed water tracers reflect the strong stratification of the water column during NE-monsoon with a mixed layer depth around 80 m. In contrast, the distribution of the carbon isotope composition in the upper 500 m is nearly homogenous in the area of upwelling during SW-monsoon. The influence of summer heating and primary production during upwelling lowers the seasonal difference at the sea surface. Therefore the strongest seasonal differences of temperature, nutrient concentrations, and $\delta^{13}C_{\Sigma CO2}$ occur between 20 and 80 m. Below 150-200 m the seasonal gradient between upwelling and non-upwelling season decreases to zero.

A comparison of ΣCO_2 data, nutrient concentrations, and phosphate/nitrate ratios between GEOSECS and our modern data suggest no variations in the hydrographic conditions. The $\delta^{13}C$ decrease of 0.3 ‰ within a period from 1977-1993 is interpreted in terms of the influence of anthropogenic $^{13}CO_2$ in the north-western Arabian Sea. This effect is evident for the data at the sea surface for both monsoon seasons. The nutrient normalised $\delta^{13}C_{\Sigma CO2}$ values are 0.2 ‰ heavier between 80-150 m during NE-monsoon season compared to upwelling situation. This might be related to a redistribution of the carbon isotope ration by marine organisms coupled with an upward mixing during upwelling.

The observed $\Delta N/\Delta P$ relations show strong deviations from the Redfield ratio, due to denitrification. The highest nitrate deficit coincides with oxygen concentrations below 20 µMol kg^{-1}. Although NO_3/PO_4 relationship shows the lowest slopes for oxygen deficient water the nutrient normalised $\delta^{13}C$ data indicate only minor additional nitrate depletion. The $\Delta N/\Delta P$ ratio of SW-monsoon samples near the sea surface as well as nutrient normalised $\delta^{13}C_{\Sigma CO2}$ values show the same characteristic as NE-monsoon samples between 150-200 m indicating this depth range as source depth of upwelled water.

6. Acknowledgements

We thank the captains and crews of *F.S. Meteor* and *R/V Tyro* for the excellent cooperation during the cruises. T. Bickert provided critical comments on an early version of the paper. The research was funded by the Bundesministerium für Bildung, Wissenschaft, Forschung und Technologie (BMBF) and is part of the NEtherlands BRemen OCeanography (NEBROC) cooperation.

The data presented in this paper are archived in the Pangea database (http://www.pangaea.de).

3. Stable isotopes in planktic foraminifera recording monsoonal upwelling in the northwest Arabian Sea

(submitted to "Marine Micropaleontology")

Christopher A. Moos[1,*], Ralf Schiebel[2], Ralph R. Schneider[1], and Gerold Wefer[1]

[1] Universität Bremen, Fachbereich Geowissenschaften, Klagenfurter Straße, Postfach 330 440, D-28359 Bremen, Germany

[2] Universität Tübingen, Institut und Museum für Geologie und Paläontologie, Sigwartstr. 10, D-72076 Tübingen, Germany

Abstract

Stable isotope results of different foraminiferal species were compared with the seasonal hydrographic conditions and carbon isotope variations of seawater. For the determination of oxygen isotope equilibrium values we additionally analyzed the oxygen isotope composition of ambient seawater and calculated the $\delta^{18}O$/salinity relationships for three important water masses of the northwest Arabian Sea. The aim was to reveal whether changes in upwelling conditions are recorded in oxygen and carbon isotope composition of planktic foraminifera, and may be preserved in sediment assemblages. Planktic foraminifera *Globigerinoides ruber* (white variety), and *Neogloboquadrina dutertrei* were available from plankton tows and sediment surface samples. The oxygen and carbon isotopes of *G. ruber* (w) and *N. dutertrei* were compared with the seasonal range of water isotope composition. The carbon isotope relationship between foraminifera and water is considered after assuming equilibrium calcification for oxygen isotopes. Under this assumption *G. ruber* (w) shows a size-related

* Corresponding author. Fax: 0049 421 218 3116; e-mail: moos@allgeo.uni-bremen.de

depletion in ^{13}C relative to the dissolved inorganic carbon of ambient seawater. The smallest $\delta^{13}C$ offset of 0.76 ‰ was observed for the largest analysed size fraction of 250-315 µm. The analysis of sediment surface samples shows that the $\delta^{13}C$ and the $\delta^{18}O$ values of *G. ruber* (w) are in accordance with sea surface conditions indicating low nutrient concentrations. In contrast, *N. dutertrei* suggests a spatial migration according to upwelling strength. The estimated depth habitat of *N. dutertrei* coincides with lowest $\delta^{13}C$ values of ambient seawater (and the highest nutrient concentrations) observed in the upper water column during upwelling season. Within the observed range of upwelling variability the carbon isotope difference between *G. ruber* (w) and *N. dutertrei* is related to upwelling intensity and documents the maximum seasonal gradient of seawater $\delta^{13}C$.

Keywords: C-13/C-12, O-18/O-16, stable isotopes, upwelling, foraminifera, monsoon, Arabian Peninsula

1. Introduction

The stable isotope composition of planktic foraminiferal tests is an important tool for paleoceanographic reconstructions. Carbon and oxygen isotopes have been used for reconstructions of temperature, salinity, and the carbon isotopic composition of dissolved inorganic carbon ($\delta^{13}C_{\Sigma CO2}$) (Shackleton and Pisias, 1985; Duplessy et al, 1988; Spero and Williams, 1990; Rostek et al., 1993; Billups and Spero, 1996; and others). Much work has been carried out using foraminiferal isotope ratios to study histories of upwelling and paleoproductivity in different regions, e.g. off Peru (Wefer et al., 1983), northwest Africa (Ganssen and Sarnthein, 1983), eastern equatorial Atlantic (Schneider et al., 1994), and in the Arabian Sea (Prell and Curry, 1981; Steens et al. 1992).

Potential problems when interpreting stable isotopes in foraminifera are unknown factors like the preferential depth habitat and season of growth for different species as well as deviations in the isotope composition of the calcareous tests relative to the isotopic equilibrium expected for inorganic calcite precipitation. For oxygen isotopes most authors find that planktic foraminifera built their tests close to equilibrium conditions and show only small and constant offsets (Bouvier-Soumagnac and Duplessy, 1985; Duplessy, 1978; Erez and Honjo, 1981, Fairbanks et al., 1982). Hence, foraminiferal $\delta^{18}O$ should be controlled by oxygen isotope composition of the seawater ($\delta^{18}O_{H2O}$) and temperature related fractionation.

In contrast, the seawater-foraminifera relationship for carbon isotopes is much more complex than for oxygen isotopes. Most planktic foraminifera show large deviations in their carbon isotope composition relative to equilibrium calcite and a clear size depended fractionation of $^{13}C/^{12}C$ (Berger, 1981; Kroon and Darling, 1995). Spero et al. (1997) showed that stable isotope ratios of foraminiferal calcite are strongly affected by pH and the concentration of seawater carbonate. Nevertheless, the fractionation of carbon isotopes in foraminiferal tests is as yet not completely understood. To further develop foraminiferal $\delta^{13}C$ to a more useful paleoceanographic indicator of past water-mass properties regional calibrations of living foraminifera from plankton tows to prevailing water conditions are necessary. In the tropical Atlantic Ocean Ravelo and Fairbanks (1992) and Mulitza et al. (1999) derived such carbon isotope disequilibria of recent planktic foraminifera from surface sediments and plankton tows. Kroon and Ganssen (1989) proposed an empirical model to explain the $\delta^{13}C$ signals of different foraminiferal species in relation to the hydrographic environment across the northern Indian Ocean and the Red Sea.

In this study we investigate the stable isotope composition of the planktic foraminiferal species *G. ruber* (w) and *N. dutertrei* in relation to the seasonal hydrographic variations in the monsoon area of the western Arabian Sea and the Gulf of Aden. For the determination of specific offsets relative to isotope equilibrium conditions we compared isotope measurements of living foraminifera from plankton tows with in situ measurements of $\delta^{13}C_{\Sigma CO2}$, temperature, and $\delta^{18}O_{H2O}$.

We used the results of the plankton tow measurements to correct foraminiferal isotope values from surface sediments for their specific offsets to $\delta^{13}C_{\Sigma CO2}$ and oxygen isotope equilibrium. Obtained by multiple measurements of the same sediment sample, variations in the $\delta^{18}O$ and $\delta^{13}C$ values of a planktic foraminiferal species can indicate variations of the hydrographic conditions, as well as seasonal growth preferences and changes in the relative depth of calcification (Mulitza et al., 1999 and references therein). When a certain number of foraminiferal specimens is analyzed, one obtains the order of magnitude for the range of $\delta^{18}O$ and $\delta^{13}C$ values contained in a sediment assemblage. The offset corrected isotope measurements of foraminiferal tests from sediment surface samples were then compared with $\delta^{13}C_{\Sigma CO2}$ measurements of both monsoon seasons and predicted oxygen isotope equilibrium. This approach allows us to identify the effects of seasonal versus depth-related calcification on the range of stable isotope values from sediment samples. We have chosen three locations for multiple measurements on tests of *G. ruber* (w) and *N dutertrei* from surface sediments

along the Arabian coast. To evaluate the effect of changes in upwelling intensity on *G. ruber* (w), and *N. dutertrei*, we measured foraminifera from surface sediments on transect from the inner Gulf of Aden into the open western Arabian Sea.

2. Oceanography of the study area

The northern Arabian Sea is strongly affected by the Indian Monsoon system. During northern hemisphere summer strong SW-monsoon winds blow parallel to the coasts of Africa and the Arabian Peninsula (Figure 1). This wind field induces Ekman drift causing intensive upwelling and an offshore transport of surface water. During upwelling cold, nutrient rich water reaches the sea surface. Lowest sea surface temperatures (SST) of ~25 °C are observed during January-February and June-August while highest values around 28 °C are reached in spring and slightly lower in fall (Wyrtki, 1971). Hence, the seasonal amplitude of SST reaches only 3 to 4 °C in the upwelling centre of the Arabian Sea. Nevertheless, due to the high fertility conditions most planktic forminifera have their maximum abundance during upwelling season (Curry et al. 1992; Peeters et al., 1999). The high nutrient concentrations of freshly upwelled water are paralleled by low $\delta^{13}C_{\Sigma CO2}$ values. Due to preferential uptake of ^{12}C during primary productivity in the upper water column after the upwelling event started the seasonal $\delta^{13}C_{\Sigma CO2}$ gradient is about 1.3 ‰ Moos et al. (submitted). Mixed layer $\delta^{13}C_{\Sigma CO2}$ values are around 1.4 ‰ during NE-monsoon season. While upwelling takes place $\delta^{13}C_{\Sigma CO2}$ drops down to ~0.7 ‰ at the sea surface and to ~0.1 ‰

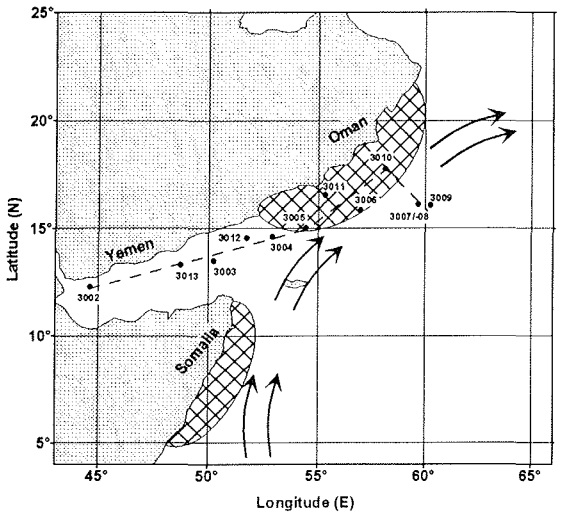

Figure 1. Map of the northwest Arabian Sea showing the sampling locations of Meteor cruise M31/3. The cross-hatched areas approximate the upwelling cells off Somalia and Oman. Arrows indicate the path of upper ocean circulation and SW-monsoon winds causing coastal upwelling during summer season. The dashed line shows the transect illustrated in Figure 8. Numbers refer to GeoB numbers (Tab. 1).

Table 1. Locations of sediment surface samples covered during Meteor cruise M31/3

Station GeoB #	Meteor #	Latitude	Longitude	depth (m)
3002-1	105	12°17,4'N	44°38,3'E	736
3003-5	106	13°29,6'N	50°17,7'E	2013
3004-9	107	14°36,3'N	52°55,1'E	1800
3005-3	108	14°58,2'N	54°22,2'E	2313
3006-2	109	15°49,7'N	56°59,7'E	3505
3007-3	111-1	16°10,2'N	59°46,3'E	1916
3008-5	111-2	16°05,5'N	59°41,1'E	2242
3009-2	110-3/-4	16°12,6'N	60°16,8'E	4071
3010-2	112	17°45,0'N	58°09,0'E	3154
3011-3	113	16°32,0'N	55°19,9'E	2624
3012-1	114	14°32,4'N	51°44,9'E	1539
3013-2	115	13°18,6'N	48°46,9'E	1729
3014-2	116	12°51,8'N	47°26,1'E	1644

between 30 and 80 m (Moos et al., submitted). Also for temperature and nutrient concentrations the observed gradients are lower at the sea surface than between 30-80 m water depth. This vertical difference during the upwelling situation has to be taken into account when dealing with the stable isotope signal of planktic foraminifera dwelling in differentwater depths. Due to the two minima of the sea surface temperature during NE- and SW-monsoon season, a combined interpretation of oxygen and carbon isotopes offers a more precise method to assign planktic foraminifera to their seasonal and vertical habitat and to reconstruct upwelling history in time series of marine sediment records.

3. Methods and Materials

3.1. Plankton tows, hydrographical data and sediment samples

In March 1995 at the end of NE-monsoon thirteen stations (Figure 1, Table 1) were sampled in the north-western Arabian Sea, along a transect off the Arabian Peninsula between 40-60° E longitude and 12-18° N latitude (Meteor cruise M31/3, Hemleben et al., 1996). At these stations plankton tows, sediment surface samples, and water samples were taken for isotope analysis of planktic foraminifera and ambient seawater. Water samples were collected with an automatic rosette of 12*12 l Niskin bottles for determination of stable oxygen and carbon isotope ratios. For oxygen isotope analysis water samples of 50 ml were taken and stored in brown borosilicate glass bottles. The bottles were sealed with melted paraffin and stored at 7 °C till measurements were carried out made at the University of Bremen.

Table 2. Locations of Plankton hauls and CTD stations selected during Meteor cruise M31/3

Station Pl. Tow #	Meteor #	Latitude (N)	Longitude (E)	CTD station GeoB #	Meteor #
898	105	12°17,3'N	44°37,5'E	3002-2	105
900	106	13°29,5'N	50°17,8'E	3003-1	106
903	107	14°36,3'N	52°55,1'E	3004-3	107
905	108	14°59,3'N	54°23,7'E	3005-1	108
906	108	14°59,7'N	54°24,8'E	3005-1	108
908	109	15°50,0'N	57°00,1'E	3006-1	109
910	111-1	16°10,1'N	59°45,9'E	3008-4	111-2
913	110-3/-4	16°13,0'N	60°16,2'E	3008-4	111-2
914	110-3/-4	16°13,0'N	60°16,1'E	3008-4	111-2
916	113	16°32,2'N	55°20,0'E	3011-4	113
917	113	16°32,9'N	55°20,1'E	3011-4	113
921	115	13°18,4'N	48°47,1'E	3013-3	115

Information of the hydrographic conditions were obtained, using a *GO 7* rosette equipped with a CTD profiler containing pressure-, temperature-, conductivity- and oxygen sensors (Table 2). On 11 stations plankton tows with a mesh size of 100 µm were used to collect foraminifera from the water column between 0-500 m. Sampling intervals were 0-20-40-60-

80-100-200-300-400-500 m. The preparation of plankton tow samples is described in Schiebel et al. (1995).

3.2. $\delta^{18}O$ and $\delta^{13}C$ measurements of planktic foraminifera

Isotope analyses were carried out using a FINNIGAN/MAT-252 mass-spectrometer equipped with an automatic carbonate preparation device. Precision based on replicates of an internal limestone standard, was better than 0.07 ‰ for $\delta^{18}O$ and 0.05 ‰ for $\delta^{13}C$.

From each plankton tow sample 8 to 12 specimens of *G. ruber* (w) (150-200 µm, 200-250 µm and 250-315 µm) were picked for isotope analyses. Multiple measurements of sediment surface samples were done with five specimens of *G. ruber* (w) (250-300 µm) and 3-4 individuals of *N. dutertrei* (315-400 µm or greater 315 µm). In case of single analyses 10-12 specimens of *G. ruber* (w) and *N. dutertrei* (315-400 µm) were used.

3.3. $\delta^{18}O$ measurements of water samples

For oxygen isotope measurements we used a fully automatic CO_2/H_2O equilibration device designed for 24 water samples, which was coupled with a mass spectrometer type FINNIGAN MAT-DELTA PLUS. The analytical procedure for CO_2 preparation corresponds to the water equilibration method of Epstein and Mayeda (1953). As laboratory standard we used deionised water, which had been calibrated to VSMOW. To convert the $\delta^{18}O$ values of seawater from the SMOW to the PDB scale we added a constant of -0.27 ‰ (Hut, 1987).

We equilibrated CO_2 with 7 µl of a seawater sample under constant temperature conditions of 24 °C. The time for equilibration varied between 7 h for the first and 25 h for the last sample of each run. Normal runs contained 18 actual samples and six laboratory standards. The positions of standards changed for each run by a rotating system. Considering replicate standard values, the overall analytical precision (one sigma) over several months is ± 0.02 ‰.

For $\delta^{13}C$ analysis dissolved inorganic carbon was extracted as CO_2 gas from the water samples, in general following the acid extraction of ΣCO_2 described by Kroopnick (1974). The carbon isotopes of the CO_2 gas were measured using triple collector mass spectrometer. Measurements of duplicate ΣCO_2 samples show a statistical reproducibility of ± 0.16 ‰. The sampling and preparation technique for carbon isotope measurements of $\delta^{13}C_{\Sigma CO2}$ is described in detail in Moos et al. (submitted).

4. Results and Discussion

4.1. $\delta^{18}O_{H2O}$ /salinity relationship in Arabian Sea water masses

In general the oxygen isotope composition of seawater is the major component influencing the $^{18}O/^{16}O$ ratio of inorganic calcite. The strong linear correlation between oxygen isotopes of seawater and salinity allows to calculate $\delta^{18}O_{H2O}$ values or to reconstruct seawater salinity. The general relationship between $\delta^{18}O_{H2O}$ and salinity for different oceans was provided in Craig and Gordon (1965).

The $\delta^{18}O_{H2O}$ measurements of Meteor cruise M31/3 samples cover a transect along the coasts off Yemen and Oman (Figure 1). Three linear $\delta^{18}O/S$ relationships can be distinguished and assigned to different depth of the water column: (1) surface and thermocline water (SW), (2) sub-thermocline water (STW) (except Red Seawater), and (3) Red Seawater (RSW) (700-900 m, ($\sigma\theta$) 27.0-27.4 kg m^{-3}). The classification of the water types SW and STW is based on the thermocline definition of Hastenrath & Merle (1987). Linear regressions for the $\delta^{18}O_{H2O}$-salinity relationships of the different water types are given in Figure 2. The $\delta^{18}O_{H2O}$ values STW samples (-0.05 to 0.45 ‰) show the lowest scatter in the $\delta^{18}O/S$ relationship. The scattering becomes larger for higher $\delta^{18}O_{H2O}$ and salinity values typical for SW and RSW. Due to local differences in the hydrography and the kinetics of evaporation at the sea surface the standard deviation of values for samples of the mixed layer relation is much larger than for the STW water approximation.

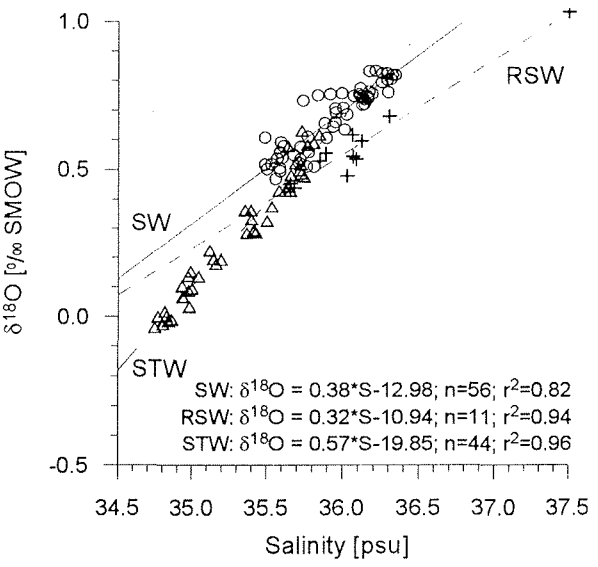

Figure 2. $\delta^{18}O$ measurements of water samples versus salinity; open circles - samples of the upper 300 m (SW); crosses - Red Sea outflow water (RSW) in the Gulf of Aden indicated by a density of 27.3 g cm^{-3}; triangles – sub thermocline water (STW). The straight line represents the regression for surface and thermocline samples used for calculation of predicted oxygen isotope equilibrium calcite.

Because salinity data are availability for both monsoon seasons the $\delta^{18}O$/salinity relationships allow to approximate seasonal $\delta^{18}O_{H2O}$ values and thus to calculate oxygen isotope composition of inorganic calcite precipitated in equilibrium.

4.2. Isotope composition of living planktic foraminifera *G. ruber* (w)

Planktic foraminifera were most frequent in the upper 100 m of the water column. Below 100 m only a few individuals were found. Most abundant species in surface waters were *G. ruber* (w), *Globigerinita glutinata,* and *Globigerinoides sacculifer*. These species always represented more than 50 % of the total assemblage. The test size of *G. ruber* (w) was restricted to >200 μm below a water depth of 100 m. Smaller individuals were concentrated in the uppermost 60 m.

To derive the relationship of the isotope composition of *G. ruber* (w) to calcite precipitated in equilibrium we plotted the isotope values of the foraminiferal tests minus $\delta^{18}O$ of ambient seawater versus temperature (Figure 3a). Plankton tow samples of *G. ruber* (w) collected within the uppermost 100 m follow the $\delta^{18}O/T$ relationships of Duplessy (1981) and Bemis et al. (1998) (Figure 3a, b). Samples collected below a water depth of 100 m show an increasing deviation up to 2.2 ‰ from oxygen isotope equilibrium with increasing sampling depth. Due to sinking of dead individuals and possible vertical migrations of planktic foraminiferal species during ontogeny the sampling depth must not be identical with

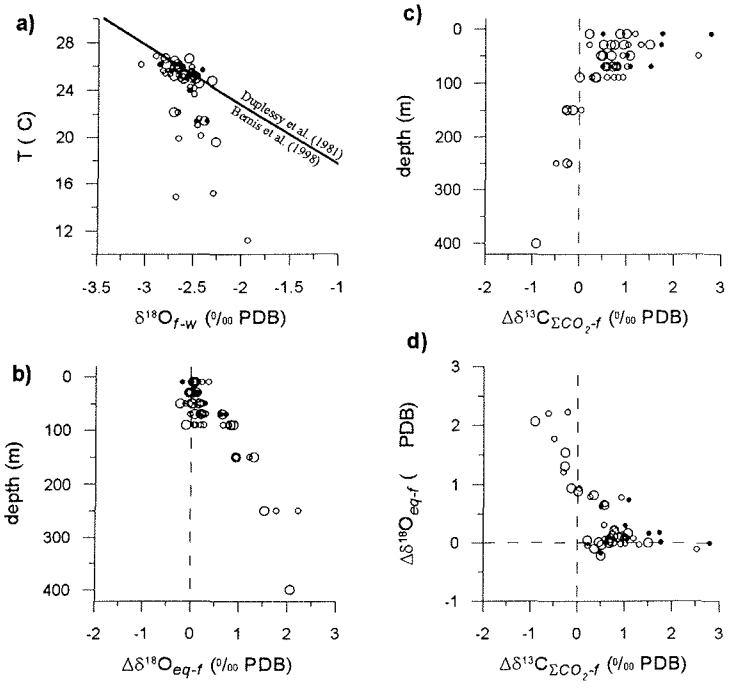

Figure 3. Isotope measurements of *G. ruber* (w) derived from plankton tows. Small filled dots - 150 to 200 μm; small open circles - 200 to 250 μm; large open circles - 250 to 315 μm. a) average temperature of sampling interval versus foraminiferal calcite minus $\delta^{18}O$ of ambient seawater; the straight line shows the relation of the paleotemperature equation of Bemis et al. (1998); b) depth related deviation to oxygen isotope equilibrium; c) depth related deviation of carbon isotope composition to $\delta^{13}C_{\Sigma CO2}$ ambient seawater; d) relation of oxygen isotope equilibrium versus deviation of foraminiferal $\delta^{13}C$ to seawater.

the depth of calcification. Hence, we compared the $\delta^{18}O$ values of samples collected below 100 m with calculated isotope equilibrium conditions as defined by Bemis et al. (1998) and displayed by the samples of the upper 100 m. Calculation of isotope equilibrium based on in situ temperature and $\delta^{18}O_{H2O}$ measurements. The results of stable isotope measurements of

plankton tow samples and the offsets to oxygen isotope equilibrium and to $\delta^{13}C_{\Sigma CO2}$ are summarised in Table 3. Assuming for all individuals calcification in oxygen isotope equilibrium the resulted depth habitat of *G. ruber* (w) specimens greater 200 µm ranges between the sea surface and 112 m. In contrast smaller *G. ruber* (w) individuals (150-200 µm) are restricted to the uppermost 30 m of the water column. The observed, as well as the estimated calcification depths of oxygen isotope equilibrium are in agreement with results derived from plankton tows of the Pacific and the Atlantic Ocean presented by Ortiz et al. (1995) and Ravelo et al. (1990).

To derive specific carbon isotope offsets for different size classes of *G. ruber* (w) we determined the deviation of foraminiferal $\delta^{13}C$ to $\delta^{13}C_{\Sigma CO2}$ (Figure 3c, Table 3). The carbon isotope composition of ambient seawater compared with foraminiferal calcite of *G. ruber* (w) again shows clear differences between samples of the upper water column and samples collected below 100 m (Figure 3c). In the uppermost 100 m the foraminiferal $\delta^{13}C$ values are 0.1 to 2.8 ‰ lower than $\delta^{13}C_{\Sigma CO2}$ (indicated by positive values in Figure 3c). In the upper 100 m the difference of foraminiferal $\delta^{13}C$ to ambient seawater decreases with increasing test size between 1.37 ‰ (± 0.76) and 0.67 ‰ (± 0.35) for *G. ruber* (w), while the standard deviation becomes smaller (Figure 4; Table 3). Below 100 m water depth carbon isotope values of *G. ruber* (w) are about 0.35 ‰ (± 0.31) lower than ambient seawater with $\delta^{13}C_{\Sigma CO2}$ values

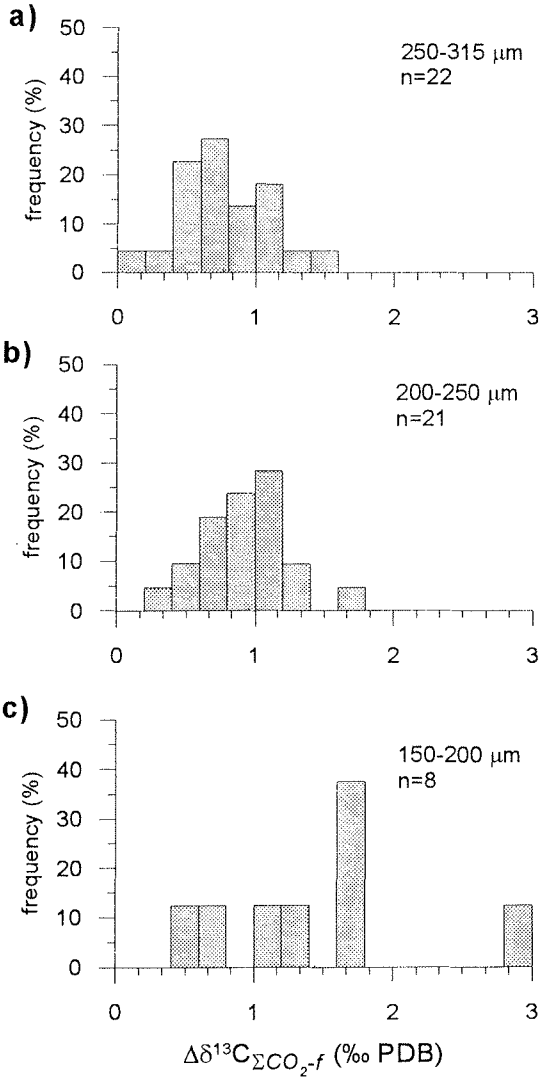

Figure 4. Distribution of the deviation of foraminiferal calcite to ambient seawater of plankton tow samples (interval size = 0.2 ‰). Depth of $\delta^{13}C_{\Sigma CO2}$ values correspond to predicted calcification depth with respect to oxygen isotope equilibrium; dashed vertical lines mark the average $\delta^{13}C$ deviation; a)-c) distribution of different size classes.

about 0.0 ‰. The $\Delta\delta^{13}C_{(\Sigma CO2\text{-}f)}$ values plotted versus $\Delta\delta^{18}O_{(eq\text{-}f)}$ same samples high deviations to $\delta^{18}O$ of equilibrium calcite as well as to $\delta^{13}C_{\Sigma CO2}$ of seawater. Hence, if we assign the depth habitats of the *G. ruber* (w) according to oxygen isotope equilibrium conditions the standard deviation of the resulted $\delta^{13}C$ offsets becomes smaller and samples collected below 100 m show differences to $\delta^{13}C_{\Sigma CO2}$ within the same range as observed for samples of the upper 100 m. For the depth habitats of oxygen isotope equilibrium the $\Delta\delta^{13}C_{(\Sigma CO2w\text{-}f)}$ values show a symmetrical scatter around the average values of 0.96 ‰ (± 0.33) and 0.76 ‰ (± 0.33) in the size classes of 200-250 µm and 250-315 µm. The higher variability of ± 0.74 observed for the size fraction of 150-200 µm might be related to the higher metabolic rate of small specimens associated with the high dynamic and biological productivity near the sea surface.

Table 3. Results of isotope measurements of plankton tow samples in relation to predicted equilibrium conditions, subdivided into samples collected above and below a water depth of 100 m; Oxygen isotope equilibrium refers to the paleotemperature equation of Bemis, et al. (1998).

Size (µm)	s.d. < 100 m				s.d. > 100 m				assuming $\delta^{18}Oeq^*$	
	n	$\delta^{18}O(f)$	$\Delta\delta^{18}O(eq\text{-}f)$	$\Delta\delta^{13}C(w\text{-}f)$	n	$\delta^{18}O(f)$	$\Delta\delta^{18}O(eq\text{-}f)$	$\Delta\delta^{13}C(w\text{-}f)$	depth (m)	$\Delta\delta^{13}C(w\text{-}f)$
150-200	9	-2.12 (± 0.18)	0.22 (± 0.29)	1.37 (± 0.76)	-	-	-	-	5-30 14 (± 9)	1.44 (± 0.74)
200-250	21	-2.16 (± 0.16)	0.22 (± 0.26)	0.89 (± 0.53)	5	-2.08 (± 0.26)	1.67 (± 0.58)	-0.32 (± 0.26)	5-112 36 (± 30)	0.96 (± 0.33)
250-315	19	-2.12 (± 0.15)	0.16 (± 0.19)	0.67 (± 0.35)	4	-1.97 (± 0.06)	1.46 (± 0.47)	-0.39 (± 0.35)	5-97 30 (± 25)	0.76 (± 0.33)

s.d. - sampling depth; n - number of isotope measurements; $\delta^{18}O(f)$ - oxygen isotope composition of foraminiferal calcite; $\Delta\delta^{18}O(eq\text{-}f)$ - deviation of foraminiferal $\delta^{18}O$ to predicted equilibrium of sampling depth; $\Delta\delta^{13}C(w\text{-}f)$ - deviation of foraminiferal $\delta^{13}C$ to $\delta^{13}C_{\Sigma CO2}$ of ambient seawater.

These results are in agreement with previous studies indicating a strong size dependent $^{13}C/^{12}C$ fractionation for several foraminiferal species (e.g. Wefer et al., 1983; Bouvier-Soumagnac and Duplessy, 1985; Kroon and Darling, 1995; Ravelo and Fairbanks, 1995; Spero and Lea, 1996).

4.3. Isotope composition of *G. ruber* (w) and *N. dutertrei* from surface sediment samples

The isotope signal of multiple planktic foraminiferal tests taken for single sample measurements out of sediments integrates the hydrographic conditions during calcification in relation to its seasonal production. Therefore an interpretation of this signal requires knowledge of the seasonal and vertical distribution of the analysed species and its variations according to hydrographical changes. To assess the environmental sensitivity of foraminiferal

isotopes we use the frequency distribution of multiple $\delta^{18}O$ and $\delta^{13}C$ measurements from sediment samples. The total range of isotope values should recover the end-members of the prevailing hydrographic conditions. Because we needed 3-5 specimens for a single isotope measurement the resulting data display already a subdued distribution and allow only a semi quantitative interpretation with respects to absolute difference of the hydrographic conditions. However, the assessment of sedimentary values along hydrographic gradients should allow the conclusion whether the planktic foraminiferal isotope signal is reflecting $\delta^{18}O$ or $\delta^{13}C$ changes in surface water associated with changes in upwelling intensity.

Multiple measurements at individual stations

We carried out multiple measurements on tests of *G. ruber* (w) (250-315 µm) and *N. dutertrei* (315-400 µm / >400 µm) at surface sediment samples influenced differently by coastal upwelling. We have chosen three sampling locations for study in the Gulf of Aden (GeoB 3013), the coastal upwelling cell off Oman (GeoB 3005), and ~300 km offshore on the Owen Ridge (GeoB 3007). Approximately 100 *G. ruber* (w) and 50 *N. dutertrei* tests were selected from each sediment sample. To obtain the magnitude of $\delta^{18}O$ and $\delta^{13}C$ variations of both species we used the minimum number of specimens needed for a single isotope measurement. To minimise the effects of isotopic outliers we interpret the range of the data with respect to the standard deviation of $\delta^{18}O$ and $\delta^{13}C$ values.

The foraminiferal isotope results from surface sediments were compared with $\delta^{13}C_{\Sigma CO2}$ values of NE- and SW-monsoon season and predicted equilibrium $\delta^{18}O$ of inorganic calcite (Figure 5) (Moos et al., submitted). Due to the observed low variations of temperature, salinity and $\delta^{18}O_{H2O}$ along the Arabian coast during Meteor cruise M31/3 we assume that our hydrographic data represent the conditions for all of the three chosen locations during winter season.

As indicated by the plankton tow measurements of *G. ruber* (w) the predicted $\delta^{18}O$ of inorganic calcite was calculated by using the $\delta^{18}O$/temperature relationship given by Bemis et al. (1998). To calculate $\delta^{18}O_{H2O}$ we use the empirical $\delta^{18}O$/salinity calibration for surface and thermocline water of this study and salinity data obtained during NIOP cruises C1 and C2 (corresponding to $\delta^{13}C_{\Sigma CO2}$ data) (Moos et al., submitted).

To assign the carbon isotope composition of *G. ruber* (w) and *N. dutertrei* to $\delta^{13}C_{\Sigma CO2}$ we corrected for their specific offsets to seawater. As derived from our plankton tow measurements we added 0.76 ‰ to the $\delta^{13}C$ values of *G. ruber* (w) (250-315 µm). For

N. dutertrei we could not derive a calibration factor, due to the low abundance in our plankton tows. Hence, we used the offset found by Mulitza et al. (1999), who obtained a constant deviation to $\delta^{13}C_{\Sigma CO2}$ of -0.5 ‰ comparing *N. dutertrei* $\delta^{13}C$ of plankton tow samples with $\delta^{13}C_{\Sigma CO2}$ within a similar temperature range in the equatorial South Atlantic.

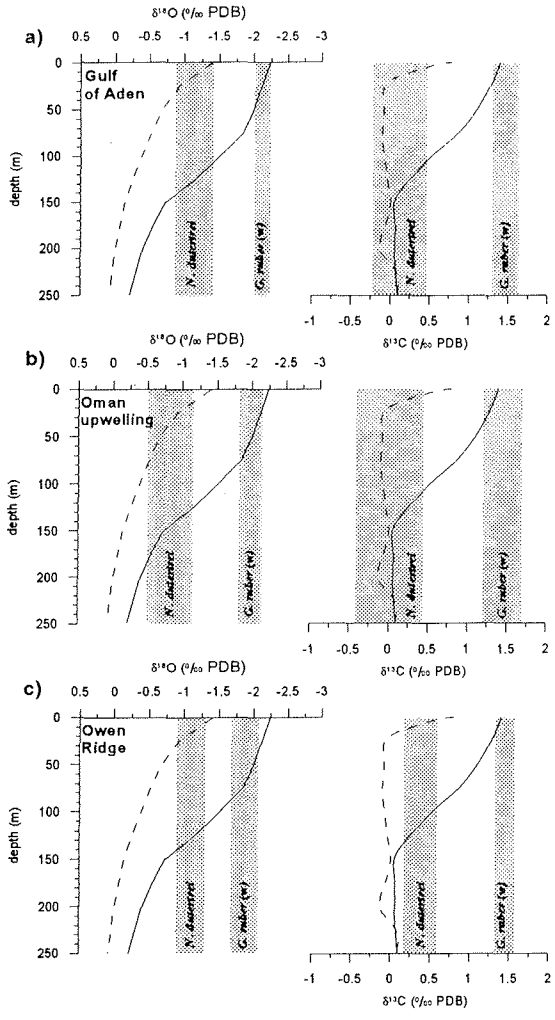

Figure 5. Comparison between foraminiferal isotopes of multiple measured sediment samples, $\delta^{18}O$ of equilibrium calcite (left panels), and seasonal measurements of $\delta^{13}C_{\Sigma CO2}$ (right panels) of the upper water column. The horizontal extend of the grey shaded areas indicates the standard deviation of a multiple measured sample. Dashed lines - SW-monsoon profiles; solid lines – NE-monsoon profiles. a) site GeoB 3013 (Gulf of Aden); b) site GeoB 3005 (Oman upwelling); c) site GeoB 3007 (Owen Ridge).

***Globigerinoides ruber* (white)**. In the Gulf of Aden the $\delta^{18}O$ data range from –2 ‰ to -2.24 ‰ and agree with predicted equilibrium $\delta^{18}O$ of the uppermost 50 m of the water column during NE-monsoon season. At the Oman upwelling site lowest $\delta^{18}O$ is 0.11 ‰ higher than predicted equilibrium at the sea surface (-2.25 ‰) during winter season. Due to a standard deviation of 0.16 the corresponding depth range covers 20 to 80 m. On the Owen Ridge the mean $\delta^{18}O$ value of –1.87 ‰ (±0.19) nearly averages predicted sea surface equilibrium of both monsoon seasons. With respect to equilibrium calcite calculated for NE-monsoon the $\delta^{18}O$ range of *G. ruber* (w) covers the deep mixed layer and the upper thermocline between 40 and 90 m.

The offset corrected *G. ruber* (w) $\delta^{13}C$ values agree with sea surface $\delta^{13}C_{\Sigma CO2}$ of NE-monsoon season at all locations. The mean values range between 1.44 ‰ and 1.46 ‰ with standard deviations of 0.17 in the Gulf of Aden and 0.13 on the Owen Ridge. For the location most influenced by coastal upwelling of Oman we found the highest standard deviation of 0.26, but no shift of the *G. ruber* (w) $\delta^{13}C$ values towards observed SW-monsoon $\delta^{13}C_{\Sigma CO2}$ of seawater. At this location $\delta^{13}C$ values display $\delta^{13}C_{\Sigma CO2}$ down to a water depth of 40 m. As shown in Figure 5a-c the majority of the *G. ruber* (w) $\delta^{13}C$ data exceed the observed sea surface $\delta^{13}C_{\Sigma CO2}$ of NE-monsoon season. An explanation might be a ^{12}C enrichment of dissolved inorganic carbon induced by fossil fuel CO_2 in the modern ocean. This effect should influence $\delta^{13}C_{\Sigma CO2}$ as well as *G. ruber* (w) $\delta^{13}C$ of plankton tow samples. In contrast individuals of a sediment assemblage should contain preferentially a preindustrial signal and thus higher $\delta^{13}C$ values.

The seasonal production rates of *G. ruber* (w) derived from sediment traps in the western Arabian Sea and off Somalia (Curry et al., 1992; Peeters et al., 1999) suggest a seasonal shell flux of *G. ruber* (w) of nearly 50 % during upwelling and non-upwelling season. The $\delta^{13}C$ values more likely display sea surface conditions of non-upwelling situation. The study of Moos et al. (submitted) suggests that photosynthesis seems to be rapid enough to strip surface water virtually free of nutrients which leads to an increase of $\delta^{13}C_{\Sigma CO2}$ values of the upwelled water in the upper 30 m. Thus, if *G. ruber* (w) calcifies close to the sea surface while upwelling occurs, the resulted $\delta^{13}C$ signal does not reflect the maximum upwelling situation. However, the carbon isotope composition of *G. ruber* (w) in surface sediments seems to reflect $\delta^{13}C_{\Sigma CO2}$ of nutrient depleted surface water. This is also indicated by the low $\delta^{13}C$ difference of about 0.1 ‰ between our plankton tow samples of NE-monsoon season and the specimens of surface sediments. These results are also supported by observations of Cayre and Bard (1999) who found an increase of the relative abundance of *G. ruber* (w) coinciding with a decrease of primary production.

Neogloboquadrina dutertrei. In the Gulf of Aden sedimentary *N. dutertrei* $\delta^{18}O$ values range from -0.86 ‰ to -1.40 ‰. These values correspond to depth ranges from 110 m to 140 m and the uppermost 35 m with accordance to winter and summer $\delta^{18}O$ equilibrium (Figure 5a). In the Oman upwelling mean $\delta^{18}O$ is with -0.82 ‰ slightly higher than in the Gulf of Aden, also is the standard deviation of 0.32 compared to 0.28 in the Gulf of Aden. The $\delta^{18}O$ values imply a depth range within the winter thermocline between 130 m and 185 m and between 20 m and 80 m with respect to $\delta^{18}O$ equilibrium of upwelling season. Oxygen

isotope results in the offshore region on the Owen Ridge are comparable to the location in the Gulf of Aden with a mean value of -1.09 ‰ (±0.21).

In the Gulf of Aden and the Oman upwelling *N. dutertrei* $\delta^{13}C$ displays seawater $\delta^{13}C_{\Sigma CO2}$ of ~25 m water depth during upwelling. In comparison to winter $\delta^{13}C_{\Sigma CO2}$ *N. dutertrei* displays again conditions below a water depth of 110 m. In the Oman upwelling *N. dutertrei* contains $\delta^{13}C$ values below the observed minimum of $\delta^{13}C_{\Sigma CO2}$. Additionally the $\delta^{13}C$ data cover the highest range of 0.08 ‰ to 0.95 ‰ although we carried out only 8 measurements at this location (Table 4). On the Owen Ridge *N. dutertrei* shows the smallest standard deviation of 0.21 and displays only sea surface conditions during SW-monsoon. The higher standard deviations observed for the locations in the Gulf of Aden and the Oman upwelling might be related to the larger size fraction (>315 µm) of foraminiferal tests used for the isotope measurements at these locations. The study of Ravelo and Fairbanks (1995) indicates for *N. dutertrei* an increase of the variation of the $\delta^{13}C$ offset with increasing test size. A strong size related fractionation of *N. dutertrei* $\delta^{13}C$ in Arabian Sea sediments is also supported by investigations of Kroon and Darling (1995).

Table 4. Summary of isotope data, measured at three core tops located in the Gulf of Aden, the Oman upwelling and the Owen Ridge.

			$\delta^{18}O$ (‰ PDB)			$\delta^{13}C$ (‰ PDB)		
station	size (µm)	n	range	mean	σ	range	mean	σ
G ruber (w)								
GeoB 3013	250-315	28	-2.34 (-) -1.83	-2.12	0.12	0.31 - 0.91	0.70	0.17
GeoB 3005	250-315	23	-2.18 (-) -1.53	-1.98	0.16	0.09 - 1.03	0.68	0.26
GeoB 3007	250-315	12	-2.04 (-) -1.53	-1.87	0.19	0.46 - 0.94	0.69	0.13
N dutertrei								
GeoB 3013	>315	12	-1.40 (-) -0.53	-1.14	0.28	0.02 - 1.11	0.62	0.35
GeoB 3005	>315	8	-1.15 (-) -0.19	-0.82	0.32	-0.18 - 0.97	0.51	0.43
GeoB 3007	315-400	29	-1.70 (-) -0.56	-1.09	0.21	0.18 - 1.25	0.85	0.26

n - number of measurements; σ - standard deviation

However, the isotope composition of *N. dutertrei* alone does not allow a clear assignment to a vertical or a seasonal habitat. Knowledge of the seasonal shell flux distribution of *N. dutertrei* offers a possibility to identify seasonal versus depth-related calcification. In contrast to *G. ruber* (w) nearly 90 % of the total annual shell flux of *N. dutertrei* occurs between July and September at the most upwelling influenced sediment trap in the Arabian Sea (Curry et al., 1992). Hence, the oxygen and carbon isotope composition of *N. dutertrei* should display the hydrographic situation of high nutrient concentrations during upwelling season.

The $\delta^{13}C$ difference between *G. ruber* (w) and *N. dutertrei* varies between 1.06 ‰ and 1.43 ‰ on the Owen Ridge and the Oman upwelling. A similar situation is found for the

oxygen isotope difference (Oman upwelling 1.16 ‰, Owen Ridge 0.78 ‰). Thus, the carbon and oxygen isotope gradients of *G. ruber* (w) and *N. dutertrei* in sediments reflect the seasonal gradients of $\delta^{13}C_{\Sigma CO2}$ and calculated $\delta^{18}O$ of equilibrium calcite. The variability of the isotope gradients is probably related to the different influence of upwelling at the three sites.

Isotope distribution along the transect of Meteor cruise M31/3

In the previous chapter we compared the isotope signals of *G. ruber* (w) and *N. dutertrei* with $\delta^{13}C_{\Sigma CO2}$ and predicted oxygen isotope profiles representing end members in the seasonal cycle. With respect to spatial variations of upwelling intensity we cannot assume similar hydrographic conditions at the three sites in the Gulf of Aden, the Oman upwelling, and the Owen Ridge. Therefore, we analysed the isotope composition of *G. ruber* (w) and *N. dutertrei* at all sediment surface samples of Meteor cruise M31/3. To indicate the strength of upwelling along the transect of Meteor cruise M31/3 we used the difference of the sea surface temperatures between May and August ($\Delta T_{(May-Aug)}$) taken from the monthly atlas data of Levitus and Boyer (1994). Due to SW-monsoon SST decreases from May to August in upwelling influenced areas of the northwest Arabian Sea. The magnitude depends mainly on the intensity of upwelling. A high positive temperature gradient suggests strong upwelling, while lower differences imply less intense upwelling. The $\Delta T_{(May-Aug)}$ data are positive at all sites indicating that strength of upwelling is high enough to cause summer-SST lower than May-SST along the coast of Arabia and the Owen Ridge. Strongest upwelling is indicated for the coastal area off Oman between about 1000 km and 1650 km of the transect (light-grey shaded area in Figure 6).

The $\delta^{18}O$ values of *G. ruber* (w) vary by about 0.3 ‰ with highest values of about -2.0 ‰ observed in the area of most intense upwelling. For *N. dutertrei* the $\delta^{18}O$ ranges from -0.35 ‰ to -1.5 ‰. The distribution of *N. dutertrei* $\delta^{18}O$ values doesn't fit the course of temperature gradients along the Arabian coast. The locations of highest $\delta^{18}O$ values are found westwards from the center of upwelling. These $\delta^{18}O$ values are possibly influenced additionally by extensions of the Somali upwelling. Such an effect must not be observed at the sea surface where upwelling water is mixed with surrounding surface water and, additionally, summer insolation may compensate the temperature signal of upwelled water. However, the spatial variability of upwelling is not reflected in the oxygen isotope composition of *N. dutertrei* and therefore not in the $\Delta\delta^{18}O$ difference between *G. ruber* (w) and *N. dutertrei*. Only oxygen

isotopes of *G. ruber* (w) seem to display the intensity of upwelling. The low magnitude of $\delta^{18}O$ variations supports the idea that *G. ruber* (w) averages the out extreme hydrographic conditions at the sea surface of both monsoon seasons, as indicated by the results of multiple surface sediment measurements discussed above.

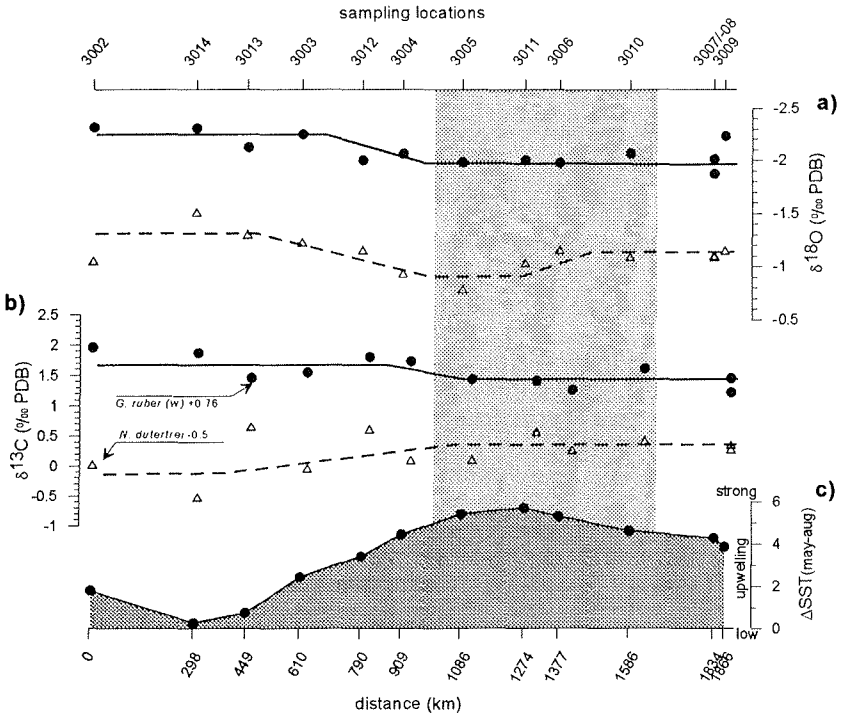

Figure 6. Isotope composition of the analysed foraminiferal species along the transect of Meteor cruise M31/3 (dashed line in Figure 1); x-Axis inscription refers to the first sampling station (GeoB 3002) of the M31/3 transect; a) spatial $\delta^{18}O$ variations; b) spatial $\delta^{13}C$ variations corrected by specific offsets to ambient seawater; c) sea surface temperature difference between May and August as indicator of upwelling intensity (temperature data of Levitus and Boyer (1994)); filled dots - *G. ruber* (w); triangles - *N. dutertrei*; lines show a schematised approximation of the isotope variations.

The $\delta^{13}C$ values of *G. ruber* (w) and *N. dutertrei* from sediments show only minor variations between sites in the Gulf of Aden, the Oman upwelling and at the Owen Ridge. For *G. ruber* (w) the $\delta^{13}C$ data are ~0.2 ‰ higher in the Gulf of Aden compared to the area of strongest upwelling. The $\delta^{13}C$ and the $\delta^{18}O$ data of *G. ruber* (w) are within the range of the multiply measured surface sediment samples. With respect to the reconstructed depth habitat the $\delta^{13}C$ values of *G. ruber* (w) suggest a preference to conditions with low nutrient concentrations close to the sea surface. Also Kroon and Ganssen (1989) found low $\delta^{13}C$ variations of *G. ruber* (w) in plankton samples along a transect in northern Indian Ocean surface waters.

Neogloboquadrina dutertrei $\delta^{13}C$ shows low variation along the Meteor transect of cruise M31/3, with slightly lower values in the Gulf of Aden. The carbon isotope values indicate a preference of *N. dutertrei* to constantly low carbon isotope levels within the water column corresponding to high food availability. This suggests a vertical migration of *N. dutertrei* to deeper water levels when strength of upwelling decreases. For *N. dutertrei* a depth habitat within the thermocline under non-upwelling conditions is also reported by Ortiz et al. (1995)

and Steens et al. (1992). For *N. dutertrei* they observed lowest $\delta^{13}C$ values in the upwelling areas off Arabia and south of India. They interpreted the carbon isotope variations of *G. ruber* (w) and *N. dutertrei* with respect to a different timing within the seasonal upwelling cycle. This is not supported by our plankton tow and sediment data. The oxygen and carbon isotope changes of *G. ruber* (w) and *N. dutertrei* are low compared to the changes of the hydrographic conditions induced by upwelling. A reason may be that the seasonal production of *G. ruber* (w) is shared to SW- and NE-monsoon season which dampens the $\delta^{13}C$ signal to shows only low variations. That we observed no changes in the isotopes of sedimentary *N. dutertrei* along the transect of M31/3 might be related to vertical compensation of the effect of variations in upwelling intensity. Nevertheless, the hydrographic variations along the Meteor transect parallel to the Arabian coast are low compared to the gradients observed by Kroon and Ganssen (1989) which cover the entire northern Indian Ocean.

Due to the opposite changes of *G. ruber* (w) and *N. dutertrei* the $\Delta\delta^{13}C$ gradient suggests a relation to the spatial variability of upwelling. However, upwelling intensity is not clearly recorded in the oxygen and carbon isotopes of *G. ruber* (w) and *N. dutertrei*. Within the expected hydrographic variations $\delta^{13}C$ values in sediment assemblages display end member of $\delta^{13}C_{\Sigma CO2}$ and nutrient concentrations of the upper 150 m of the water column.

5. Conclusions

Globigerinoides ruber (w) build its tests close to oxygen isotope equilibrium with accordance to the paleotemperature equation of Bemis et al. (1998) and reflects the hydrographic conditions of the sea surface. The $\delta^{13}C$ deviation of *G. ruber* (w) to ambient seawater amounts to 0.76 ‰ within the size class of 250-315 µm. The mean offset and the scatter of the $\delta^{13}C$ values increase with decreasing test size.

Oxygen and carbon isotopes of *G. ruber* (w) derived from surface sediment samples are related to sea surface conditions. The values display the hydrographic situation of NE-monsoon in the Gulf of Aden. An increase of about 0.3 ‰ in the $\delta^{18}O$ data indicates additional upwelling influences to the oxygen isotope values of G. ruber (w) in areas of strongest upwelling. The $\delta^{13}C$ values of *G. ruber* (w) derived from sediment surface samples display $\delta^{13}C_{\Sigma CO2}$ of nutrient depleted surface water. With accordance to upwelling intensity $\delta^{13}C$ values of *G. ruber* (w) are only little affected. In the centre of upwelling $\delta^{13}C$ values are about 0.2 ‰ lower compared to the Gulf of Aden.

For *N. dutertrei* oxygen isotope values suggest a depth habitat between 20 m and 80 m with respect to hydrographic conditions of its highest seasonal production during the period of upwelling. The $\delta^{13}C$ values of *N. dutertrei* display the lowest $\delta^{13}C_{\Sigma CO_2}$ values observed in the water column of the upper 150 m indicating a relation to water depths where productivity delivers a lot of food due to high nutrient concentrations. The small changes of the $\delta^{13}C$ values along the Arabian coast suggest for *N. dutertrei* a migration to deeper levels at locations with low upwelling intensity. This supports again that carbon isotopes of *N. dutertrei* are a measure for nutrient concentrations of source water-masses affected by upwelling. Because *G. ruber* (w) displays nutrient depleted surface water the offset corrected $\delta^{13}C$ difference between both species displays hydrographic end member of $\delta^{13}C_{\Sigma CO_2}$ and nutrient concentrations in the upwelling system of the northwest Arabian Sea.

The carbon isotope compositions of *G. ruber* (w) and *N. dutertrei* show opposite variations with respect to locations influenced by more or less upwelling intense. Thus, although $\delta^{13}C$ variations of both species are low, the $\delta^{13}C$ difference between *G. ruber* (w) and *N. dutertrei* is lower in the Oman upwelling than in the Gulf of Aden. Nevertheless, the magnitude of changes in upwelling intensity is not recorded in the oxygen and carbon isotopes of *G. ruber* (w) and *N. dutertrei*.

Acknowledgements- We thank captain and crew of *F.S. Meteor* for the excellent cooperation during the cruises. Ch. Hemleben kindly provided samples for plankton tow investigations. S. Mulitza provided critical comments on an early version of the manuscript. The research was funded by the Bundesministerium für Bildung, Wissenschaft, Forschung und Technologie (BMBF) and is part of the NEtherlands BRemen OCeanography (NEBROC) cooperation.

The data presented in this paper are archived in the Pangea database (http://www.pangaea.de).

4. Carbon isotopes of planktic foraminifera recording nutrient and productivity variations in the northwestern Arabian Sea during the past 300,000 yr

(to be submitted to "Geology")

Christopher A. Moos*, Dörte Budziak, Ralph R. Schneider and Gerold Wefer

Universität Bremen, Fachbereich Geowissenschaften, Klagenfurter Straße, Postfach 330 440, D-28359 Bremen, Germany

Abstract

Carbon isotopes of planktic foraminifera display nutrient related $\delta^{13}C$ variations of dissolved inorganic carbon ($\delta^{13}C_{\Sigma CO2}$) in the coastal upwelling area of the NW-Arabian Sea and identify nutrients as a major control mechanism of productivity variations during the past 307,000 yr. The carbon isotope composition of *Globigerinoides ruber* (w) and *Neogloboquadrina dutertrei* from site GoeB 3005 was compared with changes in global deep ocean $\delta^{13}C_{\Sigma CO2}$. The $\delta^{13}C$ record of *G. ruber* (w), revealing nutrient depleted surface water, is coherent and in phase with the global $\delta^{13}C_{\Sigma CO2}$ signal at the primary orbital periods. Additionally, the *G. ruber* (w) $\delta^{13}C$ signal contains variability at higher frequencies. The $\delta^{13}C$ of *N. dutertrei*, living deeper in the water column than *G. ruber* (w), shows stronger deviations relative to the global $\delta^{13}C_{\Sigma CO2}$. The difference between the carbon isotope records of *G. ruber* (w) and *N. dutertrei* ($\Delta\delta^{13}C$ *r-d*) of core GeoB 3005 displays nutrient variations in the coastal upwelling area. Frequency analyses of the $\Delta\delta^{13}C$ *r-d* time series suggests cyclic changes in nutrient availability in tune with Earth's orbital parameters of eccentricity and precession, as well as at periods of 12,500 yr and 7,700 yr. To unravel the dependencies of upwelling related productivity on nutrient availability of subsurface water masses and SW-monsoon wind strength during the late Pleistocene, the abundance of *G. bulloides* (ODP site

* Corresponding author. Fax: 0049 421 218 3116; e-mail: moos@allgeo.uni-bremen.de

723B) was compared with $\Delta\delta^{13}C$ *r-d* (GeoB 3005) and lithogenic grain size records (RC27-61). The results of cross-spectral analyses indicate that productivity depends mainly on nutrient availability, while upwelling intensity seems to be of lower importance during the past 307,000 yr.

Introduction

Enhanced productivity during the summer season is a major characteristic of monsoon related upwelling in the northwestern Arabian Sea. Today, about 70% of the total annual productivity takes place during the upwelling season from June to August (Smith et al., 1998). Various tracers were used to study Arabian Sea upwelling history with respect to productivity e.g.: the relative abundance of the planktic foraminifera *Globigerina bulloides* (Anderson and Prell, 1991; 1993; Prell, 1984a), the stable isotope composition of planktic and benthic foraminifera (Niitsuma et al., 1991; Steens et al., 1992), organic carbon (Budziak et al., in press; Emeis et al., 1995) and opal fluxes (Murray and Prell, 1992). Nevertheless, productivity variations are not only controlled by upwelling intensity but are additionally dependent on the nutrient concentrations of the subsurface water masses, which are to be transported into the photic zone by upwelling. While modern nutrient concentrations in intermediate water masses of the northwestern Arabian Sea were nearly constant over the past decades (Moos et al., in press) cadmium contents and carbon isotopes of benthic foraminifera imply nutrient-depleted conditions in intermediate waters during glacial times in the Indian Ocean (Boyle, 1992; Kallel et al., 1988).

In this study $\delta^{13}C$ records of planktic foraminifera were used to investigate $\delta^{13}C$ variations of dissolved inorganic carbon ($\delta^{13}C_{\Sigma CO2}$) and nutrient concentrations in surface waters of the northwestern Arabian Sea during the past 307,000 yr. To interpret the carbon isotope time series of planktic foraminifera in terms of nutrient concentrations it is necessary to define a $\delta^{13}C$ reference reflecting constant nutrient levels. Therefore, the carbon isotope values of *G. ruber* (w) and *N. dutertrei* were corrected for their specific offsets relative to ΣCO_2 based on calibrations of Moos et al. (submitted) and Mulitza et al. (1999). Today, the offset corrected carbon isotopes of *G. ruber* (w) display surface water $\delta^{13}C_{\Sigma CO2}$ stripped virtually free of nutrients, while *N. dutertrei* prefers high nutrient levels associated with low $\delta^{13}C_{\Sigma CO2}$ (Moos et al. submitted). Based on the recent calibration of Moos et al. (submitted) the carbon isotope difference between *G. ruber* (w) and *N. dutertrei* ($\Delta\delta^{13}C$ *r-d*) is interpreted with respect to nutrient gradients within Arabian Sea surface water masses.

To assess the contribution of global and regional effects to the carbon isotope signals of *G. ruber* (w) and *N. dutertrei* both records were compared with the global deep ocean $\delta^{13}C_{\Sigma CO2}$ signal estimated from the benthic foraminifera *Universa sentocosa* of the core V19-30 located in the equatorial Pacific Ocean (Shackleton et al., 1983).

Additionally, the relationships between nutrient availability, productivity, and the intensity of monsoonal upwelling during the late Pleistocene were investigated. Productivity in the northwestern Arabian Sea is mainly controlled by the combined influence of nutrient availability in the photic zone and upwelling intensity. Variations in nutrient concentrations depend on changes in ocean circulation, while upwelling intensity is mainly controlled by the strength of the SW-monsoon winds.

Clemens and Prell (1990) and Clemens et al. (1991) established lithogenic grain size records of Arabian Sea sediments as a measure of SW-monsoon wind strength, responsible for coastal upwelling off Oman. Coastal upwelling and the associated enhanced productivity are major features of SW-monsoon hydrography in the northern Indian Ocean. Productivity variations are indicated by the relative abundance of the planktic foraminiferal species *G. bulloides*, which is widely used to trace changes in upwelling intensity (Anderson and Prell, 1991; 1993; Prell, 1984a). Although the upwelling related productivity (% *G. bulloides*) and the eolian dust deposits (lithogenic grain size) seem to be related to the SW-monsoon circulation, differences were found between the time series of the associated monsoon tracers (Clemens et al. 1996; Anderson and Prell, 1991). Hence, additional mechanisms causing environmental variations have to be taken into consideration.

To study the coupling between the fertility of Arabian Sea water masses, upwelling related productivity as well as SW-monsoon wind strength, we compared $\Delta\delta^{13}C$ *r-d* record of core GeoB 3005 with the % *G. bulloides* of the coastal ODP site 723B (Anderson and Prell, 1991) and the lithogenic grain size of core RC27-61 located on the Owen Ridge (Clemens et al., 1991; Clemens and Prell, 1990).

Oceanography of the study area

The northern Arabian Sea is strongly affected by the Indian Monsoon system. During northern hemisphere summer strong SW-monsoon winds blow parallel to the coasts of Africa and the Arabian Peninsula driving the ocean surface circulation (Figure 1). This wind field induces Ekman drift causing an offshore transport of surface water. Upwelling of cold and nutrient-rich subsurface water-masses into the photic zone is the result (Wyrtki, 1971). Due to

the high fertility conditions numerous planktic forminifera are most abundant during the upwelling season (Curry et al., 1992; Peeters et al., 1999). Additionally, the high nutrient concentrations of freshly upwelled water are documented by low $\delta^{13}C_{\Sigma CO2}$ values. The $\delta^{13}C_{\Sigma CO2}$ difference between winter and summer season ranges from 0.7 ‰ at the sea surface to 1.3 ‰ between 30 m and 80 m, with mixed layer values about 1.4 ‰ during the NE-monsoon season (Moos et al, submitted).

From previous paleoceanographic studies it became evident that SW-monsoon winds and related upwelling intensity have varied mainly with a major periodicity of orbital precession (Prell, 1984b; Prell and Van Campo, 1986). Additionally, tracers of productivity indicate higher fertility during interglacial periods and lower during glacial times (Clemens et al., 1991). Carbon isotopes of benthic foraminifera suggest that the hydrographic conditions of intermediate and deep water have been different from the present situation (Kallel et al., 1988). The hydrography of intermediate water masses changes with sea level variations, because of a reduced contribution of Red Sea Water and Persian Gulf Water during times of low sea levels. In contrast, there might be an increased through-flow of pacific water masses into the Indian Ocean and a higher influence of Antarctic Intermediate Water during glacial times as revealed by carbon isotope records of planktic foraminifera (Duplessy et al., 1989). These suggest that hydrographic variations affect the transport of nutrients into the northwestern Arabian Sea.

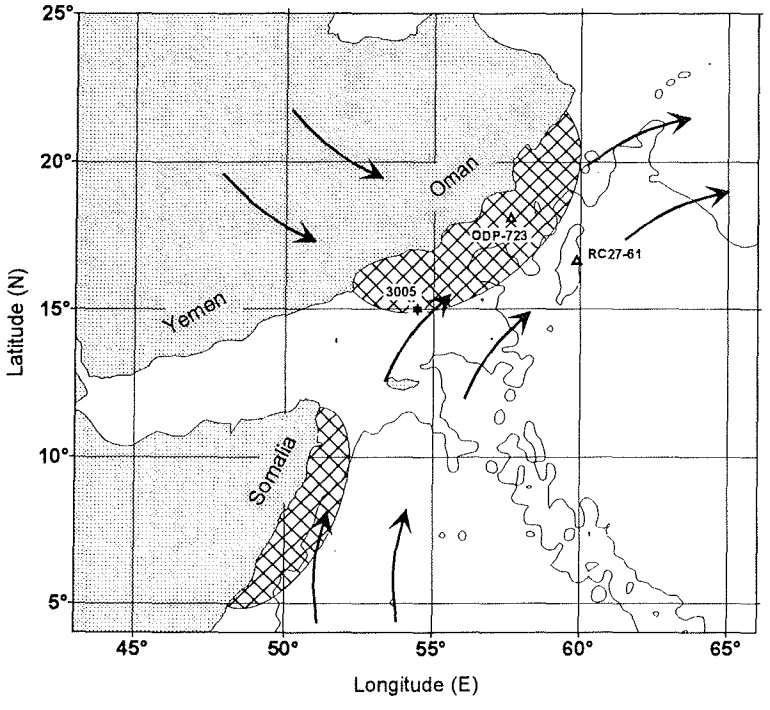

Figure 1. Map of the northwestern Arabian Sea including site locations of core GeoB 3005, RC27-61, and ODP 723B. The crosshatched areas indicate the upwelling cells off Somalia and Oman. Arrows show Shamal and SW-monsoon winds causing coastal upwelling during summer season.

Materials and Methods

We studied core GeoB 3005 which was recovered off the Arabian coast during R/V Meteor cruise M31/3 in 1995 (14°58,3'N, 54°22,2'E; 2318 m) (Figure 1), for the isotope composition of planktic foraminifera.

Isotope analyses on the planktic foraminifera *G. ruber* (w) and *N. dutertrei* were carried out using a FINNIGAN/MAT-252 mass-spectrometer equipped with an automatic carbonate preparation device. Precision based on replicates of an internal limestone standard was better than 0.07 ‰ for $\delta^{18}O$ and 0.05 ‰ for $\delta^{13}C$. From each sediment sample 8 to 12 specimens of *G. ruber* (w) (250-315 μm) and *N. dutertrei* (>315 μm) were picked out for isotope analysis.

The stratigraphic framework of GeoB 3005 was derived from graphic correlation of the $\delta^{18}O$ record of *N. dutertrei* with the SPECMAP $\delta^{18}O$ reference stack (Imbrie et al. 1984). Further details on that chronology are given in Budziak et al. (in press). According to this age model the core resolves the last 307,000 yr showing an average sedimentation rate of about 7/1000 cm yr^{-1} and a mean time resolution of about 700 years at sample intervals of 5 cm.

To identify the dominant periodicities in each time series and to estimate the correlation between the single records cross-spectral analyses were carried out. All analyses were calculated by the Cross-Blackman-Tukey method (Jenkins and Watts, 1968) using the software package 'AnalySeries 1.0a7' developed by Paillard et al. (1996). For the comparison of the $\delta^{13}C$ records of GeoB 3005 with the deep water $\delta^{13}C$ signal of *Universa senticosa* of east Pacific core V19-30, which can be considered as a global signal for $\delta^{13}C$ change (Shackleton et al., 1983). The original time series were converted to 750 yr time intervals by linear interpolation. Due to the time resolution of the *G. bulloides* and the grain size records all time series were linearly interpolated at intervals of 2000 yr for the purpose of cross-spectral analysis between the $\Delta\delta^{13}C$ *r-d* record of core GeoB 3005 and tracers of monsoon wind strength (lithogenic grain size, RC27-61) and productivity (% *G. bulloides*, ODP 723B). With respect to this rather coarse resolution we only report cyclical changes of the primary orbital periods.

Results and Discussion

$\delta^{13}C$ of planktic foraminiferal time series (GeoB 3005)

***Globigerinoides ruber* (w)**. The $\delta^{13}C$ data of *G. ruber (w)* of core GeoB 3005 range from 2.5 ‰ during the Holocene to 0.5 ‰ during isotope stage 6 (Figure 2a). The long-term variations show a good agreement with the benthic $\delta^{13}C$ record of *Universa senticosa* of core V19-30. Compared to the global variations the $\delta^{13}C$ record of *G. ruber (w)* reveals by about 0.9 ‰ higher $\delta^{13}C$ values during the Holocene. Deviations to higher $\delta^{13}C$ values occurred also during isotope stage 8. The results of the frequency analyses carried out on the time series of *G. ruber* (w) and *Universa senticosa* $\delta^{13}C$ show similar distributions of spectral power, except for the period of 29,000 yr, where variance is more pronounced in the $\delta^{13}C$ signal of *G. ruber* (w) (Figure 3a). Cross-spectral analysis indicates that both $\delta^{13}C$ records are coherent and in phase with each other at the primary frequency bands of eccentricity, obliquity, and precession. Thus, both time series seem to be controlled equally by the same mechanisms.

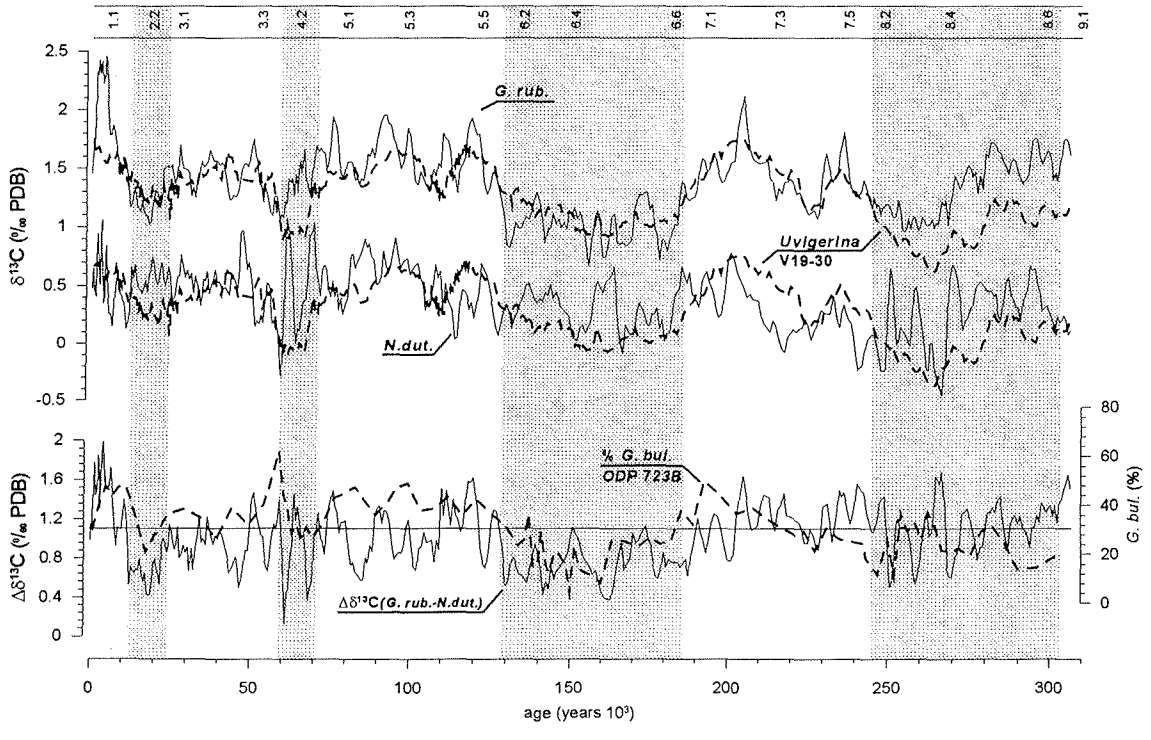

Figure 2. Carbon isotope records of core GeoB 3005. a) comparison of *G. ruber* (w) and *N. dutertrei* (straight lines) with the $\delta^{13}C$ time series of the benthic foraminifera *Universa senticosa* of the pacific core V19-30 (fat dashed line). Time series of *G. ruber* (w) and *N. dutertrei* are corrected for their specific offsets to $\delta^{13}C_{\Sigma CO2}$ given by Moos et al. (submitted) and (Mulitza et al., 1999). The record of *Universa senticosa* was shifted for the best fit relative to *G. ruber* (w) and *N. dutertrei*. b) straight lines indicate offset corrected carbon isotope difference between *G. ruber* (w) and *N. dutertrei* ($\Delta\delta^{13}C$ *r-d*). This approach only shifts the $\Delta\delta^{13}C$ curve to more positive values. Values above the horizontal line indicate $\delta^{13}C_{\Sigma CO2}$ values and nutrient concentrations higher as observed in surface sediments. Dashed line - relative abundance of G. bulloides of ODP Site 723B.

To explain the similarities of the two foraminiferal $\delta^{13}C$ records constant nutrient concentrations are required at both sites. With accordance to the modern calibration (Moos et al., submitted) *G. ruber* (w) seems to display nutrient depleted surface waters during the past 307,000 yr, which is also supported by results of Cayre and Bard (1999). Thus, the carbon isotope variations of *G. ruber* (w) indicate changes of Arabian Sea surface water masses and can be used as reference to evaluate nutrient dependent $\delta^{13}C_{\Sigma CO2}$ variations.

Neogloboquadrina dutertrei. The $\delta^{13}C$ values of *N. dutertrei* range from about -0.2 ‰ to 1.1 ‰ and show a higher variability than the *Universa senticosa* record (Figure 2a), which is additionally revealed by cross-spectral analyses (Figure 3b). While *Universa senticosa* shows a high variance in the main orbital periods, *N. dutertrei* has extra spectral power superimposed in the precessional frequency bands of 23,000 yr and 19,000 yr and in sub-Milankovitch periods. The phase relationship between both records indicates a more differentiated timing than found for *Universa senticosa* and *G. ruber* (w). These differences are interpreted in terms of regional $\delta^{13}C_{\Sigma CO2}$ variations superimposed on the global signal in the carbon isotope record of *N. dutertrei*.

$\Delta\delta^{13}C$ r-d. While *G. ruber* (w) documents generally $\delta^{13}C_{\Sigma CO2}$ of nutrient depleted surface waters, *N. dutertrei* is strongly adapted to high nutrient conditions during the upwelling season. Thus, the $\Delta\delta^{13}C$ *r-d* gradient displays the inter-annual end member of $\delta^{13}C_{\Sigma CO2}$ depending on variations in nutrient concentrations. During glacial periods the calculated down core $\Delta\delta^{13}C$ *r-d* gradient is equal or smaller compared to the recent surface sediments indicating higher nutrient gradients at about 6000 yr, 120,000 yr, 205,000 yr, 240,000, and 265,000 yr (Figure 2b).

The spectral peaks found in the $\Delta\delta^{13}C$ *r-d* spectrum allow a clear relation to the $\delta^{13}C$ spectra of *N. dutertrei* and *G. ruber* (w). The spectral power of the $\Delta\delta^{13}C$ *r-d* record that is concentrated near the period of Earth's eccentricity depends on the phase angle between $\delta^{13}C$ of *G. ruber* (w) and *N. dutertrei* as derived from the different phase relationships relative to the $\delta^{13}C$ record of *Universa senticosa*. The variance concentrated at the precessional periods as well as in the sub-Milankovitch frequency bands is related to the *N. dutertrei* spectrum with spectral power concentrated at 12,500 yr and 7,700 yr (Figure 3c). Only the period of 29,000 yr is related to *G. ruber* (w). A 29,0000 yr component is neither observed for

N. dutertrei, nor for the global variations of ΣCO_2. However, this period is also found in a sea surface temperature record of the southern Indian Ocean and interpreted as a component of monsoon variation related to latent heat transport (Clemens and Prell, 1991). Nevertheless, we found no clear relationship to monsoonal upwelling variations for *G. ruber* (w).

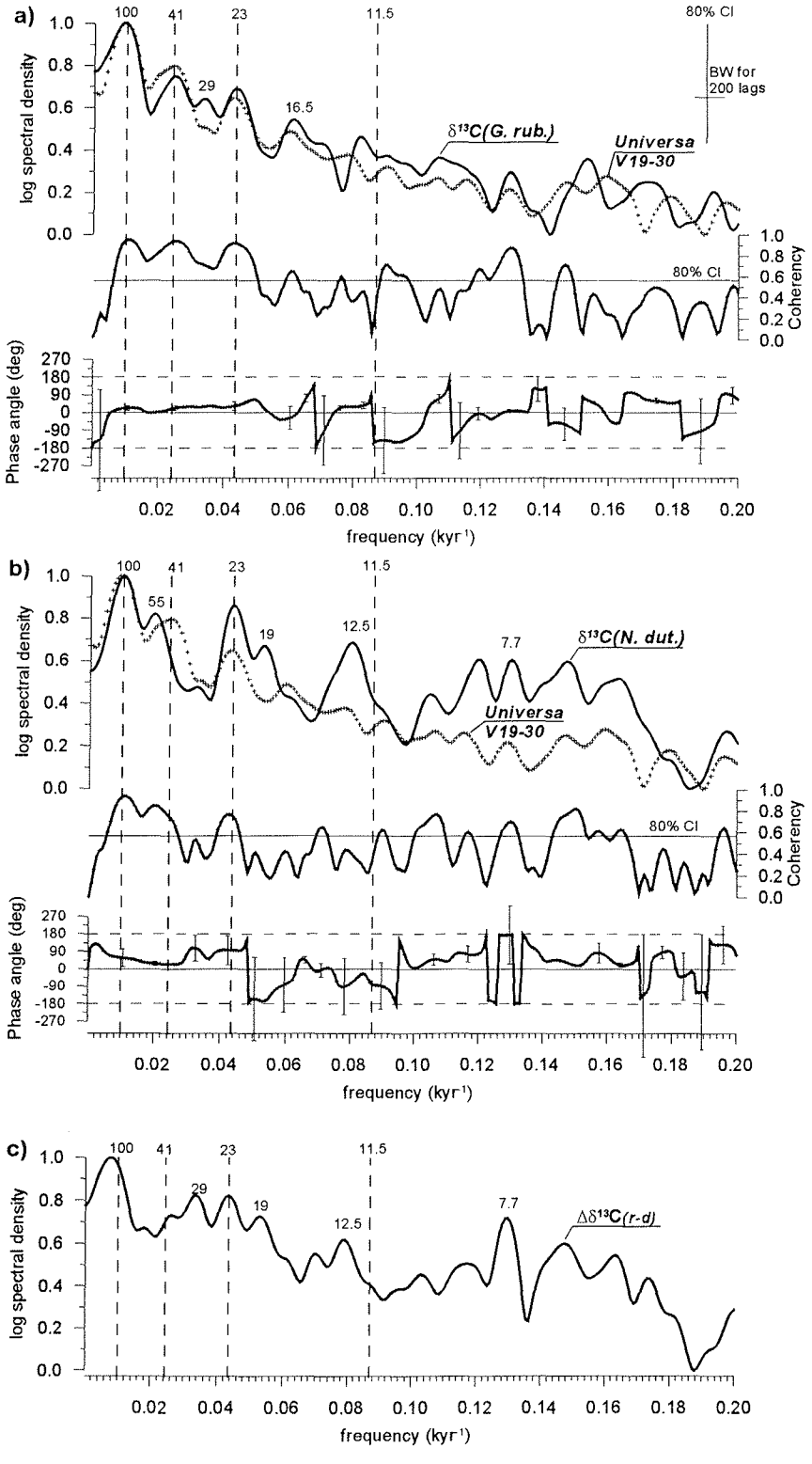

Figure 3. Spectral density, cross-coherency, and phase angles versus frequency. Time series interpolated at 750 yr from 0-307,000 yr. a) $\delta^{13}C$ of *G. ruber* (w) and *Universa senticosa*, b) $\delta^{13}C$ of *N. dutertrei* and *Universa senticosa*, c) carbon isotope difference between *G. ruber* (w) and *N. dutertrei* ($\Delta\delta^{13}C$ *r-d*).

Comparison of nutrients, productivity, and upwelling intensity

To determine the varying influence of nutrient concentrations and upwelling intensity on the productivity signal we compared the $\Delta\delta^{13}C$ *r-d* record of core GeoB 3005 with the relative abundance of *G. bulloides* from ODP Site 723B from the coastal upwelling region off Oman (Anderson and Prell, 1991) and with the record of lithogenic grain size of core RC 27-61 (Clemens and Prell, 1990) indicating upwelling related productivity and SW-monsoon wind strength, respectively. Due to its elevated location on the Owen Ridge the lithogenic component of site RC27-61 depends on eolian dust alone and is unaffected by sediments from the Oman margin and the Indus Fan (Clemens et al., 1991; Clemens and Prell, 1990).

Nutrient variations and upwelling related productivity ($\Delta\delta^{13}C$ r-d - % *G. bulloides*). A visual comparison of the $\Delta\delta^{13}C$ *r-d* record of core GeoB 3005 with the abundance of *G. bulloides* of ODP site 723B suggests a general agreement in long-term variations (Figure 2b). In accordance to a confidence level of 80 % the results show a significant coherence for the periods of highest variance in the eccentricity and precessional frequency band (120,000 yr and 23,000 yr) as revealed in Figure 4a. Coherence and phase relationship close to zero indicate the same control mechanisms with similar timing for eccentricity and to a slightly lower degree for precession. In contrast, close to the coherence between both records at 26,000 yr the time of highest *G. bulloides* abundance leads the maximum of $\Delta\delta^{13}C$ *r-d* by approximately ¼ cycle.

The results of cross-spectral analyses show a relationship between $\Delta\delta^{13}C$ *r-d* and *G. bulloides* abundance at frequencies close to the eccentricity and the precession band indicating that productivity is mainly affected by nutrient variations at these periods. Nevertheless, some differences exist in the distribution of spectral power, and coherence as well as phase angles, indicating changes of productivity (% *G. bulloides*) independent of nutrient variations at periods of 41,000 yr, 26,000, and 17,000 yr. These variations might be controlled by the intensity of upwelling and related monsoonal wind strength. On the other hand, there are nutrient variations at periods of 29,000 yr and 19,000 yr that do not affect productivity. Possibly these nutrient variations compensated by opposite changes of upwelling intensity.

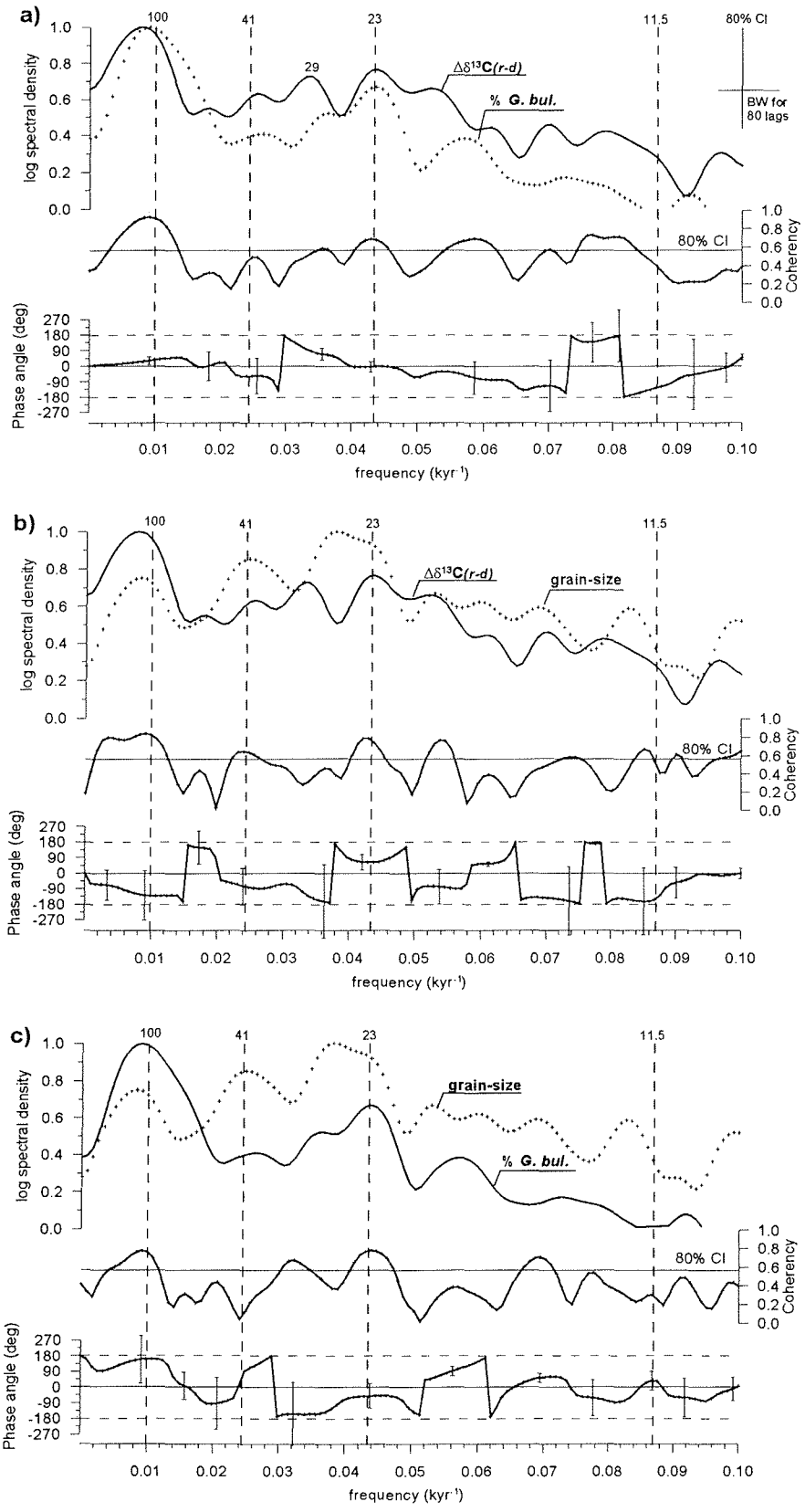

Figure 4. Spectral density, cross-coherency, and phase angles versus frequency. Time series were interpolated at 2000 yr from 4-306,000 yr. a) $\Delta\delta^{13}C$ *r-d* (GeoB 3005) and abundance of *G. bulloides* (ODP 723B), b) $\Delta\delta^{13}C$ *r-d* (GeoB 3005) and lithogenic grain size (RC27-61), c) lithogenic grain size (RC27-61) and the abundance of *G. bulloides* (ODP 723B). Note, that the differences of the $\delta^{13}C$ *r-d* spectra illustrated in Figure 3 and 4 depend on the different statistical parameters and resolutions of the time series (750 yr and 2000 yr).

Nutrient variations and monsoon wind strength ($\Delta\delta^{13}C$ r-d - grain size). The distribution of spectral variance, coherence, and the phase relationship between the records of $\Delta\delta^{13}C$ *r-d* and lithogenic grain size, indicating nutrients and monsoon wind strength, respectively, should help to explain the primary features of productivity variations. The results of cross-spectral analyses show significant coherence at the three primary orbital periods including the 19,000 yr component of precession (Figure 4b). The lithogenic grain size contains highest variance at periods from 23,000 yr to 25,000 yr and close to 41,000 yr. Concentration of spectral power in the frequency band of eccentricity is obviously lower compared to $\Delta\delta^{13}C$ *r-d* or % *G. bulloides*. The phase angles between $\Delta\delta^{13}C$ *r-d* and lithogenic grain size range from a quarter to a half cycle and suggest that enhanced productivity is not driven by these two mechanisms at the same time. The coherence at 19,000 yr and average phase angle of a quarter cycle combined with a large phase uncertainty (indicating instability of the phase relation) might explain the absence of the 19,000 yr component in the productivity record of *G. bulloides*. This could also be true for the frequency band of earth obliquity.

Upwelling related productivity and monsoon wind strength (G. bulloides - grain size). To complete the evaluation of productivity we additionally compared the strength of monsoon winds with productivity intensity, indicated by lithogenic grain size and the relative abundance of *G. bulloides*, respectively. The records are coherent at periods of 23,000 yr and 100,000 yr. The low spectral density of the grain size record and the phase angle in the low frequency domain versus *G. bulloides* suggests low variations of upwelling intensity and a minor influence on productivity for the frequency band of eccentricity. For the frequency band of precession the phase relationship suggests a time lag of about 3,000 yr.

Conclusions

A comparison of the planktic foraminifera *G. ruber* (w) $\delta^{13}C$ with global variations of $\delta^{13}C_{\Sigma CO2}$ derived from the benthic foraminiferal species *Universa senticosa* indicates that *G. ruber* (w) preferred nutrient depleted surface water conditions during the past 307,000 yr. This is also supported by results of Cayre and Bard (1999). Based on a recent calibration and additionally suggested by the strong deviations of *N. dutertrei* versus the global $\delta^{13}C_{\Sigma CO2}$ signal, *N. dutertrei* displays highest nutrient levels of sub-surface water masses affected by upwelling. The carbon isotope difference between *G. ruber* (w) and *N. dutertrei* can be used to trace nutrient gradients in the northwestern Arabian Sea.

The $\Delta\delta^{13}C$ *r-d* gradient indicates strong nutrient variations in the upwelling area of the northwestern Arabian Sea during the past 307,000 yr. Variations show significant periodicities close to the primary orbital periods of Earth's eccentricity and precessional components of 23,000 yr and 19,000 yr. Additionally, the distribution of spectral variance indicates variations near the half cycle of precession at 12,500 yr as well as at 7,700 yr.

In a simplified system variations of productivity are interpreted as the residuum of the superimposition of nutrient concentration and upwelling intensity. Geological records of foraminiferal carbon isotope gradients and lithogenic grain size were used to investigate the influence of nutrient availability and monsoon wind strength to productivity as indicated by the relative abundance of *G. bulloides*. The results of cross-spectral analyses suggest that variations of *G. bulloides* are more affected by nutrient availability than by changes in upwelling intensity. Especially at the frequency band of eccentricity and the 23,000 yr component of precession the *G. bulloides* and $\Delta\delta^{13}C$ *r-d* records are coherent and in phase with each other. In contrast, the phase relationship between the time series of *G. bulloides* and lithogenic grain size indicates a different timing of productivity and monsoon wind strength. Wind strength and nutrient records seem to be coherent with one another at all significant periods, but are out of phase. Additionally large phase errors might suggest a more differentiated superimposition of both control mechanisms on productivity.

Acknowledgements- We thank captain and crew of *F.S. Meteor* for the excellent cooperation during the cruises. The research was funded by the Bundesministerium für Bildung, Wissenschaft, Forschung und Technologie (BMBF) and is part of the NEtherlands BRemen OCeanography (NEBROC) cooperation.

The data presented in this paper are archived in the Pangea database (http://www.pangaea.de).

Part III - Conclusions and Implications for future research

1 Conclusions

Stable oxygen and carbon isotope records of the surface foraminifera *G. ruber* (w) and the deeper dwelling species *N. dutertrei* were used to reconstruct environmental variations of the upwelling area in the northwestern Arabian Sea during the late Pleistocene. The study provides the first calibration of modern foraminiferal isotope data based on seasonal hydrographic observations of the NE- and the SW-monsoon. A 307,000 yr marine sediment record off Oman yields foraminiferal isotope time series with a mean temporal resolution of about 700 yr documenting monsoon climate history.

- A comparison of carbon isotope measurements of Arabian Sea water samples from 1993 with former data from GEOSECS 1977 displays a lowering of $\delta^{13}C_{\Sigma CO2}$ values about 0.3 ‰ resulting from fossil fuel combustion during the past 2-3 decades. This effect is evident for data of both monsoon seasons, although the coastal areas off Somalia, Yemen and Oman represent CO_2 sources during the upwelling period. Nevertheless, the anthropogenic lowering of $\delta^{13}C_{\Sigma CO2}$ in Arabian Sea water masses is comparable to oligotrophic areas of the world oceans.
- Seasonal hydrographic observations in the upwelling region off Yemen and Oman showed, that the strongest differences between upwelling and non-upwelling season occur at water depth of 20 to 80 m. Summer heating and primary production lower the seasonal gradients of temperature, phosphate, and $\delta^{13}C_{\Sigma CO2}$ at the sea surface.
- For living specimens of the planktic foraminifera *G. ruber* (w) and *N. dutertrei* specific deviations to $\delta^{13}C_{\Sigma CO2}$ were identified by a comparison of foraminiferal $\delta^{13}C$ with ambient seawater. The $\delta^{13}C$ values of *G. ruber* (w) are about 0.76 ‰ lower than those of the ΣCO_2, related to a size fraction of 250-315 µm. In contrast, *N. dutertrei* (315-400 µm) shows 0.5 ‰ heavier $\delta^{13}C$ values than ambient seawater as derived from plankton tow samples from the equatorial South Atlantic.
- The stable carbon isotope composition of living *G. ruber* (w) and *N. dutertrei* specimens approximate the modern seasonal end member of $\delta^{13}C_{\Sigma CO2}$ in Arabian Sea surface waters. Offset corrected $\delta^{13}C$ values of sedimentary *N. dutertrei* display the low $\delta^{13}C_{\Sigma CO2}$ values of subsurface waters rising during upwelling season. The analyses of stable oxygen and carbon

isotopes indicate that *N. dutertrei* preferentially lives in water depth where productivity delivers high food supply due to high nutrient concentrations. In contrast, the isotope compositions of *G. ruber* (w) display low nutrient conditions at the sea surface.

- The carbon isotopes of *G. ruber* (w) from the Arabian Sea display general variations of regional water mass properties during the late Pleistocene, as indicated by the modern calibration and by the similarity to previous estimates of global $\delta^{13}C_{\Sigma CO2}$ variations. Hence, carbon isotopes of *G. ruber* (w) are independent from upwelling intensity and can be used as reference versus carbon isotope variations of foraminifera related to the upwelling season like *N. dutertrei.*
- The carbon isotope difference between *G. ruber* (w) and *N. dutertrei* reveals the history of productivity influenced by monsoonal upwelling during the past 307,000 years. Although the process of upwelling dominates the annual productivity, the $\Delta\delta^{13}C$ *r-d* signal and the *G. bulloides* abundance are different from paleo-indicators of monsoonal wind strength. Hence, upwelling intensity and nutrient concentrations are decoupled to some extent, as long as upwelling is effective enough to maintain the advection of nutrients. It is therefore suggested that productivity mainly depends on the nutrient concentrations in the upwelled sub-surface water, while variations of monsoon and upwelling intensities are secondary modifiers.
- Derived from down core $\Delta\delta^{13}C$ *r-d* data the nutrient gradients in Arabian Sea surface waters, which are affected by SW-monsoon upwelling, are generally lower during glacial periods compared to the modern situation. In contrast, nutrient availability seems to be higher at 6 kyr, 120 kyr 205 kyr, 240 kyr, and 265 kyr. Additionally, water mass properties and nutrient availability show cyclical variability at the primary orbital periods of Earth's eccentricity and precession as well as near 12,5 kyr and 7,7 kyr.

Based on the recent calibration of the foraminiferal isotope signal and with respect to the high resolution of the foraminiferal isotope time series the results of this study allow a more differentiated analysis of the oceanographic response to atmospheric forcing of the Indian Monsoon circulation. The carbon isotopes of planktic foraminifera represent an important component to distinguish between different control mechanisms of SW-monsoon related productivity.

2 Implications for future research

- When dealing with stable oxygen and carbon isotopes of planktic foraminifera an important aspect is the recent calibration of the analysed species. The habitat within the annual cycle and the water depth occupied by a foraminiferal species depend on several controlling factors like temperature, food, and light. Because each foraminiferal species reacts differently to changes of one or more of these parameters its behaviour with respect to environmental variations must be known. Plankton tows along hydrographic gradients, carried out during different seasons, allow evaluating the abundance and the distribution of foraminiferal species within the water column.
- Furthermore, sediment traps yield important information on the annual foraminiferal distribution and abundances during both monsoon seasons. Long-term monitoring will help to investigate interannual variations mentioned briefly by Curry et al. (1992) and Peeters et al. (1999). Hence, long-term monitoring of foraminiferal production over a couple of years will add to our understanding of sedimentary assemblages, which integrate hundreds to thousands of years.
- The monsoonal rainfall during summer season is essential for the surrounding populations of India and Southeast Asia and its variation is a main incentive to a better understanding of monsoonal climate. The amount of summer precipitation over India defines the all-India summer rainfall index (Mooles and Parthasarathy, 1984), an important index of modern monsoon strength. Currently, there is no proxy-parameter indicating the amount of paleo-monsoonal rainfall anomalies. Key-regions for investigations of monsoon rainfall reconstructions might be areas where strong freshwater input, due to monsoonal rainfall, takes place and reduces salinity and possibly influences additional water mass properties. Possible areas could be the mouth of the Indus River or the Gulf of Bengal. River discharge affects locally the nutrient concentrations as well as the salinity and the carbon and oxygen isotope signatures of ocean surface waters. Variations of freshwater input should be displayed in changes of foraminiferal assemblages and in the carbon and oxygen isotope composition of foraminiferal tests. Recently some investigations deal with salinity changes in the Gulf of Bengal (e.g. Rosteck et al., 1993). Hence, besides the northwestern Arabian Sea the Gulf of Bengal area might be another key region for understanding of monsoonal rainfall and comparisons between both regions might improve the understanding of the oceanic response to monsoonal forcing.

• Recently, investigations start to take the influence of the NE-monsoon circulation into consideration for interpreting paleo-time series. Yet no proxy for the NE-monsoon period was found. A important goal of future research would be to find those tracers for both paleo- and recent-time series from the northern Indian Ocean and the Gulf of Bengal. Recent studies indicate general changes of northern Indian Ocean hydrography and oceanographic circulation during the late Pleisticene mainly traced by the water mass originates in the Gulf of Bengal (e.g. Prell. et al., 1980 and Kallel et al., 1988). Water from the Gulf of Bengal is mainly transported to the north during NE-monsoon season. Thus, reconstructions of the distribution of this water mass would allow a better understanding of NE-monsoon variability and its contribution to monsoonal climate in general. Due to the exceptional signature of Gulf of Bengal water suitable water mass tracers could allow to reconstruct its distribution in the northern Indian Ocean. The wide distribution and the sensitivity to discrete hydrographic conditions raise again planktic foraminifera to potential tools tracing distinct water mass properties in the northern Indian Ocean.

Part IV - References

Arntz WE, Fahrbach E (1991) El Niño: Klimaexperiment der Natur: Basel, Birkhäuser, 264 p.

Anderson DM, Prell WL (1991) Coastal upwelling gradient during the late Pleistocene. In: Emeis K-C, Meyers PA, Niitsuma N, Prell WL (eds), Proceedings of the Ocean Drilling Program, Scientific Results. Ocean Drilling Program, College Station, Texas, pp 265-276.

Anderson DM, Prell WL (1993) A 300 kyr record of upwelling off Oman during the Late Quaternary: Evidence of the Asian southwest monsoon. Paleoceanography 8: 193-208.

Arz H, Pätzold J, Wefer G (1998) Short-term climate fluctuations in the western tropical Atlantic for the past 85,000 years revealed by a sediment core off NE-Brazil. Quat Res 50:157-166.

Baars MA, Ed. (1994) Monsoon and Pelagig Systems, Report on the three cruises of RV Tyro in the Somali Current, the Gulf of Aden and the Red Sea during the southwest monsoon of 1992 and the northeast monsoon of 1993. Cruise Reports Netherlands Indian Ocean Program. Leiden, National Museum of History.

Bacastow RB, Keeling CD, Lueker CD, Wahlen M, Mook WG (1996) The ^{13}C Suess effect in the world surface oceans and its implications for oceanic uptake of CO_2: Analysis of observations at Bermuda. Global Biogeochemical Cycles 10: 335-346.

Banse K, McClain CR (1986) Winter blooms of phytoplankton in the Arabian Sea as observed by the Coatal Zone Color Scanner. Marine Ecology Progress Series 34: 201-211.

Bard E, Arnold M, Maurice P, Duplessy JC (1987) Measurements of bomb radiocarbon in the ocean by means of accelerator mass spectrometry: technical aspects. Nuc Inst Meth Phys Res B29: 297-301.

Bard E (1988) Correction of acceleratur mass spectrometry ^{14}C ages measured in planktonic foraminifera: Paleoceanographic implications. Paleoceanography 3: 635-645.

Bemis BE, Spero HJ (1997) The influence of temperature on the carbon isotopic composition of planktonic foraminiferal shell calcite. EOS 78: 361.

Bemis BE, Spero HJ, Bijma J, Lea DW (1998) Reevaluation of the oxygen isotopic composition of living planktonic foraminifera: Experimantal results and revised paleotemperature equation. Paleoceanography 13: 150-160.

Berger WH (1971) Sedimentation of planktonic foraminifera. Marine Geology 11: 325-358.

Berger WH, Gardner JV (1975) On the determination of Pleistocene temperatures from planktic foraminifera. Journal of Foraminiferal Research 5: 102-113.

Berger WH, Killingley JS (1977) Glacial-Holocene transition in deep-sea carbonates: Selective dissolution and stable isotope signal. Science 197: 563-566.

Berger WH (1981) Oxygen and carbon isotopes in foraminifera: an introduction. Paleogeography, Paleoclimatology, Paleoecology 33: 3-7.

Berger WH, Vincent E (1986) Deep-sea carbonates: reading the carbon-isotope signal. Geologische Rundschau 75: 249-269.

Billups K, Spero HJ (1996) Reconstructing the stable isotope geochemistry and paleotemperaturers of the equatorial Atlantic during the last 150,000 years: Results from individual foraminifera. Paleoceanography 11: 217-238.

Bonneau MC, Vergnaud-Grazzini C, Berger WH (1980) Stable isotope fractionation and differential dissolution in recent planktonic foraminifera from Pacific box-cores. Oceanol Acta 3: 377-382.

Bouvier-Soumagnac Y, Duplessy J (1985) Carbon and oxygen isotopic composition of planktonic foraminifera from laboratory culture, plankton tows and Recent sediment: implications for the reconstruction of paleoclimatic conditions and of the global carbon cycle. J Foraminiferal Res 15: 302-320.

Boyle EA, Keigwin L (1987) North Atlantic thermohaline circulation during the past 20,000 years linked to high-latitude surface temperatures. Nature 330: 35-40.

Boyle EA (1988) Cadmium: Chemical Tracer of deepwater paleoceanography. Paleoceanography 3: 471-489.

Boyle E, Rosenthal Y (1996) Chemical hydrography of the Southern Ocean during the last glacial maximum: Cd vs. $\delta^{13}C$. In: Wefer G, Berger WH, Siedler G, Webb DJ (eds), The South Atlantic: Present and Past Circulation. Springer, Berlin, Heidelberg, New York: 423-443.

Broecker WS, Peng TH (1982) Tracers in the Sea. Lamont Doherty Geol. Obs. Publication, Columbia University, New York, 689 p.

Broecker WS, Maier-Reimer E (1992) The influence of air and sea exchange on the carbon isotope distribution in the sea. Global Biogeochemical Cycles 6: 315-320.

Broecker WS, Peng TH (1993) Evaluation of the ^{13}C constraint on the uptake of fossil fuel CO_2 by the ocean. Global Biogeochemical Cycles 7: 619-626.

Brummer G-JA, Kroon D (1988) Planktonic foraminifers as tracers of ocean-climate history. Amsterdam. Free University Press, Amsterdam, 346 p.

Budziak D, Schneider RR, Rostek F, Müller PJ, Bard E, Wefer G (in press) Late Quaternary insolation forcing on total organic carbon and C37 alkenone variations in the Arabian Sea. Paleoceanography.

Carstens J, Hebbeln D, Wefer G (1997) Distribution of planktic foraminifera at the ice margin in the Arctic (Fram Strait). Mar Micropal 29: 257-269.

Cayre O, Bard E (1999) Planktonic Foraminifera and Alkenon Records of the Last Deglaciation from the Eastern Arabian Sea. Quaternary Research 52: 337-342.

Charles CD, Fairbanks RG (1990) Glacial to interglacial changes in the isotopic gradients of the Southern Ocean surface water. In: Bleil U, Thiede J (eds), Geological history of the Polar Oceans: Artic versus Antarctic. Kluwer, Dordrecht: 519-538.

Charles CD, Wright JD, Fairbanks RG (1993) Thermodynamic influence on the marine Carbon Isotope Record. Paleoceanography 8: 691-697.

Charles CD, Lynch-Stieglitz J, Ninnemann US, Fairbanks RG (1996) Climate connections between the hemisphere revealed by deep sea sediment core/ice core correlations. Earth and Planetary Science Letters 142: 19-27.

Clemens SC, Prell WL (1990) Late Pleistocene variability of Arabian Sea summer monsoon winds and continental aridity: Eolian records from the lithogenic component of deep-sea sediments. Paleoceanography 5: 109-145.

Clemens SC, Prell WL (1991) Late Quaternary Forcing of Indian Ocean Summer-Monsoon Winds: A comparison of Fourier Model and General Circulation Model Results. Journal of Geophysical Research 96: 22,683-22,700.

Clemens S, Prell W, Murray D, Shimmield G, Weedon G (1991) Forcing mechanisms of the Indian Ocean monsoon. Nature 353: 720-725.

Clemens SC, Murray DW, Prell WL (1996) Nonstationary Phase of the Plio-Pleistocene Asian Monsoon. Science 274: 943-948.

Conkright ME, Boyer TP, Levitus S, 1994. Quality control and processing of historical oceanographic data. NOAA Technical Rep NESDIS. Washington, DC, NOAA, pp. 75.

Coplen TB (1996) Editorial: More uncertainty than necessary. Paleoceanography 11: 369-370.

Craig H (1953) The geochemistry of the stable carbon isotopes. Geochim Cosmochim Acta 3: 53-92.

Craig H, Gordon LI (1965) Deuterium and oxygen-18 variations in the ocean and the marine atmosphere. In: Tongiorgi E (eds), Stable isotope in oceanographic studies and

paleotemperatures. Spoleto, Pisa (Consiglio Nazionale delle Ricerche, Laboratorio di Geologia Nucleare), pp 9-130.

Curry WB, Duplessy JC, Labeyrie LD, Shackleton NJ (1988) Changes in the distribution of $\delta^{13}C$ of deep water ΣCO_2 between the last glaciation and the Holocene. Paleoceanography 3: 317-341.

Curry WB, Ostermann DR, Guptha MVS, Ittekkot V (1992) Foraminiferal production and monsoonal upwelling in the Arabian Sea: evidence from sediment traps. In: Summerhayes CP, Prell WL, Emeis KC (eds), Upwelling systems: Evolution Since the Early Miocene. Geological Society Special Publication, pp 93-106.

Dansgaard W, Tauber H (1969) Glacier oxygen-18 content and pleistocene ocean temperatures. Science 166: 499-502.

Dickson AG, Goyet C, Eds. (1994). Handbook of Methods for the Analysis of the Various Parameters of the Carbon Dioxide System in Sea Water, version 2. Rep. ORNL/CDIAC-74.

Duplessy JC, (1972). La geochimie des isotopes stables du carbone dans la mer. Centre d'Etudes Nucléaires de Saclay. Saclay, pp. 196.

Duplessy JC (1978) Oxygen isotope studies and Quaternary marine climates. In: Berger WH (eds), Climate Variations and Variability: Facts and Theories. Reidel, pp 181-192.

Duplessy J-C, Blanc PL (1981) Oxygen-18 enrichment of planktonic foraminifera due to gametogenic calcification below the euphotic zone. Science 213: 1247-1250.

Duplessy JC, Be AWH, Blanc PL (1981) Oxygen and carbon isotopic composition and the biogeographic distribution of planktonic foraminifera in the Indian Ocean. Palaeogeography, Palaeoclimatology, Palaeoecology 33: 9-47.

Duplessy JC, Shackleton NJ, Fairbanks RG, Labeyrie L, Oppo D, Kallel N (1988) Deepwater source variations during the last climatic cycle and their impact on the global deepwater circulation. Paleoceanography 3: 343-360.

Duplessy JC, Labeyrie L, Kallel N, Juillet-Leclerc A (1989) Intermediate And Deep Water Characteristics During The Last Glacial Maximum. In: Berger A (eds), Climate and Geo-Sciences. Kluwer Academic Publishers, pp 105-120.

Duplessy JC, Labeyrie L, Paterne M, Hovine S, Fichefet T, Duprat J, Labracherie M (1996) High Latitude Water Sources During the Last Glacial Maximum and the Intensity of the Global Oceanic Circulation. In: Wefer G, Berger WH, Siedler G, Webb DJ (eds), The South Atlantic - Present and Past Circulation. Springer, Berlin, pp 445-460.

Emeis K-C, Anderson DM, Doose H, Kroon D, Schulz-Bull D (1995) Sea-Surface Temperatures and the History of Monsoon Upwelling in the Northwest Arabian Sea during the Last 500,000 Years. Quartenary Research 43: 355-361.

Emrich K, Ehhalt DH, Vogel JC (1970) Carbon isotope fractionation during the precipitation of calcium carbonate. Earth Planet Sci Lett 8: 363-371.

Epstein S, Buchsbaum R, Lowenstam HA, Urey HC (1953) Revised carbonate-water isotopic temperature scale. Bull Geol Soc Am 64: 1315-1325.

Epstein S, Mayeda T (1953) Variation of O^{18} content of water from natural sources. Geochemica et Cosmochemica Acta 4: 213-224.

Erez J, Honjo S (1981) Comparison of isotopic composition of planktonic foraminifera in plankton tows, sediment traps and sediments. Palaeogeogr Palaeoclimatol Palaeocol 33: 129-156.

Fairbanks RG, Sverdlove M, Free R, Wiebe PH, Bé AWH (1982) Vertical distribution and isotopic fractionation of living planktonic foraminifera from the Panama Basin. Nature 298: 841-844.

Findlater J (1974) The low-level cross-equatorial air current of the western Indian Ocean during the Northern Summer. Weather 29: 411-416.

Flohn H (1950) Neue Anschauungen über die allgemeine Zirkulation der Atmosphäre un ihre klimatische Bedeutung. Erdkunde 4: 141-162.

Francois R, Altabet MA, R. G, McCorkle DC, Brunet C, Poisson A (1993) Changes in the $\delta^{13}C$ of surface water particulate organic matter across the subtropical convergence in the SW Indian Ocean. Global Biogeochemical Cycles 7: 627-644.

Francois R, Altabet MA, Yu EF, Sigman DM, Bacon MP, Frank M, Bohrmann G, Bareille G, Labeyrie LD (1997) Contribution of Southern Ocean surface-water stratification to low atmospheric CO_2 concentrations during the last glacial period. Nature 389: 929-935.

Frank M, Gersonde R, Rutgers van der Loeff M, Kuhn G, Mangini A (1996) Late Quaternary sediment dating and quantification of lateral sediment redistribution applying $^{230}Th_{ex}$: a study from the eastern Atlantic sector of the Southern Ocean. Geol Rundsch 85: 554-566.

Friedli H, Lötscher H, Oeschger H, Siegenthaler U, Stauffer B (1986) Ice core record $^{13}C/^{12}C$ ratio of atmospheric CO_2 in the past two centuries. Nature 324: 237-241.

Ganssen G (1983) Dokumentation von küstennahem Auftrieb anhand stabiler Isotope in rezenten Foraminiferen vor Nordwest-Afrika. "Meteor"-Forschungsergebnisse 37C: 1-46.

Ganssen G, Sarnthein M (1983) Stable-isotope composition of foraminifers: The surface and botoom water record of costal upwelling. In: Suess AE, J. T (eds), Coastal Upwelling, Its Sediment Record, Part A,. pp

Gordon AL (1981) South Atlantic thermocline ventilation. Deep-Sea Res 28A: 1239-1264.

Goyet C, Coatanoan C, Eischeid G, Amaoka T, Okuda K, Healy R, Tsunogai S (1999) Spatial variation of total CO_2 and total alkalinity in the northern Indian Ocan: A novel approach for the quantification of anthropogenic CO_2 in seawater. Journal of Marine Research 57: 135-163.

Gruber N, Sarmiento JL (1997) Global patterns of marine nitrogen fixation and denitrification. Global Biogeochemical Cycles 11: 235-266.

Harkness DD (1979) Radiocarbon dates from Antarctica. British Antarctic Survey Bulletin 47: 43-59.

Hart TJ, Currie RI (1960) 'Discovery'. Report 31: 123-298.

Hastenrath S, Merle J (1987) Annual cycle of subsurface thermal structure in the Tropical Atlantic Ocean. Journal of Physical oceanography 17: 1518-1538.

Hays JD, Imbrie J, Shackleton NJ (1976) Variations in the earth's orbit: pacemaker of the Ice Ages. Science 194: 1121-1132.

Heimann M, Maier-Reimer E (1996) On the relations between the oceanic uptake of CO2 and its carbon isotopes. Global Biogeochemical Cycles 10: 89-110.

Hemleben C, Spindler M, Breitinger M, Deuser W (1985) Field and laboratory studies on the ontogeny and ecology of some globorotaliid species from the Sagasso Sea of Bermuda. J Foram Res 15: 254-272.

Hemleben C, Spindler M, Anderson OR (1989) Modern planktonic foraminifera,'. Springer, New York, 363 pp.

Hemleben C, Roether W, Stoffers P, Eds. (1996) Östliches Mittelmeer, Rotes Meer, Arabisches Meer, Cruise No. 31. Meteor Berichte. Hamburg, Leitstelle Meteor, Institut für Meereskunde.

Hoefs J (1987) Stable isotope geochemistry. Springer, Berlin, 241 pp.

Hupe A, van Bennecom J, Thomas H, Ittekkot V (1998) Redfield stoichiometriy in the Arabian Sea subsurface waters. EOS, Transactions 79.

Hupe A, Karstensen J (2000) Redfield stoichiometry in the Arabian Sea subsurface waters. Global Biogeochemical Cycles (in press).

Hut G (1987) Stable isotope reference samples for geochemical and hydrological investigations, Consultants' Group Meeting IAEA, Vienna, 16.-18.04.1985. In: Report to the Director General I (eds), Vienna, pp 1-42.

Imbrie J, Hays JD, Martinson DG, McIntyre A, Morley JJ, Pisias NG, Prell WL, Shackleton NJ (1984) The orbital theory of Pleistocene climate: support from a revised chronology of the marine $\delta^{18}O$ record. In: Berger A, Imbrie J, Hays J, Kukla G, Saltzman B (eds), Milankovitch and Climate, Part I. D. Reidel Publishing Co., Dordrecht (Netherlands), pp 269-305.

Jenkins GM, Watts DG (1968) Spectral analysis and its applications. Holden-Day, San Francisco, Cambridge, London, Amsterdam, 525 pp.

Jochem FJ, Pollehne F, Zeitschel B (1993) Productivity regime and phytoplankton size structure in the Arabian Sea. Deep-Sea Research II 40: 711-735.

Joos F, Bruno M (1998) Long-term variability of the terrestrial and oceanic carbon sinks and the budgets of the carbon isotopes ^{13}C and ^{14}C. Global Biogeochemical Cycles 12: 277-295.

Kallel N, Labeyrie LD, Juillet-Leclerc A, Duplessy J-C (1988) A deep hydrological front between intermediate and deep-water masses in the glacial Indian Ocean. Nature 333: 651-655.

Keeling CD, Whorf TP (1998) Atmospheric CO_2 records from sites in the SIO air sampling. In: (eds), Trends: A Compendium of Data on Global Change. Carbon Dioxide Information Center, Oak Ridge National Laboratory, Oak Ridge, Tenn., U.S.A., pp

Keir R, Rehder G, Erlenkeuser H, Suess E (1998) The d13C anomaly in the northeastern Atlantic. Global Biogeochemical Cycles 12: 467-477.

Kirst GJ, Schneider RR, Wefer G (1998) Late Quaternary temperature variability in the Benguela Current system derived from Alkenones. Quat Res, in press.

Kohfeld KE, Fairbanks RG, Smith SL, Walsh ID (1997) *Neogloboquadrina pachyderma* (sinistral coiling) as paleoceanographic tracers in polar oceans: Evidence from Northeast Water Polynya plankton tows, sediment traps, and surface sediments. Paleoceanography 11: 679-699.

Kroon D, Ganssen G (1989) Northern Indian Ocean upwelling cells and the stable isotope composition of living planktonic foraminifers. Deep-Sea Research 36: 1219-1236.

Kroon D, Darling K (1995) Size and upwelling control of the stable isotope composition of *Neogloboquadrina dutertrei* (d'Orbigny), *Globigerinoides ruber* (d'Orbigny) and

Globigerina bulloides d'Orbigny: examples from the Panama Basin and the Arabian Sea. Journal of Foraminiferal Research 25: 39-52.

Kroopnick P (1974) The dissolved O_2-CO_2-^{13}C system in the eastern equatorial Pacific. Deep-Sea Research 21: 211-227.

Kroopnick PM, Margolis SV, Wong CS (1977) $\delta^{13}C$ variations in marine carbonate sediments as indicators of the CO_2 balance between the atmosphere and oceans. In: Andersen NR, Malahoff A (eds), Fate of fossil CO_2 in the oceans. Plenum Press, New York, pp 295-321.

Kroopnick PM (1985) The distribution of ^{13}C of ΣCO_2 in the world oceans. Deep-Sea Research 32: 57-84.

Labeyrie LD, Duplessy JC (1985) Changes in the oceanic $^{13}C/^{12}C$ ratio during the last 140,000 Years: High-latitude surface water records. Palaeogeogr, Palaeoclim, Palaeoecol 50: 217-240.

Lea DW (1995) A trace element perspective on the evolution of Antarctic Circumpolar Deep Water chemistry. Paleoceanography 10: 733-747.

Levitus S, Boyer T (1994) World Ocean Atlas 1994. U.S. Department of Commerce, Washington, D.C., pp.

Lohmann GP (1995) A model for variation in the chemistry of planktonic foraminifera due to secondary calcification and selectiv dissolution. Paleoceanography 10: 445-457.

Lynch-Steglitz J, Fairbanks RG, Charles CD (1994) Glacial-interglacial history of Antarctic Intermediate Water: Relative strengths of Antarctic versus Indian Ocean sources. Paleoceanography 9: 7-29.

Lynch-Stieglitz J, Stocker TF, Broecker WS, Fairbanks RG (1995) The influence of air-sea exchange on the isotopic comosition of oceanic carbon: observations and modelling. Glob Biogeochem Cycl 9: 653-665.

Mackensen A, Hubberten H-W, Bickert T, Fischer G, Fütterer DK (1993) The $\delta^{13}C$ in benthic foraminiferal tests of *Fontbotia wuellerstorfi* (Schwager) relative to the $\delta^{13}C$ of dissolved inorganic carbon in southern ocean deep water: implication for glacial ocean circulation models. Paleoceanography 8: 587-610.

Mantoura RFC, Law CS, Owens NJP, Burkill PH, Woodward EMS, Howland RJM, Llewellyn CA (1993) Nitrogen biogeochemical cycling in the northwestern Indian Ocean. Deep-Sea Research II 40: 651-671.

McConnaughey TA, Burdett J, Whelan JF, Paull CK (1997) Carbon isotopes in biological carbonates: Respiration and photosynthesis. Geochim Cosmochim Acta 61: 611-622.

Michel E, Labeyrie LD, Dupllessy J-C, Gorfti N (1995) Could deep Subantarctic convection feed the world deep basins during the last glacial maximum? Paleoceanography 10: 871-880.

Millero FJ, Degler EA, O'Sullivan DW, Goyet C, Eischeid G (1998) The carbon dioxide system in the Arabian Sea. Deep-Sea Research II 45: 2225-2252.

Molinelli EJ (1981) The Antarctic influence on Antarctic Intermediate Water. J Mar Res 39: 267-293.

Mook WG, Boomerson JC, Staverman WH (1974) Carbon isotope fractionation between dissolved bicarbonate and gaseous carbon dioxide. Earth and Planetary Science Letters 22: 169-176.

Mooley DA, Parthasarathy B (1984) Fluctuations in all-India summer monsoon rainfall during 1871-1978. Climatic Change 6: 287-301.

Moos CA, Brummer G-JA, Ganssen G, Helder W, Hupe A, Kloosterhuis R, Lendt R, Schneider RR, Wefer G (submitted) Seasonal and decadal changes in carbon isotope composition of the north western Arabian Sea. Deep-Sea Research I.

Moos C, Schiebel R, Schneider RR, Wefer G (submitted) Stable isotopes in planktic foraminifera recording monsoonal upwelling in the northwestern Arabian Sea. Marine Micropaleontology.

Morrison JM, Codispoti LA, Gaurin S, Jones B, Manghnani V, Zheng Z (1998) Seasonal variation of hydrographic and nutrient fields during the US JGOFS Arabian Sea Process Study. Deep-Sea Research II 45: 2053-2101.

Mulitza S, Dürkoop A, Hale W, Wefer G, Niebler H-S (1997) Planktonic foraminifera as recorders of past surface-water stratification. Geology 25: 335-338.

Mulitza S, Rühlemann C, Bickert T, Hale W, Pätzold J, Wefer G (1998) Late Quaternary $\delta^{13}C$ gradients and carbonate accumulation in the western equatorial Atlantic. Earth and Planetary Letters 155: 237-249.

Mulitza S, Arz H, Kemle-von Mücke S, Moos C, Niebler H-S, Pätzold J, Segl M (1999) The South Atlantic Carbon Isotope Record of Planktic Foraminifera. In: Fischer G, Wefer G (eds), Use Of Proxies In Paleoceanography. Springer, Berlin, New York, pp 427-445.

Murray DW, Prell WL (1992) Late Pliocene and Pleistocene climate oscillations and monsoon upwelling recorded in sediments from the Own Ridge, northwestern Arabian Sea. In: Summerhayes CP, Prell WL, Emeis KC (eds), Upwelling Systems: Evolution Since the Early Miocene. Geological Society Special Publication, pp 301-321.

Naqvi SWA, Sen Gupta R (1985) 'NO', a useful tool for the estimation of nitrate deficits in the Arabian Sea. Deep-Sea Research 32: 665-674.

Naqvi SWA (1987) Some aspects of the oxygen deficient conditions and denitrification in the Arabian Sea. Journal of Marine Research 45: 1049-1072.

Naqvi SWA, Noronha RJ (1991) Nitrous oxide in the Arabian Sea. Deep Sea Research 38: 871-890.

Neftel A, Friedli H, Moos E, Lötscher H, Oeschger H, Siegenthaler U, Stauffer B (1994) Historical CO_2 record from the Siple Station ice core. In: Boden TA, Kaiser DP, Sepanski RJ, Stoss FW, Logsdon GM (eds), Trends '93: A Compendium of Data on Global Change. Carbon Dioxide Information Center, Oak Ridge National Laboratory, Oak Ridge, Tennessee, U.S.A., pp 11-14.

Niebler H-S (1995) Rekonstruktionen von Paläo-Umweltparametern anhand von stabilen Isotopen und Faunen-Vergesellschaftungen planktischer Foraminiferen im Südatlantik. Alfred Wegner Institute for Polar and Marine Research, 198 pp.

Niitsuma N, Oba T, Okada M (1991) Oxygen and carbon isotope stratigraphy at Site 723, Oman Margin. In: Emeis K-C, Meyers PA, Niitsuma N, Prell WL (eds), Proceedings of the Ocean Drilling Program, Scientific Results. Ocean Drilling Program, College Station, Texas, pp 321-341.

Ninnemann US, Charles CD (1997) Regional differences in Quaternary Subantarctic nutrient cycling: Link to intermediate and deep water ventilation. Paleoceanography 12: 560-567.

Oppo DW, Fairbanks RG (1987) Variability in the deep and intermediate water circulation of the Atlantic ocean during the past 25,000 years: Northern hemisphere modulation of the Southern ocean. Earth Planetary Sci Letters 86: 1-15.

Oppo DW, Fairbanks RG (1989) Carbon isotopic composition of tropical surface water during the past 22,000 years. Paleoceanography 4: 333-351.

Ortiz JD, Mix AC, Collier RW (1995) Environmental control of living symbiotic and asymbiotic foraminifera of the California Current. Paleoceanography 10: 987-1009.

Ortiz JD, Mix AC, Rugh W, Watkins JM, Collier RW (1996) Deep-dwelling planktonic foraminifera of the northeastern Pacific Ocean reveal environmental control of oxygen and carbon isotopic disequilibria. Geochemica et Cosmochemica Acta 60: 4509-4523.

Owens NJP, Burkill PH, Mantoura RFC, Woodward EMS, Bellan IE, Aiken J, Howland RJM, Llewellyn CA (1993) Size-fractionated primary production and nitrogen assimilation in the northwestern Indian Ocean. Deep-Sea Research II 40: 697-709.

Paillard D, Labeyrie L, Yiou P (1996) Macintosh program performs time-series analysis. EOS, Transactions, AGU 77: 379.

Parthasarathy B, Munot AA, Kothawale DR (1994) All-India monthly and seasonal rainfall series: 1871-1993. Theoretical and Applied Climatology 49: 217-224.

Pastouret L, Chamley H, Delibrias G, Duplessy JC, Thiede J (1978) Late Quaternary climatic changes in western tropical Africa deduced from deep-sea sedimentation off the Niger delta. Oceanol Acta 1: 217-232.

Peeters F, Ivanova E, Conan S, Brummer G-J, Ganssen G, Troelstra S, Hinte Jv (1999) A size analysis of planktic foraminifera from the Arabian Sea. Marine Micropaleontology 36: 31-63.

Prell WL, Hutson WH, Williams DF, Bé AWH, Geitzenauer K, Molfino B (1980) Surface circulation of the Indian Ocean during the last glacial maximum, approximately 18,000 yr B. P. Quat Res 14: 309-336.

Prell WL, Curry WB (1981) Faunal and isotopic indices of monsoonal upwelling: Western Arabian Sea. Oceanologica Acta 4: 91-98.

Prell WL (1984a) Monsoonal climate of the Arabian Sea during the late Quaternary: A response to changing solar radiation. In: Berger A, Imbrie J, Hays J, Kukla G, Saltzman B (eds), Milankovitch and Climate, Part I. D. Reidel Publishing Co., Dordrecht (Netherlands), pp 349-366.

Prell WL (1984b) Variation of monsoonal upwelling: A response to changing solar radiation. In: Hansen JE, Takahasi T (eds), Geophysical Monograph Series. American Geophysical Union, Washington, D.C., pp 48-57.

Prell WL, Van Campo E (1986) Coherent response of Arabian Sea upwelling and pollen transport to late Quaternary monsoonal winds. *Nature* 323: 526-528.

Quay PD, Tilbrook B, Wong CS (1992) Oceanic uptake of fossil fuel CO_2: Carbon-13 evidence. Science 256: 74-79.

Rau GH, Froehlich PN, Takahashi T, Des Marais DJ (1991) Does sedimentary organic $\delta^{13}C$ record variations in Quaternary ocean [$CO_{2(aq)}$]?. Paleoceanography 6: 335-347.

Ravelo AC, Fairbanks RG, Philander SGH (1990) Reconstructing tropical Atlantic hydrography using planctonic foraminifera and an ocean model. Paleoceanography 5: 409-431.

Ravelo AC, Fairbanks RG (1992) Oxygen isotopic composition of multiple species of planktonic foraminifera: Recorders of the modern photic zone temperature gradient. Paleoceanography 7: 815-831.

Ravelo AC, Fairbanks RG (1995) Carbon isotopic fractionation in Multiple species of planktonik Foraminifera from Core-Tops in the Tropical Atlantic. Journal of Foraminiferal Research 25: 53-74.

Redfield AC, Ketchum BH, Richards FA (1963) The influence of organisms on the composition of sea-water. In: Hill MN (eds), The Sea. Interscience, New York, pp 26-77.

Robinson C, Williams PJl (1991) Development and assessment of an analytical system for the accurate and continual measurement of total dissolved inorganic carbon. Marine Chemistry 34: 157-175.

Romanek CS, Grossman EL, Morse JW (1992) Carbon isotopic fractionation in synthetic aragonite and calcite: effects of temperature and precipitation rate. Geochimica et Cosmochimica Acta 56: 419-430.

Rostek F, Ruhland G, Bassinot FC, Müller PJ, Labeyrie LD, Lancelot Y, Bard E (1993) Reconstructing sea surface temperature and salinity using $\delta^{18}O$ and alkenone records. Nature 364: 319-321.

Rühlemann C, Mulitza S, Müller PJ, Wefer G, Zahn R (1998) Tropical Atlantic warming during conveyor slowdown. Nature, subm.

Savin SM, Douglas RG (1973) Stable isotope and magnesium geochemistry of recent planktonic foraminifera from the South Pacific. Geol Soc Am Bull 84: 2327-2342.

Schiebel R, Hiller B, Hemleben C (1995) Impacts of storms on recent planktic foraminiferal test production and $CaCO_3$ flux in the North Atlantic at 47 degrees N, 20 degrees W (JGOFS). Marine Micropaleontology 26: 115-129.

Schneider R, Dahmke A, Kölling A, Müller PJ, Schulz HD, Wefer G (1992) Strong deglacial minimum in the $\delta^{13}C$ record from planktonic foraminifera in the Benguela Upwelling Region: paleoceanographic signal or early diagenetic imprint. In: Summerhayes CP, Prell WL, Emeis KC (eds), Upwelling systems: Evolution since the early Miocene. Geological Society Special Publication no. 63, 285-297.

Schneider RR, Müller PJ, Wefer G (1994) Late Quaternary paleoproductivity changes off the Congo deduced from stable carbon isotopes of planktonic foraminifera. Palaeogeogr, Palaeoclim, Palaeoecol 110: 255-274.

Schott F, Swallow JC, Fieux M (1990) The Somali Current at the equator: annual cycle of currents and transports in the upper 1000 m and connection to neighbouring latitudes. Deep-Sea Research 37: 1825-1848.

Shackleton NJ, Opdyke ND (1973) Oxygen isotope and paleomagnetic stratigraphy of equatorial Pacific core V 28-238: Oxygen isotope temperatures and ice volumes on a 10^5 year scale. Quartenary Research 3: 39-55.

Shackleton NJ, Opdyke ND (1976) Oxygen-isotope and paleomagnetic stratigraphy of Pacific Core V28-239: late Pliocene to latest Pleistocene. Geol Soc Amer Mem 145: 449-464.

Shackleton NJ (1977) Carbon-13 in *Uvigerina*: tropical rainforest history and the equatorial Pacific carbonate dissolution cycles. In: Andersen NR, Malahoff A (eds), The Fate of Fossil Fuel CO_2 in Oceans. Plenum Press, New York, pp 401-427.

Shackleton NJ, Imbrie J, Hall MA (1983) Oxygen and carbon isotope record of East Pacific core V19-30: implications for the formation of deep water in the late Pleistocene North Atlantic. Earth and Planetary Science Letters 65: 233-244.

Shackleton NJ, Pisias NG (1985) Atmospheric carbon dioxide, orbital forcing , and climate. In: Sundquist ET, Broecker WS (eds), The carbon cycle and atmospheric CO_2: Natural variations Archean to Present. American Geophysical Union, Washington, pp 303-318.

Shetye SR, Gouveia AD, Shenoi SSC, Michael GS, Sundar D, Almeida AM, Santanam K (1991) The coastal current off western India during the northeast monsoon. Deep Sea Research 38: 1517-1529.

Short DA, Mengel JG, Crowley TJ, Hyde WT, North GR (1991) Filtering of Milankovitch cycles by Earth's geography. Quat Res 35: 157-173.

Siegenthaler U, Münnich KO (1981) 13C/12C Fractionation during CO_2 Transfer from Air to Sea. In: Bolin B (eds), Carbon CycleModelling. John Wiley & Sons, New York, pp 249-257.

Siegenthaler U, Sarmiento JL (1993) Atmospheric carbon dioxide and the ocean. Nature 365: 119-125.

Sirocko F, Garbe-Schönberg D, McIntyre A, Molfino B (1996) Teleconnections between the subtropical monsoon and high-latitude climates during the Last Deglaciation. Science 272: 526-529.

Smith SL, Codispoti LA, Morrison JM, Barber RT (1998) The 1994-1996 Arabian Sea Expedition: An integrated, interdisciplinary investigation of the response of the northwestern Indian Ocean to monsoonal forcing. Deep-Sea Research II 45: 1905-1915.

Spero HJ, Williams DF (1990) Evidence for seasonal low salinity surface waters in the Gulf of Mexico over the last 16,000 years. Paleoceanography 5: 963-975.

Spero HJ, Lea DW (1993) Intraspecific stable isotope variability in the planktic foraminifera Globigerinoides sacculifer: Results from laboratory experiments. Marine Micropaleontology 22: 221-234.

Spero HJ, Lea DW (1996) Experimental determination of stable isotope variability in Globigerina bulloides: implications for paleoceanographic reconstructions. Marine Micropaleontology 28: 231-246.

Spero HJ, Bijma J, Lea DW, Bemis BE (1997) Effects of sea-water carbonate chemistry on planktonic foraminiferal carbon and oxygen isotope values. Nature 390: 497-500.

Steens TNF, Ganssen G, Kroon D (1992) Oxygen and carbon isotopes in planktonic foraminifera as indicators of upwelling intensity and upwelling-induced high productivity in sediments from the northwestern arabian Sea. In: Summerhayes CP, Prell CP, Emeis KC (eds), Upwelling Systems: Evolution Since the Early Miocene. Geological Society Special Publication, pp 107-119.

Steinberg PA, Millero FJ, Zhu X (1998) Carbonate system response to iron enrichment. Marine Chemistry 62: 31-43.

Swallow JC (1984) Some Aspects of the Physical Oceanography of the Indian Ocean. Deep-Sea Research 31: 639-650.

Tans PP, Berry JA, Keeling RF (1993) Oceanic $^{13}C/^{12}C$ observations: a new window on ocean CO_2 uptake. Global Biogeochemical Cycles 7: 353-368.

Tomczak M, Godfrey JS (1994) Regional Oceanography: An Introduction. Butler and Tanner, London, 422 pp.

Tsuchia M, Talley LD, McCartney MS (1994) Water-mass distributions in the western South Atlantic; A section from South Georgia Island (54S) northward across the equator. J Mar Res 52: 55-81.

Turner JV (1982) Kinetic fractionation of carbon-13 during calcium carbonate precipitation. Geochim Cosmochim Acta 46: 1183-1191.

Van Hinte JE, van Weering TCE, Troelstra SR, Eds. (1995). Tracing a seasonal upwelling. Cruise Reports Netherlands Indian Ocean Program. Leiden, National Museum of History.

Webster PJ, Magana VO, Palmer TN, Shukla J, Tomas RA, Yanai M, Yasunari T (1998) Monsoon: Processes, predictability, and the prospects for prediction. Journal of Geophysical Research 103: 14,451-14,510.

Wefer G, Dunbar RB, Suess E (1983) Stable isotopes of foraminifers off Peru recording high fertility and changes in upwelling history. In: Thiede J, Suess E (eds), Coastal Upwelling: Its Sediment Record. New York, pp 295-308.

Wefer G (1985) Die Verteilung stabiler Isotope in Kalkschalen mariner Organismen. Geologisches Jahrbuch A 82: 1-112.

Wefer G, Berger WH (1991) Isotope paleontology: growth and composition of extant calcareous species. Marine Geology 100: 207-248.

Wefer G, Berger WH, Bickert T, Donner B, Fischer G, Kemle-von Mücke S, Meinecke G, Müller PJ, Mulitza S, Niebler HS, Pätzold J, Schmidt H, Schneider RR, Segl M (1996) Late Quaternary Surface Circulation of the South Atlantic: The Stable Isotope Record and Implications for Heat Transport and Productivity. In: Wefer G, Berger WH, Siedler G, Webb DJ (eds), The South Atlantic - Present and Past Circulation. Springer, Berlin, pp 461-502.

Wefer G, Berger WH, Bijma J, Fischer G (1999) Clues to Ocean History: a Brief Overview of Proxies. In: Fischer G, Wefer G (eds), Use Of Proxies In Paleoceanography. Springer, Berlin, New York, pp 1-68.

Weischet W (1988) Einführung in die Allgemeine Klimatologie. Teubner Stuttgart, 264 pp.

Wolff T, Grieger B, Hale W, Dürkoop A, Mulitza S, Pätzold J, Wefer G (1999) On the Reconstruction of Paleosalinities. In: Fischer G, Wefer G (eds), Use Of Proxies In Paleoceanography. Springer, Berlin, New York, pp 207-228.

Wu G, Berger WH (1989) Planktonic foraminifera: Differentail dissolution and the Quaternary stable isotope record in the West Equatorial Pacific. Paleoceanography 4: 181-198.

Wyrtki K (1971) Oceanographic Atlas of the International Indian Ocean Expedition. National Science Foundation, Washington, pp 531.

Wyrtki K (1973) Physical Oceanography of the Indian Ocean. In: Zeitschel B (eds), The Biology of the Indian Ocean. Springer-Verlag, Berlin, pp 18-36.

Zahn R, Sarnthein M (1987) Benthic isotope evidence for changes of the Mediterranean Outflow during the Late Quaternary. Paleoceanography 2: 543-559.

Zielinski U, Gersonde R, Sieger R, Fütterer D (1998) Quaternary surface water temperature estimations: Calibration of a diatom transfer function for the Southern Ocean. Paleoceanography 13: 365-383.

Danksagung

Bei Herrn Professor Dr. Gerold Wefer möchte ich mich für die Vergabe und Betreuung der Arbeit, sowie für sein stets, anregend kritisches Interesse an der Entstehung der Dissertation bedanken. Gleichfalls geht mein besonderer Dank an Dr. Ralph Schneider, von dessen Unterstützung und Engagement die Arbeit entscheidend profitierte.

Für die freundliche Übernahme des zweiten Gutachtens danke ich Herrn PD Dr. Andreas Mackensen.

Aus der nie endenden Diskussionsbereitschaft meiner Kollegen Helge Arz, Dörte Budziak, Thomas Felis, Sylvia Kemle- von Mücke, Henning Kuhnert, Stefan Mulitza und Thorsten Bickert profitierte diese Arbeit durch zahlreiche Anregungen und Kritiken. Auch die engagierten Diskussionen innerhalb der Arbeitsgruppe "Meeresgeologie", sowie die angenehme Arbeitsatmosphäre trugen erheblich zum erfolgreichen Gelingen dieser Arbeit bei. Frank Schmieder möchte ich für die Unterstützung bei der mathematischen Auswertung meiner Zeitreihen danken.

Für die umfassende Unterstützung bei den Laborarbeiten möchte ich meinen herzlichen Dank an Dr. Monika Segl und Birgit Meyer-Schack richten. Ohne die Unterstützung von Gisela Boelen, Carmen Murken, Adelheit Grimm-Geils und Britta Schilder wäre ich sicherlich an der ein oder anderen "Verwaltungshürde" gescheitert. Die bereitwillige und geduldige Hilfe von Thorsten Klein, Gerrit Meinecke und Götz Ruhland ermöglichte es meine Arbeit in Bits und Bytes zu fassen und zwischendurch auch auf Postern zu präsentieren.

Für die intensive und angenehme Zusammenarbeit, sowie den problemlosen Austausch wissenschaftlichen Datenmaterials möchte ich Geert-Jan Brummer, Gerald Ganssen und Ralf Schiebel herzliche danken.

Überaus dankbar bin ich Reina, für ihre Anteilnahme und die Tolerierung meiner Arbeitsweise während der letzten Jahre. Nicht zuletzt möchte ich mich bei meinem Freundes- und Bekanntenkreis sowie meiner Familie für die Unterstützung und den menschlichen Zuspruch bedanken.